



universität  
wien

# DISSERTATION

Titel der Dissertation

„Identification of novel biomarkers for severe allergic  
asthma“

Verfasser

Mag. znan. Berislav Bosnjak

angestrebter akademischer Grad

Doktor der Naturwissenschaften (Dr.rer.nat.)

Wien, 2015

Studienkennzahl lt. Studienblatt:	A 091 490
Dissertationsgebiet lt. Studienblatt:	Molekulare Biologie
Betreuer:	Ao. Univ.-Prof. Dr. Oskar Hoffmann



Diese Arbeit wurde an der Medizinische Universität Wien in der Forschungsgruppe von Dr. Michelle M. Epstein im Labor für Experimentelle Allergie an der Universitätsklinik für Dermatologie durchgeführt.



# CONTENTS

SUMMARY .....	1
ZUSAMMENFASUNG.....	4
1. INTRODUCTION.....	7
1.1. Asthma: definition, epidemiology, etiology, pathogenesis and phenotypes .....	7
1.2. Allergic asthma pathophysiology.....	10
1.3. Treatment of allergic asthma and disease severity .....	13
1.3.1. Available treatments for allergic asthma .....	13
1.3.2. Disease severity and need for novel therapies .....	16
1.4. Asthma biomarkers .....	17
1.5. Animal models of allergic asthma.....	20
1.6. Allergic asthma imaging .....	22
2. AIMS OF THE THESIS .....	26
3. PUBLICATIONS.....	28
3.1. Manuscript.....	28
3.2. Publication 1 .....	90
3.3. Publication 2 .....	100
4. CONCLUDING DISCUSSION.....	109
5. DECLARATION OF CONTRIBUTION .....	111
6. REFERENCES.....	112
7. ACKNOWLEDGMENTS.....	122
8. CURRICULUM VITAE.....	123



## SUMMARY

Asthma is a chronic inflammatory pulmonary disease characterized by recurrent episodes of wheezy, laboured breathing that affects approximately 300 million people worldwide and can be fatal. Current therapies (especially inhaled corticosteroids and  $\beta$ 2-agonists) efficiently control allergic asthma in most of the patients. Development of novel therapies is crucial, however, for disease control in 5-10% of patients with very severe forms of disease that cannot be controlled even with high doses of oral steroids. Additionally, there is still need to improve side effect profile of currently available drugs, especially as they do not cure the disease and have to be continuously administered for a lifetime of a patient.

To guide research of new treatments for asthma, it is crucial to identify and develop novel biomarkers of the disease. Moreover, clinically relevant biomarkers are crucial for understanding of asthma heterogeneity, as the disease differs in severity, natural history, comorbidities, and treatment response between patients. Development of biomarkers for distinct asthma subtypes could ultimately guide research towards development of personalized asthma medications.

The main aim of this work was to detect genomic biomarkers, to develop novel optical imaging techniques and to establish novel treatment modalities for allergic asthma. Therefore, we used 3 novel approaches to (i) provide comprehensive gene expression profile in mice with acute allergic asthma; (ii) visualize allergic inflammation in an experimental mouse model of allergic asthma; and (iii) to treat allergic asthma relapse in mice with a selective muscarinic receptor antagonist drug tiotropium bromide.

To provide a comprehensive gene expression profile in mice with acute allergic asthma, in the manuscript we analyzed 6 publically available expression datasets using a novel and innovative gene- and pathway-driven bioinformatics strategy. We generated and validated an acute asthma signature gene list

consisting of asthma-annotated genes as well as of asthma-unrelated genes that constitute an “acute allergic asthma ignorome” in mice. Further, functional and network connectivity analyses indicated that asthma-annotated and -ignorome genes cluster into 4 biologically relevant domains. Finally, within our network we discovered 12 super-connectors genes that link the complex pathophysiological mechanisms underlying asthma and are normalized upon treatment with glucocorticosteroids. Thus, our powerful bioinformatic analyses prioritized asthma-related and -ignorome genes within the clusters and biological domains to provide important insights in asthma pathophysiology.

In publication 1, we developed a novel imaging approach for detection of pulmonary inflammation. Dendritic polyglycerol sulfates selectively bind P- and L-selectins and C3 and C5 complement factors that are upregulated at the site of inflammation. Using fluorescence imaging, we detected specific accumulation of near infrared fluorescence dye labeled dendritic polyglycerol sulfates (dPGS-NIRF) in the lungs of mice with acute allergic asthma. Further, our results show that dPGS-NIRF had a faster uptake compared to other commercially available imaging probes. Altogether, these results suggest that dPGS-NIRF is a potent probe for *in vivo* monitoring of pulmonary inflammation.

Finally, in publication 2, we tested efficacy of selective long-acting muscarinic receptor antagonist tiotropium bromide in acute onset and relapsing mouse models of allergic asthma. Tiotropium bromide is important for the treatment of chronic obstructive pulmonary disease. However, it is not commonly used to treat asthma, even though the mode of action suggests that they may also be effective. Our results demonstrate that tiotropium efficiently suppressed airway hyperreactivity, mucus hypersecretion and airway inflammation in experimental allergic asthma. These data highlighted the anti-inflammatory properties of tiotropium and support its use for the treatment of asthma.

Altogether, the results presented in this thesis provide detailed gene expression profiling in acute allergic asthma, describe a novel imaging technology for visualization of allergic lung inflammation and expand armamentarium of anti-asthmatic drugs. While the gene expression data provide multiple novel bi-

omarker and treatment targets, a combination of our imaging approach with the asthma relapse model would provide an elegant experimental setting for their testing.

## ZUSAMMENFASSUNG

Asthma ist eine chronisch entzündliche Erkrankung der Lunge charakterisiert durch wiederkehrende Episoden pfeifender, schwerfälliger Atmung, von der weltweit etwa 300 Millionen Menschen betroffen sind und tödlich enden kann. Allergisches Asthma kann durch gängige Therapien, vor allem mit inhalativen Kortikosteroiden und  $\beta$ 2-Agonisten, bei den meisten Patienten effizient behandelt werden. Allerdings ist die Entwicklung neuer Therapien für 5-10% der Patienten dringend erforderlich, da diese an sehr schweren Asthma-Formen leiden, welche nicht einmal auf hohe Dosen oral verabreichter Kortikosteroide ansprechen. Außerdem ist es notwendig das Nebenwirkungsprofil erhältlicher Medikamente zu verbessern, da diese nicht zur Heilung führen, sondern lediglich die Symptome lindern und ein Leben lang eingenommen werden müssen.

Zur Erforschung neuer Therapieansätze ist die Identifizierung und Entwicklung neuartiger Asthma-Biomarker essentiell. Zudem sind klinisch relevante Biomarker notwendig, um die Heterogenität des Asthmas zu verstehen, da es sich in Entstehung, Stärke, Verlauf, Komorbiditäten und im Ansprechen auf Therapien je nach PatientIn unterscheidet. Die Entwicklung von Biomarkern für bestimmte Asthma-Subtypen könnte letztendlich zur Etablierung personalisierter Asthma Medikamente führen.

Das Ziel dieser Arbeit war es, genomische Biomarker zu finden, neue Bildgebungstechniken zu entwickeln und neue Therapien für allergisches Asthma zu etablieren. Dafür verwendeten wir 3 neue Ansätze, um (i) ein umfassendes Genexpressions-Profil in Mäusen mit allergischem Asthma zu erstellen; (ii) entzündliches Geschehen in einem experimentellen Maus-Modell für allergisches Asthma zu visualisieren; und um (iii) allergische Asthma-Rückfälle der Mäuse mit dem selektiven Muskarinrezeptor-Antagonisten Tiotropiumbromid zu behandeln.

Zur Erstellung eines umfassenden Genexpressions-Profiles in Mäusen mit allergischem Asthma, analysierten wir 6 öffentlich zugängliche Expressions-Datensätze mit einer neuartigen und innovativen Gen- und Signalweg-orientierten Bioinformatik-Strategie. Wir erstellten und validierten eine Signatur-Gen Liste für akutes Asthma in Mäusen, bestehend aus Genen, welche dem Asthma zugeordnet sind und Genen, die bisher nicht mit Asthma in Zusammenhang gebracht wurden und als akutes, allergisches „Asthma Ignorome“ bezeichnet werden. Funktionelle und Netzwerkkonnektivitäts-Analysen zeigten, dass sich bekannte Asthma Gene und „Asthma Ignorome“ Gene in 4 biologisch relevante Domänen gruppieren lassen. Des Weiteren entdeckten wir 12 Super-Konnektor Gene des Asthmas, welche komplexe pathophysiologische Mechanismen verbinden, die mit Glukokortikoid-Behandlung normalisiert werden können. Unsere leistungsstarken bioinformatischen Analysen priorisierten Asthma bezogene und „Asthma Ignorome“ Gene in den Clustern und biologischen Domänen, um wichtige Einblicke in die Asthma-Pathophysiologie zu erlangen.

In der ersten Publikation entwickelten wir eine neuartige Bildgebungstechnik, um pulmonale Entzündungen zu detektieren. Dendritische Polyglycerolsulfate binden selektiv P- und L-Selektine und die Komplementfaktoren C3 und C5, welche an Entzündungsstellen hochreguliert sind. Durch Fluoreszenzbildgebung entdeckten wir spezifische Akkumulationen von infrarotnah-fluoreszenz markierten dendritischen Polyglycerolsulfaten (dPGS-NIRF) in den Lungen von Mäusen mit allergischem Asthma. Des Weiteren zeigten unsere Resultate, dass dPGS-NIRF eine schnellere Absorption aufwies als andere kommerziell erhältliche Bildgebungs-Sonden. Zusammenfassend konnten wir demonstrieren, dass dPGS-NIRF eine potente Sonde für die *in vivo* Darstellung von Entzündungen ist.

In der zweiten Publikation untersuchten wir die Wirksamkeit des selektiven, lang-wirksamen Muskarinrezeptor-Antagonisten Tiotropiumbromid im akuten und rezidivierenden Maus-Modell für allergische Asthma. Tiotropiumbromid wird zur Behandlung der chronisch obstruktiven Lungenerkrankung eingesetzt, aber üblicherweise nicht in der Asthmatherapie verwendet, obwohl des-

sen Wirkmechanismus gute Wirksamkeit vermuten lassen. Unsere Resultate zeigen, dass Tiotropiumbromid bei experimentellem allergischem Asthma die Entzündung, Hyperreaktivität und Schleimüberproduktion der Atemwege effizient unterdrücken konnte. Diese Daten demonstrierten die entzündungshemmenden Eigenschaften von Tiotropiumbromid und bekräftigen dessen Einsatz in der Asthmatherapie.

Zusammenfassend zeigen die Resultate dieser Arbeit detaillierte Genexpressions-Profile in akut allergischem Asthma, beschreiben eine neuartige Bildgebungstechnologie zur Visualisierung von allergischen Entzündungen der Lunge und erweitern das Arsenal an anti-asthmatischen Arzneistoffen. Die Genexpressionsdaten liefern zahlreiche neuartige Biomarker und Therapieansätze, während unsere Bildgebungstechnik in Kombination mit dem rezidivierenden Asthma-Modell einen eleganten Versuchsrahmen, bietet diese Biomarker zu testen.

# 1. INTRODUCTION

## 1.1. Asthma: definition, epidemiology, etiology, pathogenesis and phenotypes

The first clinical description of asthma (coming from old greek verb ἀάζειν (aazein), meaning to exhale with open mouth, to pant) is ascribed to Aretaeus of Cappadocia in the first century AD (1). From then on, the definition of asthma has changed to include a heterogenous group of conditions that result in recurrent and reversible airway obstruction (2,3). According to the Global Strategy for Asthma Management and Prevention Report, *“Asthma is a chronic inflammatory disorder of the airways in which many cells and cellular elements play a role. The chronic inflammation is associated with airway hyper-responsiveness that leads to recurrent episodes of wheezing, breathlessness, chest tightness, and coughing, particularly at night or in the early morning. These episodes are usually associated with widespread, but variable, airflow obstruction within the lung that is often reversible either spontaneously or with treatment.”* (4).

Asthma is a common disease that affects ~300 million individuals and causes ~250, 000 deaths per year worldwide (2,4). Asthma prevalence increased substantially during second half of 20<sup>th</sup> century (5). Thereafter, it seems to have plateaued in high income countries, but still increases in many low and middle income countries (4). In Austria, the prevalence of clinical asthma is ~5% (6), and it increased from 1996 to 2002 for 16% in children aged 6-7 years and for 32% in children aged 12-14 years (7).

Multiple genetic and environmental factors are involved in asthma. Twin studies indicate that genetic effects explain 35 to 80% of the variation in the risk for the disease, while the remaining variation is due to non-shared environmental effects (8,9). Numerous genome-wide linkage, candidate gene and genome-wide association studies indicate that it is a polygenic disease with an increasingly large list of genes involved in different biological mechanisms

(2,9-11). March et al. (11) categorized asthma-related genes into broad functional groups that include:

- T helper cell type 2 (Th2)-mediated cell response (including transcription factor *GATA3*, cytokines *IL4* and *IL13*, signaling mediator *STAT6* and the beta-chain of the IgE receptor *FCER1*);
- inflammation (such as cytokine *IL18* and its receptor *IL18R1*);
- environmental sensing and immune detection (genes involved in antigen recognition like Toll-like receptor (TLR) *TLR2*, *TLR4* and human leukocyte antigen HLA class II molecule);
- airway remodeling (i.e. a disintegrin and metalloproteinase domain-containing protein 33 (*ADAM33*) that is expressed on smooth muscle cells and lung fibroblasts);
- bronchoconstriction (such as a receptor for acetylcholine *CHRNA3/5* and nitric oxide synthase *NOS1*); and
- epithelial barrier function (including filaggrin (*FLG*), anti-microbial peptide defensin-beta1 (*DEFB1*) and an inhibitor of dendritic cell-mediated Th2-cell differentiation Clara cell 16-kD protein (*CC16*).

In individuals with genetic susceptibility to asthma, environmental factors can either elicit asthma or have protective effects. Factors that contribute to asthma development or can trigger asthma attack include biologic aeroallergens (house dust mites, pollen, animal dander, molds, etc.), air pollutants from tobacco smoke or combustion devices, irritant chemicals and fumes, viruses (especially rhinoviruses), as well as extreme weather conditions and changing climate (2). On the other hand, living on a farm or exposure to day care early in life is associated with decrease risk of asthma later in life (3).

Complexity of the clinical and pathophysiological characteristics that belong to the term “asthma” has recently prompted a concept that asthma consists of multiple phenotypes (3,12-14). The term ‘phenotype’ is defined as the “*observable properties of an organism that are produced by the interactions of the genotype and the environment*” (12). According to clinical characteristics, triggers and general inflammatory processes several asthma phenotypes

have been proposed (3,12) and there are attempts to describe specific pathogenic mechanisms that might underlie a certain phenotype (13,14). An integrated view of major asthma phenotypes with relevant pathological mechanisms is presented in Table 1.

**Table 1. An integrated list of major clinical and molecular asthma phenotypes.** Source: Martinez and Vercelli, 2013, (3).

	Natural history	Clinical and physiological features	Pathobiology and biomarkers	Response to therapy
<b>Th2-high phenotype</b>				
Early-onset allergic	Early onset, mild to severe	Allergic symptoms and other diseases	Thick subepithelial basement membrane, specific IgE, Th2 cytokines	Corticosteroid-responsive, Th2-targeted
Late-onset eosinophilic	Adult onset, often severe	Sinusitis, less allergic	Corticosteroid-refractory, eosinophilia, interleukin 5	Responsive to antibody to interleukin 5 and cysteinyl leukotriene modifiers, corticosteroid-refractory
<b>Th2-low phenotype</b>				
Obesity-related	Adolescent and adult onset	Women mainly affected, very symptomatic, airway hyper-responsiveness less clear	Lack of Th2 biomarkers, oxidative stress	Responsive to weight loss, antioxidants, and possibly to hormonal therapy
Neutrophilic	Adult onset	Low FEV1, more air trapping	Sputum neutrophilia, Th17 pathways, interleukin 8	Possibly responsive to macrolide antibiotics
Th2=T-helper-type-2 cytokine. FEV1=forced expiratory volume in 1 s.				
<b>Table: An integrated view of clinical and molecular asthma phenotypes<sup>92</sup></b>				

In addition to phenotypes, recent progress in methods for molecular phenotyping grouped asthma variants into ‘endotypes’, or “*disease subtypes based on cellular and molecular mechanisms*” (14,15). Asthma endotypes, thus, represent distinct disease entities with consistent pathophysiological mechanisms related to the divergent clinical presentation, epidemiology, and response to different treatments (16). Several studies used gene expression (17,18) and proteomics (19) data to define divergent asthma endotypes. However, there are still no generally accepted criteria that for endotype definition or use in clinics (14,16).

## 1.2. Allergic asthma pathophysiology

Allergic asthma is an asthma phenotype strongly linked to atopy (a hereditary bias toward development of allergic reactions) and allergy (a type I hypersensitivity reaction to a substance that is present in amounts that do not affect most people). Atopy is a major known predisposing factor for asthma (20), and allergy is involved in ~80% of childhood asthma and in 40-50% of adult asthma (21). Clinically, it can be further subdivided into early-onset (usually during childhood) and late-onset (after 20 years of age) asthma phenotype (22).

Defining features of allergic asthma include an underlying T-helper-type-2 (Th2)-cell- and an IgE-mediated immune response against allergen, a type of antigen that is harmless to the body, but induces an abnormally vigorous immune response. The initial step is allergen sensitization that involves a complex interplay of environmental factors and host immune response ultimately leading to the differentiation of allergen specific Th2 cells (23). Airway epithelium, apart from serving as a physical barrier, is actively involved in the response to environmental insults (e.g., aerallergens that have proteolytic properties (23)) by secreting inflammatory mediators and antimicrobial peptides, including interleukin (IL)-25, IL-33 and thymic stromal lymphopoietin (TSLP) (24-26). IL-25 and IL-33 activate type 2 innate lymphoid cells (ILC2) to secrete IL-5 and IL-13 that can directly act on lung structural cells (to induce airway hyperresponsiveness (AHR) and mucus oversecretion), as well as on immune system (recruiting eosinophils or inducing alternative activation of macrophages) (27). TSLP, in contrast, induces OX40 ligand expression on dendritic cells, which then prime naïve T cells in secondary lymphatic organs to differentiate into the Th2 cell subtype (28). Th2 cells then secrete IL-4 and IL-13 and induce B-cell isotype switching leading to the generation of allergen-specific IgE and IgG1 (in mice) or IgG<sub>4</sub> (in humans) (29-31). While memory T and B cells usually provide long-term antigen-specific protective immunity to previously encountered pathogens, immunological Th2 memory plays a crucial role in pathophysiology of allergic asthma. Numerous data from animal models and clinical studies support the central role of allergen-

specific memory Th2 cells (32-35) and IgE-producing B cells (36,37) in the initiation and maintenance of the key pathophysiological features of the disease.

Re-exposure to the allergen induces, in sensitized individuals, a characteristic biphasic response that includes innate (early-phase) and adaptive (late-phase) mechanisms. In the early phase, occurring within minutes upon contact, allergen interacts with IgE bound to high-affinity Fc $\epsilon$ RI receptors on basophils and mast cells, causing their crosslinking and resulting in the release of inflammatory mediators, including histamine, leukotrienes, prostaglandins, chemokines and cytokines (38,39). These mediators, in concert, induce airway smooth muscle contraction, mucus secretion and vasodilatation of blood vessels that mediate the initial symptoms of an asthma attack. Furthermore, as the response progresses to late phase, basophil- and mast cell-derived products enable infiltration of other innate and immune cells, including eosinophils, neutrophils, T and B cells (38,39). Mast cells also secrete several mediators crucial for recruitment of memory Th2 cells and eosinophils, including prostaglandin D2 (PGD2) that binds to chemoattractant receptor homologous molecule expressed on Th2 cells (CRTH2) (40,41). The late phase usually starts a few hours after the early phase response and is mediated mainly by Th2 cells and their cytokines (particularly IL-4, IL-5 and IL-13) (38). IL-4 and IL-13 directly promote multiple features of asthma, including goblet cell metaplasia, airway hyperresponsiveness, smooth muscle remodeling and subepithelial fibrosis, while the main function of IL-5 is the stimulation of eosinophil development, survival and activation (42). Eosinophil accumulation in the lungs, mediated by chemokine CCL11 (43), is one of the defining features of allergic asthma. Their function in the pathology of asthma, however, is still not completely elucidated because of conflicting data obtained with transgenic animals and inhibition experiments (reviewed in (44)). It appears that eosinophils contribute, at least to a part, to various aspects of the disease, including Th2 cell differentiation, airway hyperresponsiveness and remodeling (44). Allergic inflammation induced by allergen re-exposure involves many other leukocytes, including B cells, other helper T cell subtypes (Th17, Th9, Th1, regu-

latory T cells), neutrophils and basophils (reviewed in (39,45)) that are interconnected in a complex network depicted in Figure 1. It is also important to note that during the inflammatory response to an allergen, leukocytes sometimes show overlapping functions and can compensate for each other.

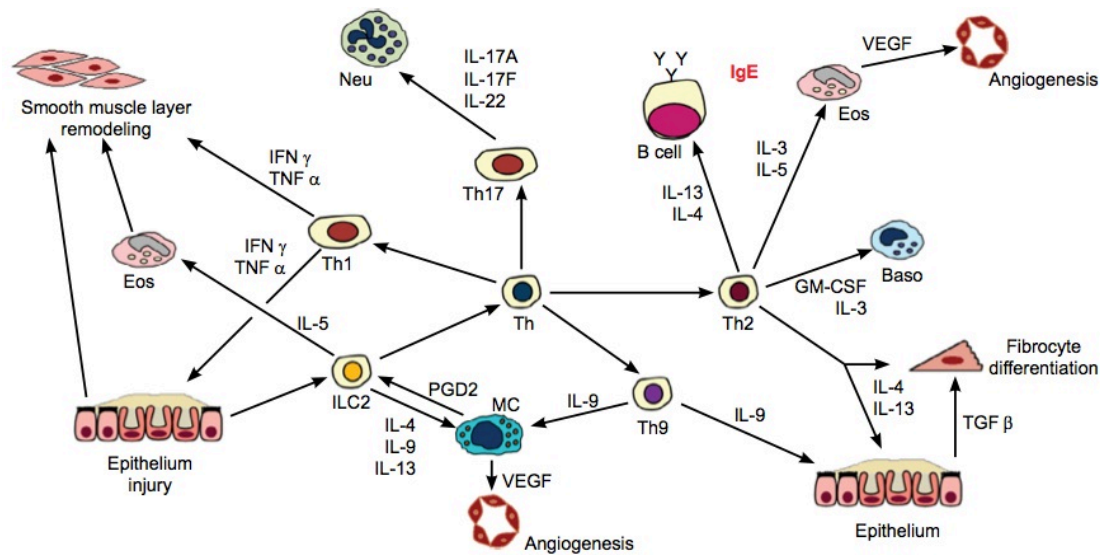


**Figure 1. The complexity of inflammatory reactions involved in allergic asthma orchestrated by T helper lymphocytes.** Abbreviations: Baso: Basophil, Eos: Eosinophil, GM-CSF: Granulocyte macrophage colony-stimulating factor, IFN $\gamma$ : interferon gamma, IgE: Immunoglobulin E, IL: Interleukin, ILC2: Innate lymphoid cell type 2, MC: Mast cell, Neu: Neutrophil, PGD2: Prostaglandin D2, Th: T helper, TGF $\beta$ : Tumor growth factor beta, TNF $\alpha$ : Tumor necrosis factor alpha, VEGF: Vascular endothelial growth factor. Source: Akdis et al 2013 (2).

Without further exposure to allergens, signs of acute disease, such as eosinophilic inflammation, mucus hypersecretion and airway hyperresponsiveness, usually resolve within few weeks (46,47). Mice recovered from acute allergic asthma, however, have inflammatory infiltrates containing memory Th2 cells in the lungs and elevated serum titers of allergen-specific IgG1 and IgE for their lifetime (48). Similarly, lungs of asthmatics contain persistent isolated aggregations of lymphoid cells containing T and B cells (49). Moreover, recent

studies suggest that lungs contain a large number of tissue-resident memory T cells (reviewed in (50)). The mechanisms underlying memory CD4<sup>+</sup> T cell retention in asthmatic lungs are still not fully elucidated and appear to involve CD69 (51) and/or chemokine receptor CCR4 (52).

Allergen re-challenge of recovered mice induces rapid reactivation of resting allergen-specific memory Th2 cells, leading to disease relapse characterized by re-occurrence of airway hyperresponsiveness (AHR), eosinophilic airway and lung inflammation and mucus hypersecretion (48). Clinically, allergic asthmatics have recurrent episodes of asthma attacks associated with allergen exposure (2). Remittent and prolonged exposure to allergens leads to a chronic disease in both experimental animals and humans that is accompanied by healing for which the end result is an altered structure referred to as an airway remodeling (38,53). In addition to other inflammatory features of the disease, changes in the airway wall of asthmatics include epithelial cell shedding, hypertrophy and hyperplasia of airway smooth muscle and increase in mucous glands, causing thickening of airway wall and permanently reducing airway caliber and ultimately leading to permanent decline in lung function (38).

### **1.3. Treatment of allergic asthma and disease severity**

#### *1.3.1. Available treatments for allergic asthma*

Allergen avoidance is one of the first described remedies for allergic asthma, dating from the Moses Maimonides in the Middle Ages (54), that remains an important cornerstone in asthma management in modern medicine (2). Besides allergens, asthmatics should also avoid risk factors for allergy and asthma, such as exposure to tobacco smoke, moisture, air pollution and respiratory virus infections (2). Inhalation of allergens or predisposing factors leads to asthma exacerbation, defined as *“an acute or subacute episodes of progressively worsening shortness of breath, cough, wheezing, and chest tightness, or some combination of these symptoms, characterized by de-*

*creases in expiratory airflow and objective measures of lung function (spirometry and peak flow)” (55). If asthma exacerbations occur regularly, unpredictably or are extremely severe, then disease treatment with long-term medications is necessary. The treatment regimes for asthma are internationally agreed upon and guidelines for the management of the disease have been developed (2,4).*

The only currently available treatment that can change the course of allergic disease and even lead to immune tolerance to allergens is allergy immunotherapy (56). Controlled administration of allergens in form of subcutaneous immunotherapy (SCIT) and/or sublingual immunotherapy (SLIT) leads to desensitization of mast cells and basophils due to suppression of allergen-specific IgE production by induction of IL-10 producing regulatory T cells (57), tolerance of allergen-specific Th2 cells or induction of Th1 immune response to allergen (58). While allergy immunotherapy is treatment of choice for allergic rhinitis, its widespread use for allergic asthma is currently hindered by lack of efficacy in some patients, high costs and long duration of treatment and possible induction of severe side effects (2,56). Development of novel allergen extracts, adjuvants and treatment regimens for allergy immunotherapy might lead to its more spread use in clinics (56).

Mainstream therapy for allergic asthma includes use of two types of drugs: relievers and controllers (2,4). Relievers are drugs used during acute asthma attack (thus on an as-needed basis) to reverse bronchoconstriction and relieve its accompanying symptoms. The main medication of choice are rapid-acting  $\beta_2$ -adrenergic receptor agonists, such as salbutamol, terbutaline, fenoterol and reproterol, while alternatives include anticholinergic bronchodilators, theophylline or systemic glucocorticosteroids (4). In contrast to relievers, controller medications have to be taken daily, long-term (usually lifelong) to keep asthma under control, mainly through their anti-inflammatory effects. The most effective anti-inflammatory controller medication for the treatment of allergic asthma is inhaled glucocorticosteroids (beclomethasone dipropionate, fluticasone propionate, budesonide) that reduce the frequency and severity of exacerbations of asthma, improve lung function and decrease airway hyper-

responsiveness (59-61). Inhaled glucocorticosteroids are usually combined with other medications for full control, including leukotriene modifiers (e.g., cysteinyl-leukotriene 1 (CysLT1) receptor antagonist montelukast or 5-lipoxygenase inhibitor zileuton), long-acting  $\beta_2$ -adrenergic receptor agonists (e.g., formoterol and salmeterol), theophylline and anti-IgE therapy (e.g., omalizumab) (4). However, all alternative controller treatments have weak anti-inflammatory effects compared to inhaled glucocorticosteroids and they may not be useful as monotherapies (4).

The main goal of asthma treatment is to achieve and maintain symptomatic control of the disease. The Global Initiative for Asthma devised a treatment strategy involving 5 steps, as depicted on Figure 2. Each treatment step provides options for increasing efficacy needed to control the disease in majority of patients (62,63).

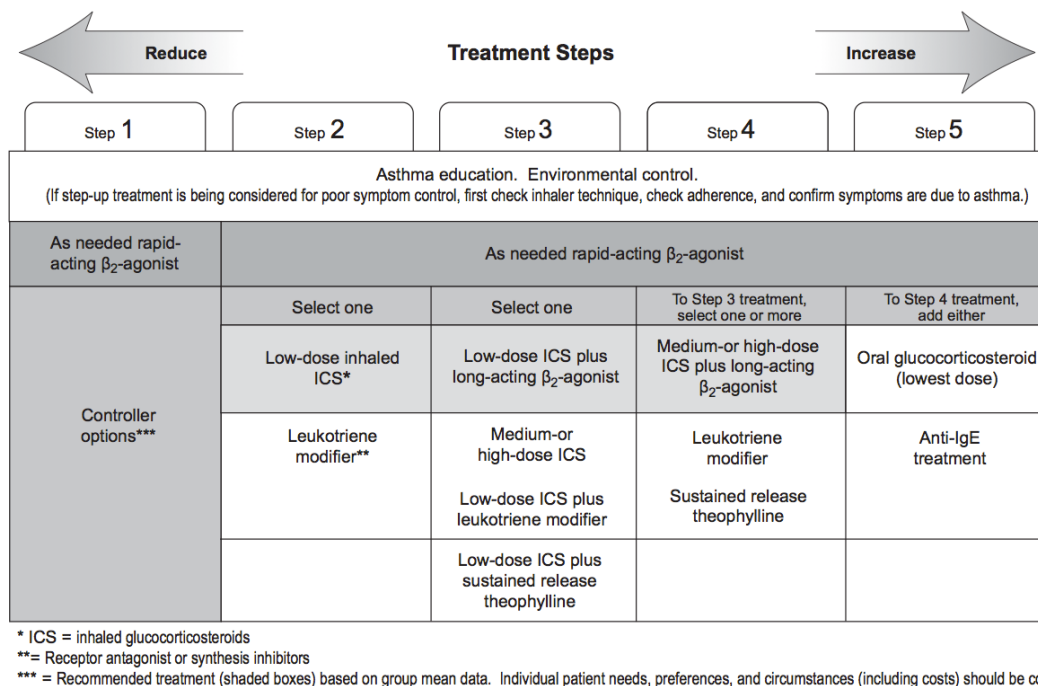


**Figure 2. Treatment strategy for allergic asthma. Abbreviations:  $\beta_2$ -agonist –  $\beta_2$ -adrenergic receptor agonists, ICS – inhaled corticosteroid. Source: Global Initiative for Asthma 2011 (4).**

### 1.3.2. Disease severity and need for novel therapies

While currently available treatments control symptoms in the majority of asthmatics, 5 to 10% of patients suffer from severe asthma that is associated with poor asthma control, increased risk of frequent severe exacerbations and/or chronic symptoms despite intensive treatment (2). The World Health Organization (WHO) defined severe asthma as: *“Uncontrolled asthma which can result in risk of frequent severe exacerbations (or death) and/or adverse reactions to medications and/ or chronic morbidity (including impaired lung function or reduced lung growth in children).”* Severe asthma is classified as (i) untreated; (ii) difficult-to-treat; and (iii) treatment-resistant (64). According to the Global Initiative for Asthma, asthma severity is determined on the basis of the treatment intensity needed to control the disease (4). According to this classification, mild asthma may be controlled with low intensity treatment (e.g., low-dose inhaled glucocorticosteroids or leukotriene modifiers), while severe asthma requires a step 4 treatment with oral glucocorticosteroids or the patient remains uncontrolled despite high intensity treatment (4). Importantly, this classification involves both severity of the underlying disease and responsiveness to treatment (65), both of which should be assessed periodically in the patient (66).

Therefore, the development of novel drugs is crucial for disease control in patients with severe, corticosteroid-resistant asthma. Additionally, existing therapies require fewer side effects. Importantly, none of the current asthma controller therapies cure the disease and symptoms usually remerge within few weeks after treatment is terminated (2,67). Furthermore, better understanding of the allergic asthma heterogeneity, consisting of multiple phenotypes and endotypes, will allow optimizing personalized treatment approaches through active case management (68). It is not surprising, thus, that many key molecules and cellular responses defined in basic research are being explored as new targets for testing in the clinics. For example, several novel treatments targeting crucial inflammatory mediators, such as the anti-IL-5 monoclonal antibody, Mepolizuman (69), Dupilumab, the anti-IL-4Ralpha monoclonal antibody that blocks the common receptor for IL-4 and IL-13 (70) and AMG157,

anti-TSLP antibody (71), have significantly reduced asthma exacerbations in clinical trials.

#### 1.4. Asthma biomarkers

In medicine, biomarker, or “biological marker”, refers to “*a broad subcategory of medical signs – that is, objective indications of medical state observed from outside the patient – which can be measured accurately and reproducibly*” (72). More precisely, the National Institutes of Health Biomarkers Definitions Working Group defined a biomarker as “*a characteristic that is objectively measured and evaluated as an indicator of normal biological processes, pathogenic processes, or pharmacologic responses to a therapeutic intervention.*” (72). A validated biomarker should represent underlying pathological mechanisms of the disease and thus enable diagnosis, indicate treatment responsiveness or allow monitoring of the disease control. The biomarker examples range from blood pressure and pulse, through basic laboratory tests such as leukocyte number in blood to sophisticated laboratory tests, such as measurement of human epidermal growth factor receptor-2 (HER2) expression to predict breast cancer treatment response (73).

Asthma diagnosis and management is based on reported asthma symptoms in combination with lung function tests measuring reversible airway hyperresponsiveness and obstruction. Although these biomarkers provide information on the extent of airflow limitation, they do not monitor the airway and lung inflammation, a central feature of allergic asthma (74-76). Management plan for asthmatic patients should, therefore, include monitoring of airway and/or lung inflammation (74-76).

Bronchoscopy with bronchoalveolar lavage and bronchial biopsy are the gold standards for assessment of extent and type of airway and lung inflammation, respectively (77). However, these invasive techniques are not suitable for routine diagnosis, especially in children (78). Therefore, multiple novel less-invasive biomarkers are being extensively validated for clinical use in asthma

(Figure 3) (68,77,79,80). Among those, sputum induction allows less invasive assessment of airway inflammation and sputum eosinophil counts have been used as biomarkers of airway inflammation and therapy success (81). Despite promising results, the wide use of this biomarker in clinics is disputed due to number of technical limitations and questionable reproducibility (77,79,82).

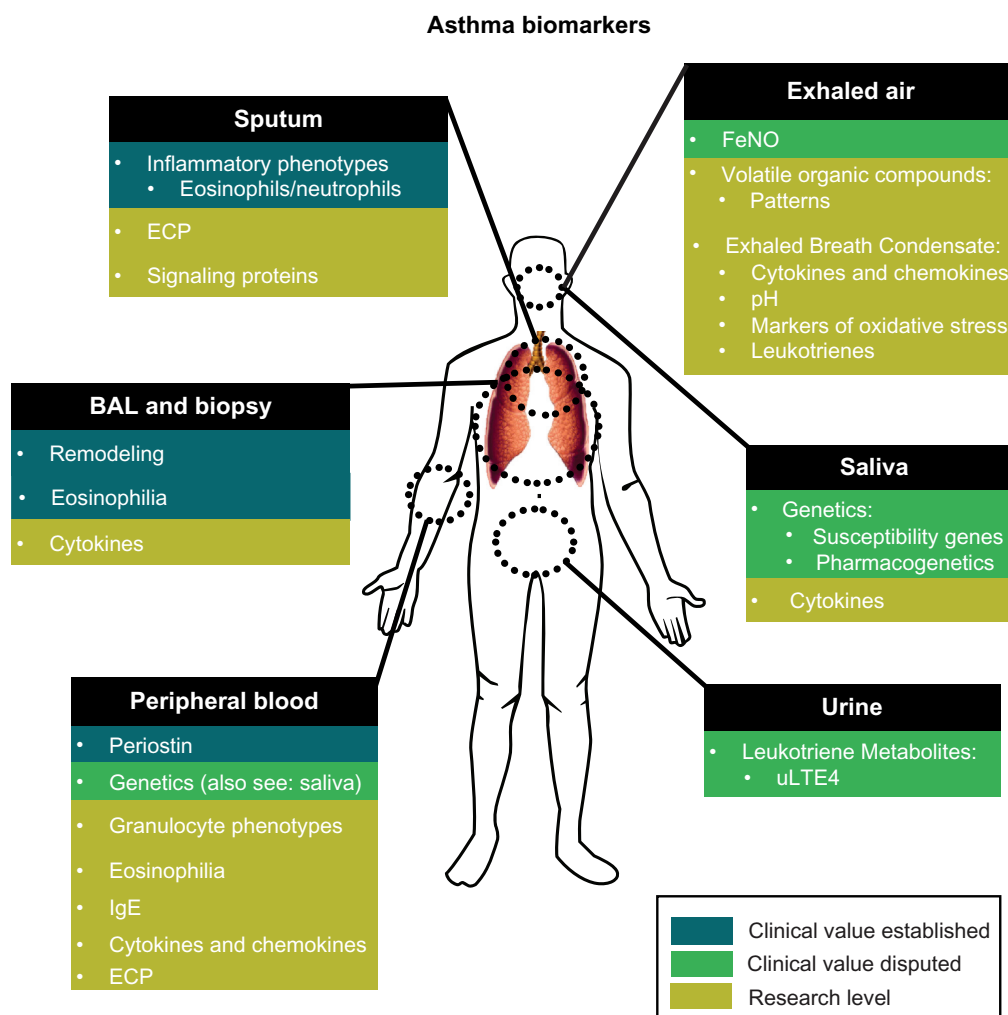


**Figure 3. Overview of asthma biomarkers used in clinical practice or currently under research.** Abbreviations: BAL, bronchoalveolar lavage; ECP, eosinophil cationic protein; FeNO, fraction of exhaled nitric oxide; IgE, immunoglobulin E; uLTE4, urinary leukotriene E4. Source: Vijverberg et al 2013 (79).

In contrast to sputum collection, more technically feasible biomarker for routine clinical use is measurement of fractional exhaled nitric oxide concentration (FeNO). Initial finding that FeNO is increased in asthmatics compared to healthy controls dates from 1994 (83), and until now its use in asthma management and diagnosis has been extensively studied. However, many factors, such as age, atopy, medication use, therapy adherence or airway infections, influence FeNO levels and preclude its acceptance as a validated biomarker for asthma inflammation (77,79).

Besides sputum induction and FeNO, other asthma biomarkers that are currently being developed include peripheral blood eosinophilia, the measurement of volatile organic compounds in exhaled breath or metabolites in urine and asthma imaging (77,79,80). In addition, unbiased high-throughput screening approaches, including genomics, transcriptomics and proteomics, are powerful techniques that allow biomarker discovery and validation (68,79). Studies using these techniques identified potential endotypes in asthma (18,84), evaluated effects of corticosteroid treatment (85) and identified genes and proteins that could serve as potential novel molecular biomarkers for asthma (17,86,87).

Altogether, combining several biomarkers could provide a more comprehensive approach to monitor the disease than any single biomarker alone (68,79). Recently, George et al. combined clinical biomarker data (including numbers of circulating white blood cells and cardiopulmonary measures) with gene expression analysis from blood to define 3 asthma endotypes (17). In another study, a non-invasive panel of inflammatory biomarkers (*ie*, FeNO, sputum eosinophil count and urinary bromotyrosine level) had better power to predict steroid responsiveness in asthmatics than each of the biomarkers alone (81). Furthermore, transcriptomic approaches provide a great potential for defining divergent asthma phenotypes and endotypes that could ultimately lead to personalized therapy (68,79,88). However, those approaches should be further investigated and eventually incorporated into clinical routine.

### 1.5. Animal models of allergic asthma

Current understanding of the pathophysiology of allergic asthma and development of novel therapies would be difficult without experimental animal models. There are numerous models of asthma in many different species, including mice, rats, sheep and monkeys (reviewed in (53)). While each animal model has advantages and disadvantages compared to human disease, mice are most widely used, primarily because of the availability of numerous immunological reagents, technologies involving gene manipulation and well-characterized inbred strains that allow for the assessment of function of specific factors and cells (53).

There are no standardized experimental protocols for the induction of allergic asthma in mice (39,53,89,90). However, most models use a two step approach that involves initial intraperitoneal sensitization with allergen and the second step is allergen exposure to the respiratory tract with the same allergen administered either in the trachea or nose or in an aerosol. The resulting response depends on the choice of allergen, the inbred mouse strain, the use of adjuvant (e.g., aluminum hydroxide) and the treatment schedule (39,53,89,90). Most models induce elevated levels of allergen-specific IgG1 and IgE, airway and lung allergic inflammation, mucus hypersecretion and airway hyperresponsiveness (53,89-91). These models induce a Th2-mediated late phase response and are successfully used to investigate inflammatory mechanisms and interplay of cells and mediators in asthmatic lungs (53,89,90). However, they do not address all aspects of human disease, including a natural sensitization to airborne allergens that occurs in asthmatics or chronic inflammation of airway wall and airway remodeling (53,89,90).

To mimic exposure of airborne allergens involves airway administration of allergen alone over several days or weeks without adjuvants (53,92). These models also induce acute asthma and allow for the investigation of the mechanisms underlying allergen sensitization via the respiratory mucosa.

To model structural/remodeling changes in the airways of asthmatics, including subepithelial fibrosis, smooth muscle thickening and increased vascularity, various protocols use an increased number of allergen exposures over many weeks (53,92). In this type of model, inflammation peaks after 2-3 weeks of exposure, while airway hyperresponsiveness and remodeling appear after 5 weeks and remain elevated for up to 9 weeks after cessation of allergen exposure (93,94).

To imitate seasonal allergic asthma, in which allergen exposure is intermittent and recurrent, mice are left to recover from acute exposure to allergen and rechallenged again with the same allergen at later time (48,53). A single secondary allergen challenge induces a robust reappearance of all disease signs (including airway and lung inflammation, airway hyperresponsiveness and mucus hypersecretion). Mice recovered from acute allergic asthma retain local (in the lungs) and systemic (in spleen) Th2 memory that it maintained for their lifetime (48). This model closely resembles patients with intermittent or seasonal asthma and allows for the investigation of Th2 immunological memory.

In summary, none of animal models can be considered perfect surrogates for human asthma, but they should be considered as models of different disease stages and/or phenotypes. Mice as a model species have several advantages over other small animals (such as detailed knowledge on the genome, availability of different reagents and techniques to generate genetically engineered animals), but also several limitations (including differences in lung structure and lack of persistent airway hyperresponsiveness) that should be taken into account when translating results from experimental research to clinical practice. Nevertheless, mouse models of allergic asthma provide an important opportunity to investigate the pathophysiology of asthma and test novel therapies in well-controlled system.

## 1.6. Allergic asthma imaging

The majority of experimental or clinical allergic asthma studies use end-point analysis of surgical or autopsy samples that preclude the possibility of repeated, longitudinal examination of disease progress. Technical progress over the last decade has led to the development of novel imaging techniques which allow non-invasive, longitudinal monitoring of dynamic pathological mechanisms involved in allergic asthma *in vivo* (95). Moreover, advances in imaging of lung of patients with asthma allows for the assessment of airway anatomy and regional lung function to further understand the differences between asthma phenotypes (96). Medical imaging techniques can be divided into 2 major categories: anatomical and functional modalities. Anatomical modalities mainly emphasize tissue structure, and include X-ray, computed tomography (CT), magnetic resonance imaging (MRI) and ultrasound. Functional modalities primarily provide information on (patho)physiological activities within the certain tissue and include single photon emission computed tomography (SPECT), positron emission tomography (PET) and fluorescence imaging. As functional modalities have limited spatial resolution and anatomical modalities provide limited information on lung function, several modalities can be combined to co-register functional information with anatomical structures.

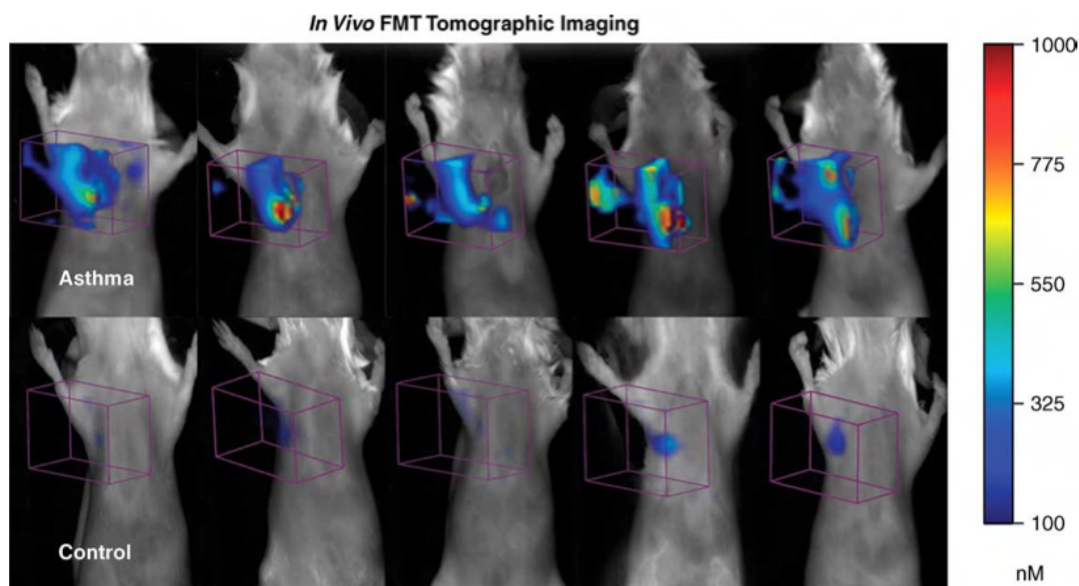
Computed tomography (CT) images constitutional contrast between air and surrounding lung tissue that allows assessment of airway wall thickness and airway obstruction. However, CT lacks spatial resolution and has to be combined with X-ray to provide anatomical evaluation of the bronchial tree and lung parenchyma. Ct was, either alone or in combination with inhalable contrast agent, successfully used in preclinical animal models to visualize airway inflammation and remodeling (97,98), as well as in clinical studies to determine lung density as a measure of airflow limitation, airway wall thickening and evaluation of therapies in long-term treatment trials (reviewed in (96)). The major drawback of this technique is exposure to high doses of radiation and long scanning times that are needed to achieve high image resolution (<0.05  $\mu\text{m}$ ) (95).

In contrast to CT, magnetic resonance imaging (MRI) is radiation free, which makes this method specially suited for longitudinal studies. Difficulties in MRI lung imaging due to low physical and proton density of the organ can be overcome with the use of safe hyperpolarized gases, such as helium-3 ( $^3\text{He}$ ). Hyperpolarized gas lung MRI imaging allows detection of ventilation defects before or after use of bronchoconstricting agents (e.g., methacholine) that can be related to asthma severity (99,100). The use of MRI for imaging asthma, however, is limited with low spatial resolution of this technique and the availability and cost of relatively short-lived hyperpolarized gases (96,101). Nevertheless, MRI was successfully used recently to quantify pulmonary inflammation induced by segmental allergen challenge (102).

In contrast to anatomical, functional imaging modalities directly or indirectly monitor cellular or molecular processes in the tissue. Most of these techniques are still under development for allergic asthma and their use is mostly limited to preclinical animal models (96). Positron emission tomography (PET) can detect tiny amounts of radioactively labeled compounds in body tissues, which was used to monitor ventilation in sheep (103) or airway inflammation in rats (104). PET in combination with radioactive-labeled fluorodeoxyglucose was used in two clinical studies on asthmatics to quantify inflammatory response with limited success (105,106). The use of radioactive markers and its low spatial resolution of about  $1\text{ cm}^3$ , however, precludes the use of PET in small animals and restricts its applicability in humans (95).

Another functional modality that provides a tool for noninvasive repeated examinations of cellular and subcellular activities in an unperturbed environment is *in vivo* fluorescence imaging (Figure 2). Fluorescent dyes that allow tracking of biological processes can be coupled directly to antibodies (107) and small molecules (108), expressed by cells (109), or generated directly in the tissue by administration enzyme-targeted probes that become fluorescent when activated by different enzymes, such as cathepsins (110) or matrix metalloproteinases (111). The fluorescent signal can be detected by intravital microscopy using fiberoptic bronchoscopy (111), 3D fluorescence molecular tomography (110) and time-domain optical imaging systems (112). Fluores-

cence imaging allows insight in early pathological processes in experimental models of asthma that cannot be accessed using other imaging methods, while its applicability in humans is still limited by the safety and specificity of fluorescent probes (95). Therefore, there is current need for development of novel specific and safe fluorescent probes that can be used in different areas of asthma research and diagnosis.



*Drug Discovery Today: Disease Models*

**Figure 4. Imaging of allergic airway inflammation with a fluorescence imaging.** Mice with acute allergic asthma show a consistent lung fluorescence 24 hours after administration of a near-infrared fluorescent probe activated by cathepsin (ProSense 680), while control mice show minimal signal in the lungs. Signals were detected using VisEn FMT 2500 in vivo imaging system. Source: Jannasch et al 2009 (95).

Altogether, each imaging modality has a unique combination of strengths and weaknesses that are summarized in Table 2. The choice of imaging method depends on the aspects of particular study. In clinics, quantitative CT and hyperpolarized gas MRI allow investigation of structural differences present in the lungs of asthmatics (96). In preclinical research, on the other hand, fluorescence imaging allows insights in inflammatory processes that cannot be assessed using other methods (95). For a detailed understanding of asthma

pathophysiology, the optimal approach would consist of a combination of different techniques that allows for simultaneous detection of structural and functional information.

**Table 2. Summary table comparing different imaging techniques for allergic asthma. Source: Jannasch et al 2009 (95).**

	<b>CT</b>	<b>PET/SPECT</b>	<b>MRI</b>	<b>Fluorescence imaging</b>
<b>Pros</b>	No limit in depth High spatial resolution	No limit in depth	No radiation No limit in depth High spatial resolution	No radiation High sensitivity
<b>Cons</b>	Radiation	Low spatial resolution Radiation	Low sensitivity Long scanning times	Limited depth Low spatial resolution
<b>Best use</b>	Morphological imaging	In combination with CT Translational research	Morphological and functional imaging	Functional imaging

## 2. AIMS OF THE THESIS

The main aim of this thesis was to detect genomic biomarkers, to develop novel optical imaging techniques and to establish novel treatment modalities for allergic asthma. Detailed molecular genetic characterization of pathophysiological responses involved in allergic asthma and development of novel imaging technologies to monitor disease progression *in vivo* will provide opportunities for new treatments. There is one manuscript and 2 published papers reported in this thesis.

In the manuscript, we show the results of a meta-analysis of 6 publically available gene expression experiments from *in vivo* mouse allergic asthma models. We created an acute asthma signature gene list consisting of 933 genes of which 493 are unrelated to asthma and constitute an “acute allergic asthma ignorome” in mice. Asthma-annotated and ignorome genes were confirmed in an independent mouse model, thus verifying the generalizability of these genes expressed in multiple experimental protocols. We ascertained through functional and network connectivity analyses that asthma-annotated and -ignorome genes clustered into 4 biologically relevant domains. Within these networks, we discovered 12 super-connectors genes that link the complex pathophysiological mechanisms underlying asthma and are normalized upon treatment with glucocorticosteroids in an independent mouse model of allergic asthma and have a strong disease phenotype. Overall, our powerful bioinformatic analyses prioritized asthma-related and -ignorome genes within the clusters and biological domains to provide important insights in asthma pathophysiology.

The published paper 1 describes a non-invasive *in vivo* imaging approach to visualize allergic inflammation in an experimental mouse model of allergic asthma. We used dendritic polyglycerol sulfates, which bind to selectins and complement factors, labeled with near infrared fluorescence dye (dPGS-NIRF) in combination with time-domain optical imager. The dye accumulated in the lungs of mice with allergic inflammation that resulted in greater fluores-

cence intensity in the thoracic area of asthmatic in comparison to healthy mice, representing a novel approach to monitor lung inflammation.

In published paper 2, we investigated the effects of tiotropium bromide, a selective long-acting muscarinic receptor antagonist, in mouse model of allergic asthma relapse. Tiotropium bromide is used for the treatment of chronic obstructive pulmonary disease, but is currently not approved for use in asthma and pre-clinical and clinical studies have to demonstrate its efficacy in this disease. We showed that tiotropium bromide efficiently suppresses airway hyperreactivity, mucus hypersecretion and airway inflammation in experimental allergic asthma. These data highlight the anti-inflammatory properties of tiotropium bromide and support its use for the treatment of asthma.

### 3. PUBLICATIONS

#### 3.1. Manuscript

##### **Revealing the acute asthma ignorome: characterization and validation of uninvestigated gene networks**

Michela Riba<sup>1\*</sup>, Jose Manuel Garcia Manteiga<sup>1\*</sup>, Berislav Bosnjak<sup>2\*</sup>, Davide Cittaro<sup>1</sup>, Pavol Mikolka<sup>2,3</sup>, Connie Le<sup>2,4</sup>, Michelle M. Epstein<sup>2§</sup> and Elia Stupka<sup>1§</sup>

<sup>1</sup>Center for Translational Genomics and Bioinformatics, San Raffaele Scientific Institute, Milan, Italy

<sup>2</sup>Experimental Allergy Lab, Department of Dermatology, DIAID, Medical University of Vienna, Austria

<sup>3</sup>Current address: Comenius University in Bratislava, Institute of Physiology (Jessenius Faculty of Medicine), Slovakia

<sup>4</sup>Current address: The University of Alberta, Faculty of Medicine, Edmonton, Alberta, Canada

\* These authors made equal contributions.

§ These authors made equal contributions.

***Submitted to: American Journal of Respiratory and Critical Care Medicine***

Revealing the acute asthma ignorome: characterization and validation of uninvestigated gene networks

Michela Riba<sup>1\*</sup>, Jose Manuel Garcia Manteiga<sup>1\*</sup>, Berislav Bosnjak<sup>2\*</sup>, Davide Cittaro<sup>1</sup>, Pavol Mikolka<sup>2,3</sup>, Connie Le<sup>2,4</sup>, Michelle M. Epstein<sup>2§</sup> and Elia Stupka<sup>1§</sup>

<sup>1</sup>Center for Translational Genomics and Bioinformatics, San Raffaele Scientific Institute, Milan, Italy

<sup>2</sup>Experimental Allergy Lab, Department of Dermatology, DIAID, Medical University of Vienna, Austria

<sup>3</sup>Current address: Comenius University in Bratislava, Jessenius Faculty of Medicine, Department of Physiology and Biomedical Centre, Martin,

<sup>4</sup>Current address: The University of Alberta, Faculty of Medicine, Edmonton, Alberta, Canada

\* These authors made equal contributions.

§ These authors made equal contributions.

Corresponding author:

Berislav Bosnjak, MSc, Experimental Allergy Lab, Department of Dermatology, DIAID, Medical University of Vienna, Währinger Gürtel 18-20, 1090 Vienna, Austria; phone: +43 1 40 160 63013; fax: +43 1 40 160 963012; e-mail: berislav.bosnjak@meduniwin.ac.at

Author contributions:

*M.R. performed multi-dataset bioinformatics analysis, network analysis and contributed to manuscript preparation; J.M.G.M. performed multi-dataset bioinformatics, network analysis and contributed to manuscript preparation; B.B. designed and performed in vivo experiments, analyzed the samples and contributed to manuscript preparation; D.C. performed and supervised computational analysis; P.M. contributed to in vivo experiments and sample analyses; C.L. participated in quantitative PCR analyses; M.M.E. designed in vivo experiments, contributed to manuscript preparation; E.S. designed and supervised*

*computational analysis, contributed to manuscript preparation. All authors read and approved final version of the manuscript.*

Sources of support: *This study was partially supported by the European Commission through an FP7- IAPP Marie Curie Action, P3AGI project (GA 230739).*

Running title: Microarray analysis reveals asthma ignorome

Descriptor number that best classifies the subject of your manuscript: 1.10  
*Asthma Mediators*

Total word count: 3336

*At a Glance Commentary: A novel multi-dataset bioinformatics strategy enabled us to unambiguously define acute asthma signature genes. A literature search indicated that 53% of those genes belong to the “acute asthma ignorome”, which are defined as genes without previous publications related to allergic asthma. An experimental validation and functional annotation of these genes indicates novel areas of biology to be pursued further and provides a novel perspective for future basic and translational asthma research.*

This article has an online data supplement, which is accessible from this issue's table of content online at [www.atsjournals.org](http://www.atsjournals.org)

**Abstract**

Rationale: Although multiple pathways involved in allergic asthma are known, work in other disease areas indicates that there is still a vast “ignorome” to be discovered, and that this can shed new insights on disease pathogenesis.

Objectives: Integrating systems biology and experimental validation to identify and validate novel asthma gene networks.

Methods: A systems biology approach on existing data provided a gene signature, evaluated by network analysis and literature mining and validated in a mouse model, with and without steroid treatment.

Measurements and Main results: We generated a signature of 933 genes and experimentally validated their deregulation in our experiment (Pearson  $r=0.86-0.88$ ). The genes grouped into 7 clusters and 4 biological domains related to inflammation, lung-specific insult response, stem cell proliferation and circadian rhythm. Literature mining showed that 13 genes account for over one third of asthma publications, and 50% of the genes are novel, making up the “acute asthma ignorome”. Two domains containing the highest proportion of ignorome genes were related to cell proliferation in CD34<sup>+</sup>, CD71<sup>+</sup>, CD105<sup>+</sup> cells and circadian rhythm. Network topology identified 1) novel hubs (e.g. IGSF6, PLEK, SLC15A3, and GSTA3) and 2) super-connector genes with robust small expression changes that linked multiple biological domains. Systemic treatment with dexamethasone targeted the super-connector, glucocorticoid receptor, *NR3C1*, reverted the majority of the inflammation-related, and partially reverted lung-specific insult response super-connectors.

Conclusions: Our approach characterizes and validates gene networks underlying acute asthma, shedding light on the asthma ignorome and key gene networks not yet investigated in the disease.

Abstract word count: 249

Key words: acute allergic asthma, ignorome, multi-dataset bioinformatics analysis, systems biology, microarray

## Introduction

Allergen exposure causes a complex interaction of cellular and molecular networks leading to allergic asthma in susceptible individuals. Experimental mouse models of allergic asthma are widely used to understand disease pathogenesis and elucidate mechanisms underlying the initiation of allergic asthma (1). For example, gene profiling of lung tissue from experimental mice during the initiation of allergic asthma in experiments with different protocols (2-7) validated well-known genes and identified new genes with roles in disease pathogenesis such as *C5* (3), *ARG1* (8), *ADAM8* (9), and *PON1* (7), and dissected pathways activated by *IL13* (10) and *STAT6* (11). Despite these datasets revealing large numbers of genes expressed in lungs during the onset of allergic asthma, there is a skewed distribution of research and literature coverage on a small number of genes, as has been noted in other fields (12-14).

To fully understand the genes and pathways in the lung that are involved in the initiation of allergic asthma, we reviewed all 23 published gene expression experiments performed on lungs from mice with allergic asthma to select those of sufficient robustness to be utilized for a multi-dataset bioinformatics analysis. We focused on 6 studies that share a common microarray platform, have a robust disease phenotype and were derived from experiments using different mouse strains and experimental protocols (2-7). We used a novel bioinformatics strategy combining gene-centric and pathway-centric approaches (see methods) to generate a stringent asthma signature list. This list included a large set of protein-coding genes that had no published function or literature connecting them to allergic asthma either at the level of the whole organism or for individual organs, tissues or cells, genes for which the term “ignorome” was recently coined (15). Here, we present a gene signature list from mice consisting of 933 genes with 440 asthma-annotated and 493 “acute allergic asthma ignorome” genes.

## Materials and methods

### *Data selection*

From the 23 experiments identified in the literature, we selected 6 datasets based on studies using the Affymetrix Mouse Genome 430 2.0 or Murine Genome U74 Version 2 Arrays microarray platform and mouse models of ovalbumin (OVA) and house dust mite induced acute asthma characterized by airway eosinophilia, airway hyperresponsiveness (AHR) and mucus hypersecretion. Within these independent datasets, we extracted in total 10 comparisons of asthmatic vs. control samples (see Table 1).

### *Multi-dataset bioinformatics analysis for selection of acute asthma signature list*

We retrieved raw data from the GEO database (16) and analyzed them using a common pipeline for signal normalization and extraction of differentially expressed genes (see supplementary methods and Figure 1). We extracted differentially regulated genes for each experiment, which were then utilized for our multi-dataset bioinformatics analysis combining two approaches: a top-down, biological process enrichment-driven approach, from now on called 'pathway-driven', and a bottom-up, 'gene-driven' approach (see supplementary methods). The two approaches were merged to generate a final union list.

### *Gene annotation for acute asthma ignorome detection and its functional annotation*

To assess the extent of the acute asthma ignorome, we performed an unambiguous literature search based on Entrez Gene and PubMed databases (see online supplementary methods). To annotate the genes from the acute asthma signature list (including the asthma ignorome), we compiled a list of human orthologs, mapped it to the STRING interaction network, and performed a topological analysis for clusters of densely connected genes ( $n \geq 5$ ; details in supplementary methods). For each cluster, we identified three sets of genes: (i) hub genes (the top 10% of the genes in the list ranked by betweenness centrality, defined as the ratio of shortest paths passing through a node, being a common measure of centrality of a node parameter in descending order); (ii) peripheral genes (1-degree nodes connected to a clique, *i.e.* a

set of nodes completely connected to each other); and (iii) super-connectors (genes connecting more than 5 clusters). Each cluster was then further characterized in terms of functional enrichment, tissue specific expression and literature representation (see supplementary methods).

### *Biological validation experiments*

We used 8-10 week old female BALB/c mice (Charles River, Sulzfeld, Germany). All experimental protocols complied with the requirements of the Animal Care Committee of the Austrian Ministry of Science. All mice were immunized with OVA (Sigma Chemical Co., St. Louis, MO) dissolved in PBS intraperitoneally on days 0 and 21 and intranasally on day 32 with OVA or PBS. In treatment experiments, we administered vehicle or dexamethasone (Sigma) intraperitoneally at 1mg/kg 30min before and 24 and 48h after challenge. Details on animal treatment and measurements of airway hyperresponsiveness, airway and lung inflammation, mucus hypersecretion and serum OVA-specific antibody titers are reported in supplementary methods. Separate groups of mice were used for lung mRNA extraction at 24 or 72h after intranasal challenge with PBS or OVA. Methods for RNA extraction, reverse-transcription, quantitative polymerase chain reaction and statistical analysis are also reported in supplementary information.

## **Results**

### *Acute allergic asthma gene signature list*

To select the datasets for analysis, we analyzed 23 microarray studies of lung RNA from mice at the initiation of allergic asthma [(16), GEO database (<http://www.ncbi.nlm.nih.gov/geo/>)]. Our selection criteria included the phenotype elicited and data robustness (see methods). Six microarray datasets [(2, 10, 17, 18), GSE1301 and GSE3184] from 5 different mouse strains, 2 allergens, 6 experimental protocols were subdivided into 10 comparisons of control vs. asthmatic mice (A-J) (Table 1 and Figure 1).

To create an acute asthma signature list from these 6 microarray datasets, we used a multi-dataset bioinformatics analysis strategy including a pathway-

driven and gene-driven approach (see methods and online supplementary methods; Figure 1) to ensure that both enriched pathways as well as robust genes not annotated to pathways were maintained in the final signature (see methods). The pathway-enrichment-driven approach yielded 493 genes, the gene-driven approach 602 genes, giving a final acute asthma signature list of 933 genes.

We validated the robustness of the signature by measuring 59 genes through qPCR in an independent experimental model of allergic asthma (Supplementary figure E1). Despite the difference in experimental setup and technology platform, we observed a significant positive correlation of 0.8660 and 0.8819 (both  $p < 0.00001$ ) between the two datasets at 24 h and 72h post-challenge, respectively (Figure 2, Supplementary figure E2). These data indicate that stringent and multi-dataset bioinformatics analysis across independent experiments can yield robust gene signatures, which are found to be applicable regardless of experimental context and are representative of general features of the disease.

#### *Allergic asthma ignorome*

To determine the already known association of the 933 genes with allergic asthma, we enumerated publications associated with asthma, as well as asthma annotation in other sources (CTD and Malacards, see supplementary methods). Figure 3A illustrates the number of genes associated with asthma using these methods. There is an inverse correlation between these data sources and the number of genes, i.e. a large number of publications are associated with relatively few genes: 13 genes (*Ccl11*, *Ccl5*, *Cd14*, *Cysltr1*, *Gstm1*, *Ifng*, *Il10*, *Il13*, *Il33*, *Il4*, *Il4ra*, *Tlr2*, and *Tlr4*) account for approximately 1/3 of the articles published on asthma for these 933 genes (Figure 3). In our dataset, there are 493 genes (Figure 3B) that are as yet unrelated to asthma and belong to the acute allergic asthma “ignorome”. These data, combined with the robustness of the gene signature shown above, substantiate that the scientific community has so far focused only on a small subset of genes which are likely to play a role in asthma and that there is a substantial set of genes which warrant further investigation.

### *Network connectivity analysis*

To define the allergic asthma gene network, we analyzed the connections of 897 human orthologs from 933 acute asthma mouse genes (see methods). We detected a network of 779 densely connected genes in which there are 7 topological clusters containing 763 genes (Figure 4A), whereas 118 genes were outside of the network (Supplementary Table E2). In the 7 topological clusters, 409 genes are associated with asthma publications (Figure 4B) and 645 are related to “inflammation or immunity” (Figure 4C) in at least one relevant publication.

The 7 topological clusters were annotated for functional enrichments (see methods) (Table 2, Supplementary figures E3-E7). The clusters fall into 4 major biological domains, of which two are well studied, and two novel: 1) inflammation, including clusters 1A-B: cytokine-cytokine receptor signaling, leucocyte endothelial migration (353 genes, 66.86% published in asthma) 2) circadian rhythm, cluster 2, including genes expressed in the lung as well as CD4<sup>+</sup>, CD8<sup>+</sup>, CD56<sup>+</sup> and CD71<sup>+</sup> cells (15 genes, 86.7% as yet unpublished in asthma), 3) lung-specific insult response including clusters 3A-C: extracellular matrix remodeling, adherens and tight junctions, and mucus secretion (309 genes, of which 48.5% are published in connection to asthma), and 4) stem cell proliferation in CD34<sup>+</sup>, CD71<sup>+</sup>, CD105<sup>+</sup> cells (82 genes, of which 85.4% unpublished in asthma) (Table 2, Figure 4A).

Investigating, in greater depth, the connectivity between the genes contained in these domains (see supplemental methods) enabled the characterization of the connectivity hierarchy amongst them (Figure 5). As expected, clusters belonging to the inflammation domain have the strongest connectivity between themselves, as well as lung to inflammation domains. Interestingly, the genes within the 2 novel domains identified (stem cell proliferation and circadian rhythm) are strongly connected to a specific cluster within the lung-specific insult response, *i.e.* extracellular matrix remodeling. The same domains are also interconnected by a single gene, *RORα* that belongs to the circadian rhythm domain and couples the stem cell proliferation and the

extracellular matrix remodeling cluster in the lung-specific insult response domain (Figure 5).

When these novel clusters are annotated for publications in inflammation or immunity, they reveal a substantially larger body of literature (73.3% of circadian rhythm genes and 56.1% of the stem cell genes are associated), indicating that their role in the broader field of immunology is already being investigated, although not yet associated specifically to asthma.

The reliability of the identified functional gene clusters is corroborated by manual inspection of well established key genes in asthma, e.g. the inflammation cluster contains lung allergic immune response genes (e.g. cluster 1A: *Il4*, *Il4r*, *Il13*, *Il33*, *CCL11*, *CCL17* and *CCL22*; and cluster 1B: *Cysltr1*, *Alox5ap*, *Arg1*, *Adam8* and *Fcer1g*), the lung-specific insult response clusters with known extracellular matrix remodeling, tight junctions, and mucus production genes (e.g. *Gstm1*, *Vegfa*, *Chi3l1*, *Pcna*, in cluster 3B, e.g. *Pard3*, *Prkci*, and in cluster 3C, e.g. *muc4*, *muc5B* and *muc5AC*). In contrast, stem cell proliferation clusters contain genes that are essential for DNA replication and cell proliferation, which were not previously attributed to asthma. Enrichment analysis indicated that these genes are expressed mainly in cells that mediate leukocyte proliferation [CD34<sup>+</sup> and CD71<sup>+</sup> cells; (19-21)] and tissue regeneration [CD105<sup>+</sup> cells; (22)] in allergic asthma. Cluster 2 contains well-known circadian rhythm genes e.g. *NR1D1* [or *Rev-Erba*], *NR1D2*, *PER2*, *PER3*. Most of them have not been related to asthma yet, but growing evidence suggests they play a role in the immune system (23, 24). This evidence suggests that our approach is able to identify valid functional clusters within the overall acute asthma gene signature and to identify genes that are less explored in the context of asthma.

We utilized the network connectivity information to prioritize specific genes that are likely to play an important role in the above domains. We concentrated on two categories of genes: hub genes, i.e. genes that are central, given the network structure and peripheral genes, i.e. genes which, despite not having a large number of connections themselves, are connected to a set of genes having full mutual interplay (*cliques*, see methods). The assumption

is that hub genes play an important role in the overall network, while peripheral genes have reciprocal influence on specific *cliques*. This approach led to the identification of 34 hub genes and 8 peripheral genes in the inflammation domain, and 29 hub genes and 11 peripheral genes in the lung-specific insult response domain. The majority of the peripheral genes (14/22) have not yet been associated with asthma, but most of them have been associated with inflammation (17/22). In contrast, only 11/61 hub genes have not been associated with asthma, and 4/61 have not been associated with inflammation. Interestingly, some well-studied genes are hubs, e.g. as *IFNG*, *TLR4* and *PTPRC*, but several others are not, e.g. *IL13*, *IL4* and *IL4R*. The ignosome hubs and peripheral genes are summarized in Table 3. They include *IGSF6* and *SLC15A3*, which are expressed on antigen presenting cells and involved in antigen recognition (25, 26), as well as the peripheral gene *CLEC5A* (also known as *MDL-1*), which is involved in the innate immune response to microorganisms (27-29). Within the lung-specific insult response domain, a hub gene *TGFBI* and a peripheral gene *BAMBI* belong to the *TGF $\beta$*  signaling pathway, important for lung remodeling (30).

#### *Super-connector genes link functional domains*

We then searched for “super-connectors”, *i.e.* genes that link at least 5 clusters, and thus, identified 12 genes (Figure 6). There are 9 super-connectors in the inflammation domain that are cytokines *IL6* and *IL1 $\beta$* , cell surface receptors *CD4* and *CD44*, signaling molecules *STAT1*, *TRAF6* and *RELA*, as well as *CADM1*, a receptor that mediates mast cell adhesion to lung structural cells (31) and the glucocorticoid receptor *NR3C1*. The other 3 of 12 molecules belong to cluster 3 (extracellular matrix remodeling) and include *PRKCD*, a protein kinase that plays an important role in tissue remodeling (32), an anti-hemophilic factor *VWF* with multiple pro-inflammatory roles (33) and *ERBB2*, an orphan tyrosine kinase that plays an important role in cancer (34)).

The super-connector fold change fluctuated considerably, albeit in limited ranges, as indicated by the median fold changes that ranged from -0.01 and 0.32 within each microarray comparison (Figure 7). This finding is consistent with a previous analysis (35), indicating that genes with high connectivity have

minimal fold change in gene expression. Despite this, we found that the expression change determined by qPCR was significant for 9/12 genes and concordant with the microarray data for 8 of 12 (67%) super-connector genes (Figure 7). Moreover, we observed a significant positive correlation of 0.69 ( $p = 0.0132$ ) between the two datasets at 72h post-challenge (Supplementary figure E8). These data indicate that genes, which are likely to play an important role, would often escape attention in a single experiment analysis due to their minimal fold-change, but can emerge from an approach that combines computational dataset analysis and gene network connectivity investigation.

#### *Dexamethasone treatment reverts super-connector gene expression*

The glucocorticoid receptor *NR3C1* is the only super-connector that linked all 4 major domains and robustly changed expression across microarray comparisons and our qPCR. Given existing knowledge of the role of *NR3C1* in allergic asthma, we tested the effect of dexamethasone, a steroid that binds to *NR3C1* (36), in our animal model on both the disease phenotype and super-connector gene expression. As expected, dexamethasone significantly suppressed airway and lung inflammation, mucus hypersecretion and lung Th2 cytokine gene expression (Supplementary figure E9). Out of the 9 super-connector genes that were significantly deregulated in our model, dexamethasone partially or completely reverted 7 genes towards control values (Figure 8). Although *STAT1* was not deregulated in our model, it was down-regulated significantly after dexamethasone treatment, which is in agreement with a previous study (37). *TRAF6* and *VWF* were the only 2 super-connectors significantly down-regulated in our model that were unaffected by dexamethasone treatment. Out of the 9 super-connectors belonging to the inflammation domain, 6 were partially or completely reverted by dexamethasone treatment, whereas of the 3 super-connectors belonging to extracellular matrix remodeling, *ERBB2* is partially reverted by dexamethasone, *PKRCD* is not deregulated, and *VWF* is not reverted by the treatment. In conclusion, systemic treatment with glucocorticoids modulated the majority of the super-connectors belonging to the inflammation domain, but only partially reverts one gene belonging to the extracellular matrix remodeling domain.

## Discussion

Here, we implement a novel computational approach used to analyze multiple microarray datasets derived from lungs of mice with acute onset allergic asthma and integrate it with independent experiments to unravel the asthma ignorome and dissect it into domains, clusters, hubs and peripheral genes.

Technical limitations reduce the power of microarrays in detection of potentially important genes with limited variation in expression levels, especially when the sample size is small (38, 39). Gene signals from small specific cell populations in complex tissues, such as lung, are hence diluted to low levels that are not accurately detected by microarray analyses (38, 39). Using our approach, we reduced biological noise and detected genes with significant  $< 1.5$ -fold changes that were excluded from previous individual microarray studies (2, 10, 17, 18) and meta-analysis (40), which generated a reliable, robust gene expression signature for acute allergic asthma in mice.

Our signature gene list consists of 41% asthma-annotated genes and 59% of genes not previously associated with disease, defined as the ignorome (15). Of the asthma-annotated genes, 13 genes associated with Th2 and inflammatory responses account for 1/3 of all asthma related publications and the remaining genes play roles in inflammation. Strikingly, there are a large number of ignorome genes involved in inflammatory pathways, DNA replication, cell cycle and wound healing, which may include important disease targets. Taken together, these data support the notion that biomedical research is skewed towards a relatively small number of 'successful' genes (12, 13, 15, 41). We argue that novel insights into the pathogenesis of allergic asthma should be achieved irrespective of the current literature bias. The main ignorome clusters relate to stem cell proliferation and circadian rhythm domains. Both functional domains are well established in asthma (19, 20, 22, 42) and yet the individual genes identified in this study have as yet not been associated to it, thus providing interesting candidates to pursue these functional areas in the disease.

Understanding hubs (predominantly asthma-annotated) and peripheral genes (mostly ignorome) is essential for establishing functional interplay within the clusters and determining why key Th2 genes e.g. *IL13*, *IL4* and *IL4R* are neither hub nor peripheral genes (43, 44). These data support the finding that there is no correlation between a gene's degree of interaction, importance in the pathogenesis, and frequency of occurrence in the scientific literature (14).

Notably, all super-connectors are asthma-annotated and belong to either inflammation or lung-specific insult response domains. In our dexamethasone experiment, we found that only *TRAF6* and *VWF* had not changed expression levels. However, it is possible that they might have changed, if higher steroid doses were used, especially because steroids are known to increase *VWF* (45, 46) and *TRAF6* (47) expression. Although we focused on these super-connectors, there is evidence that 41% (314) of genes interconnect 3 or more clusters, 1/3 of them being an ignorome, further demonstrating a large constellation of interrelated clusters across tissues and biological domains.

There are caveats regarding the signature gene list and analyses presented here. Firstly, these analyses are based on the early events at the initiation of acute allergic asthma in the lungs of mice and may not reflect the same multiplicity of clusters and biological domains that would appear when testing chronic disease or disease relapse. Secondly, according to the current paradigm, genes in the inflammatory and immune response are expected, however, the remodeling response appears earlier than expected and these genes may reflect an early response of the lung to inflammatory signals and may represent the activation of healing mechanisms. Thirdly, it is not known whether human gene expression profiles from patient lungs would produce a similar gene list and functional clusters. Asthma is a heterogeneous disease that includes several distinct disease phenotypes and endotypes (48) and is not usually studied at acute onset, but rather during ongoing disease. Multiple dataset analyses including more gene expression profiles from mouse and man and at different stages of disease and in distinct patient subgroups may result in the prioritization of essential genes and networks at the core of disease and simultaneously highlight molecular differences between phenotypes.

In conclusion, the integration of prior literature knowledge and unbiased multiple dataset analysis paradigms through the lens of systems biology provides important insights into asthma pathogenesis, allowing to bring novel biology and existing knowledge on a balanced plate, highlighting connections between the two and providing novel avenues to combat the disease.

### **Acknowledgments**

The authors acknowledge excellent technical help of Drs. Rui-Yun Lee, Gordana Mokrovic and Daniela Reiner in various stages of experimental work.

## Tables

**Table 1.** Gene expression studies of asthma used for the bioinformatics analysis.

No.	Study				Affimerix Mouse Array	Mice	Antigen (Mice number)	No. of challenges	Sampling time (hr after last challenge)
	GSE	GPL	PMID	Comparison					
1	13032	1261	19491150	A	Genome 430 2.0	A/J	PBS (3) OVA (3)	3	3
				B		B6	PBS (3) OVA (3)		
2	6858	1261	17437023	C	Genome 430 2.0	BALB/c	PBS (4) OVA (4)	7	24
3	9465	1261	19057703	D	Genome 430 2.0	A/J	PBS (3) OVA (3)	1	96
4	1301	339-340	-	E	U74 Version 2	BALB/c	PBS (3) HDM (3)	2	72
5	3184	339	-	F	U74 Version 2	C3H	PBS (5) OVA (5)	1	6
				G		C3H	PBS (5) OVA (5)		
				H		A/J	PBS (5) OVA (5)	1	6
				I		A/J	PBS (5) OVA (5)		
6	18010	1261	19770271	J	Genome 430 2.0	B6.114raQ576/Q576 B6.114raQ576/Q576/IL-13tg	- (5) IL-13 (8)	7	24

Six GEO Datasets (<http://www.ncbi.nlm.nih.gov/gds/>) studies were selected for meta-analysis on the basis of the microarray platform and *in vivo* experimental protocol. From those 6 studies, 10 asthmatic vs. healthy control comparisons (A to J) have been extracted and further analyzed.



**Table 3.** List of hub and peripheral genes related to acute asthma ignorome.

Gene Name	Network role	Functional Domain	Published in inflammation&immunity
<i>C1QA</i>	Hub	Inflammation	Yes
<i>IFITM</i>	Hub	Inflammation	Yes
<i>HCLS1</i>	Hub	Inflammation	Yes
<i>IGSF6</i>	Hub	Inflammation	No
<i>PLEK</i>	Hub	Inflammation	No
<i>SLC15A3</i>	Hub	Inflammation	No
<i>CLEC5A</i>	Peripheral	Inflammation	Yes
<i>COTL1</i>	Peripheral	Inflammation	Yes
<i>MTPN</i>	Peripheral	Inflammation	No
<i>PRICKLE1</i>	Peripheral	Inflammation	No
<i>SDPR</i>	Peripheral	Inflammation	No
<i>GSTA3</i>	Hub	Lung-specific insult response	No
<i>CYP2B6</i>	Hub	Lung-specific insult response	Yes
<i>TGFBI</i>	Hub	Lung-specific insult response	Yes
<i>COL1A2</i>	Hub	Lung-specific insult response	Yes
<i>FGF1</i>	Hub	Lung-specific insult response	Yes
<i>BEX1</i>	Peripheral	Lung-specific insult response	No
<i>EFHD2</i>	Peripheral	Lung-specific insult response	No
<i>BAMBI</i>	Peripheral	Lung-specific insult response	Yes
<i>CHST2</i>	Peripheral	Lung-specific insult response	Yes
<i>ITGB1BP2</i>	Peripheral	Lung-specific insult response	Yes
<i>MYO1B</i>	Peripheral	Lung-specific insult response	Yes
<i>TFPI2</i>	Peripheral	Lung-specific insult response	Yes
<i>TMEM173</i>	Peripheral	Lung-specific insult response	Yes
<i>TSPAN7</i>	Peripheral	Lung-specific insult response	Yes

## Figures

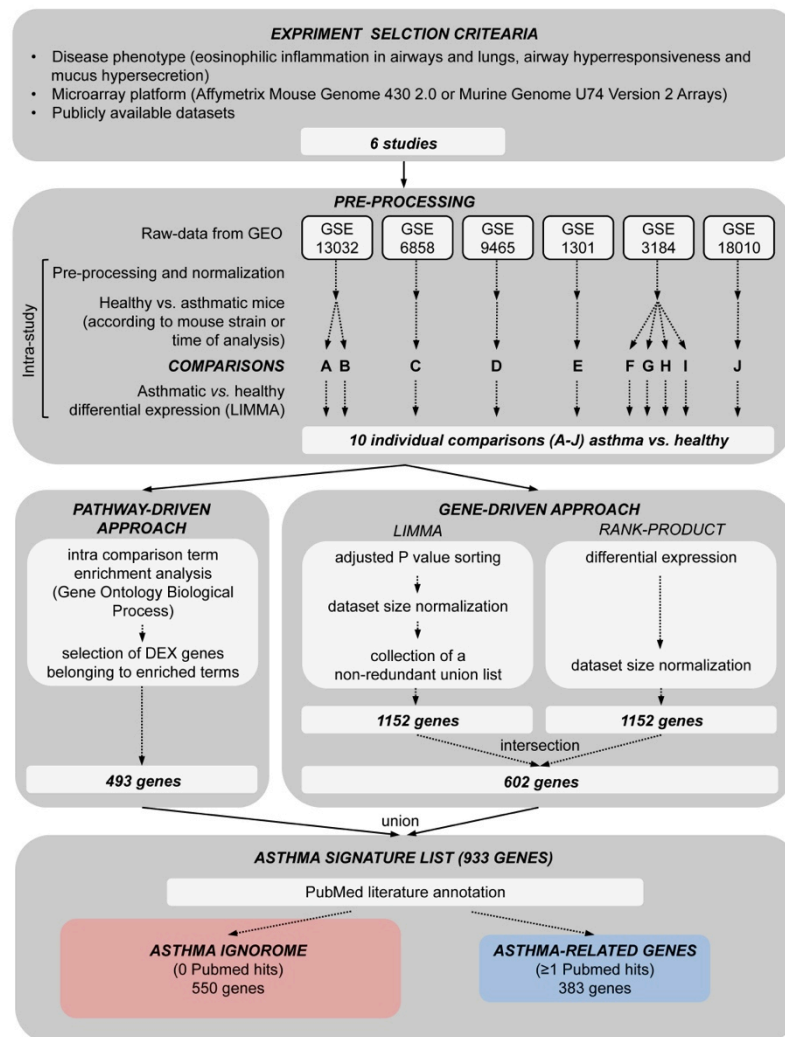


**Figure 1. Schematic overview of analysis pipeline.** Using experiment selection criteria, we selected six studies that were further subdivided into 10 comparisons of control and asthmatic mice according to mouse strain and time of analysis. After initial analysis with linear models to obtain differential gene expression, data from each comparison were re-analyzed using pathway- and gene-driven approaches (for details please refer to online supplementary methods). Lists of differentially regulated genes generated in the 2 approaches were merged into a final asthma signature list of 933 genes, which was used for literature-coverage searches in PubMed.

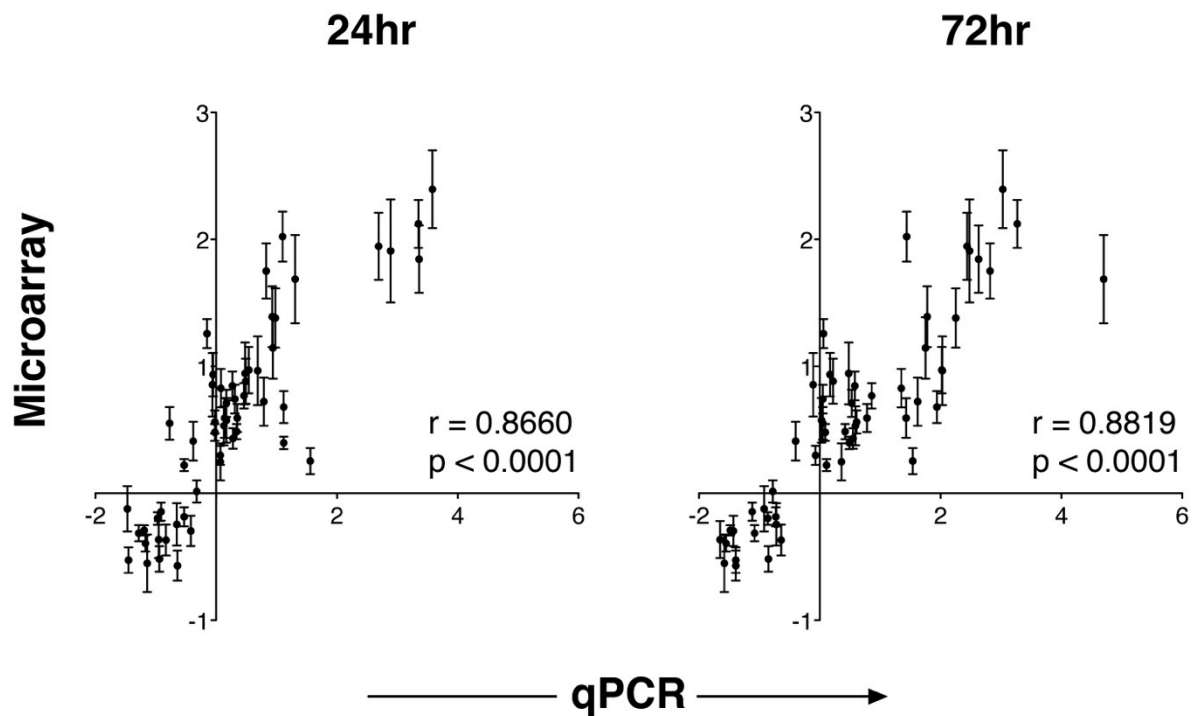


**Figure 2. Microarray data for 59 randomly selected genes from 10 comparisons of control and asthmatic mice correlate to quantitative PCR data from our independent mouse asthma model.** For qPCR, ovalbumin (OVA)-sensitized BALB/c mice received PBS (controls) or OVA challenge (A) 24h or (B) 72h before extraction of total lung RNA. Pearson r coefficients and p values for each correlation are indicated.



lacards; shown as lines). (B) List of MGI gene symbols for 933 asthma signature genes according to their number of asthma-annotated literature in PubMed according to the method described in online supplementary methods and exact number of publications is listed in Supplementary table E2.

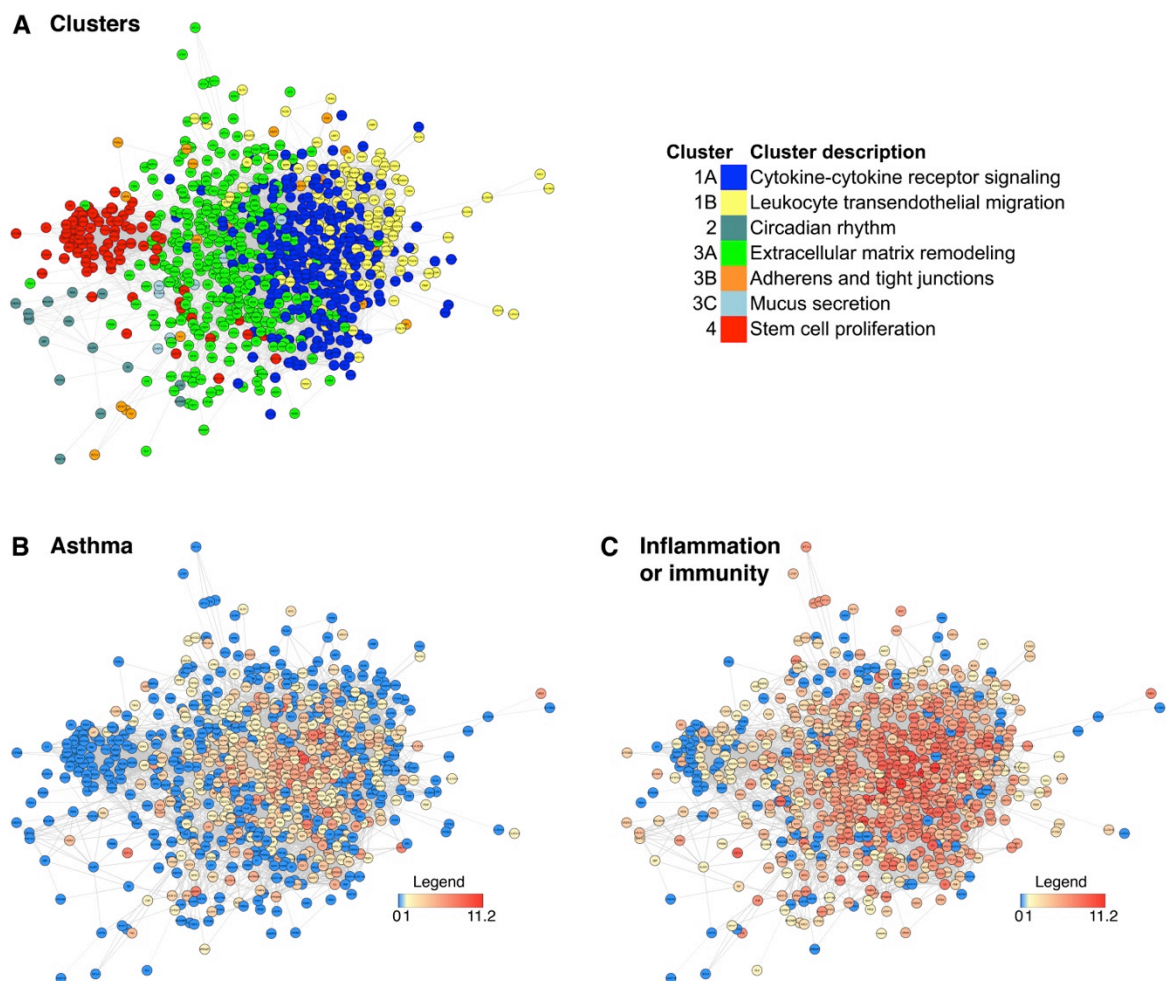


**Figure 4. Network representation of 759 human ortholog genes in 7 clusters from our asthma-signature list.** (A) Within the network we have detected 7 main clusters using STRINGdb library in Bioconductor that were further functionally annotated to reveal biological functions with online tool EnrichR (for details please refer to Online supplementary material). Genes are colored according to literature number associating each gene to (A) “asthma” or (B) “inflammation OR immunity”. For each gene, we have retrieved number of publications in PubMed in November 2014

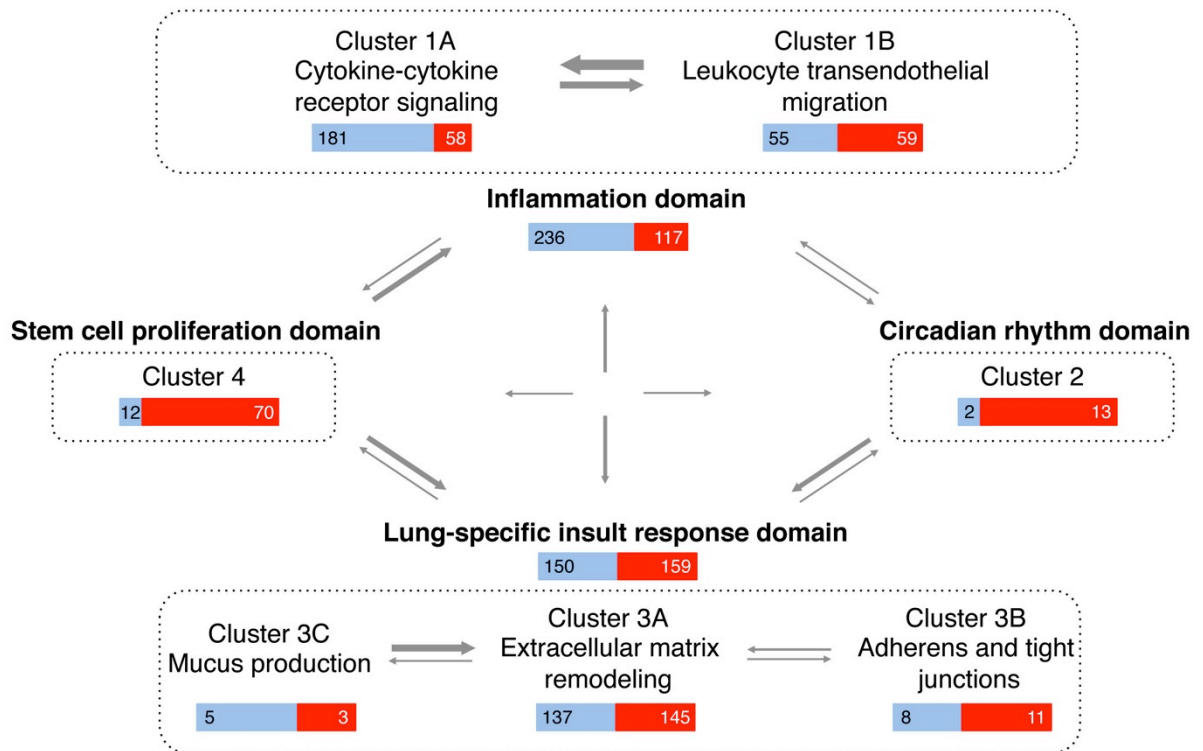


**Figure 5. Schematic diagram depicting connectivity between 4 domains and individual clusters in acute asthma signature list.** Bars indicate number of asthma-related (blue) and -ignorome (red) genes in each cluster or domain. Arrows indicating connections between clusters or domains are scaled according to relative connection strength between clusters and domains (see supplementary methods for details).

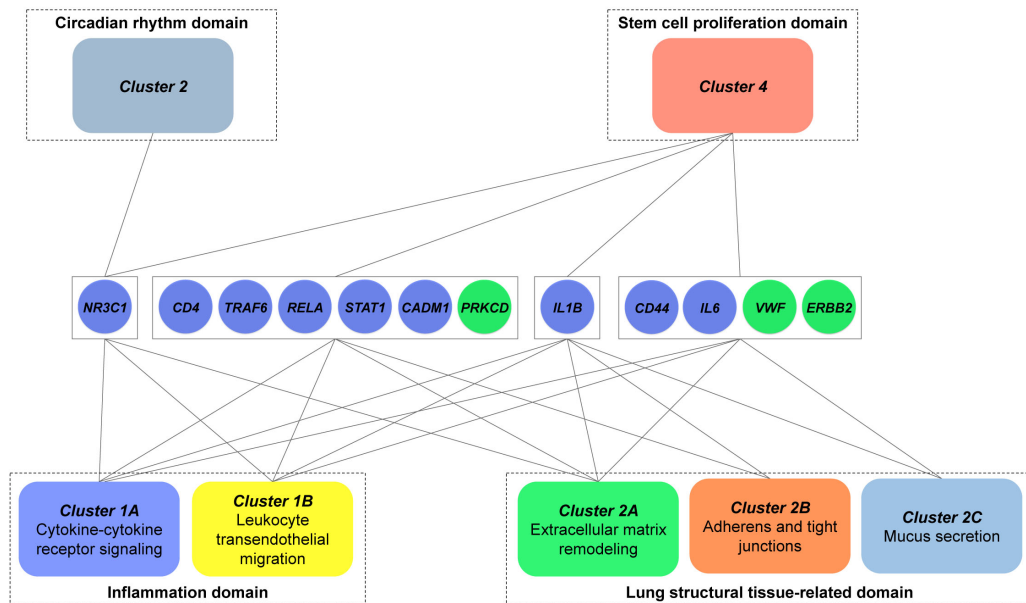


**Figure 6. Schematic diagram depicting 12 super-connector genes in the asthma-signature gene list.** Gene circle color indicates the cluster of origin and connected to the pertaining topological cluster. Topological clusters are grouped into 4 biological domains by dotted rectangles.

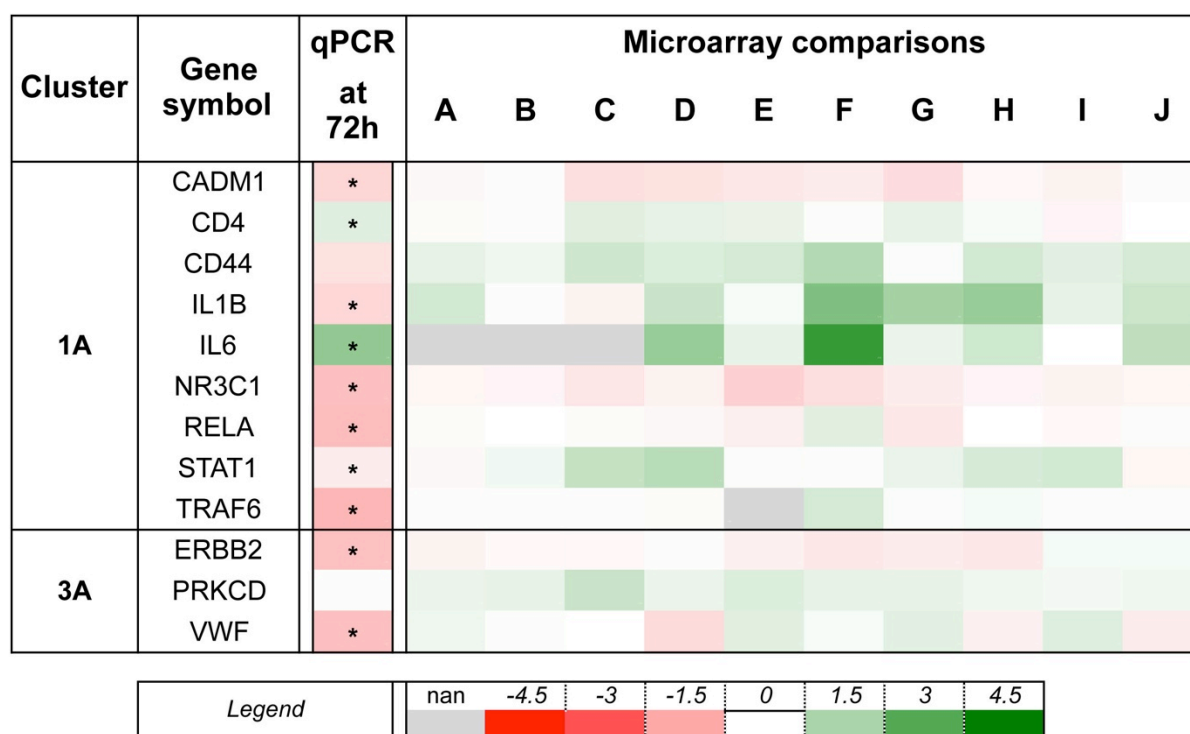


**Figure 7. Expression profiles of 8 from 12 super-connectors were confirmed with quantitative PCR.** Data are presented as mean log<sub>2</sub> fold changes of gene expression by quantitative real-time PCR and microarray relative to control mice. Quantitative real-time PCR data were determined in whole lung extracts and are pooled from 2 independent experiments (n=6). Microarray data are from 6 publicly available datasets broken down into 10 direct comparisons of asthmatic and control mice (please refer to Supplementary data and Figure 1 for details). \* p < 0.05 compared with PBS challenged mice (unpaired *t*-test).

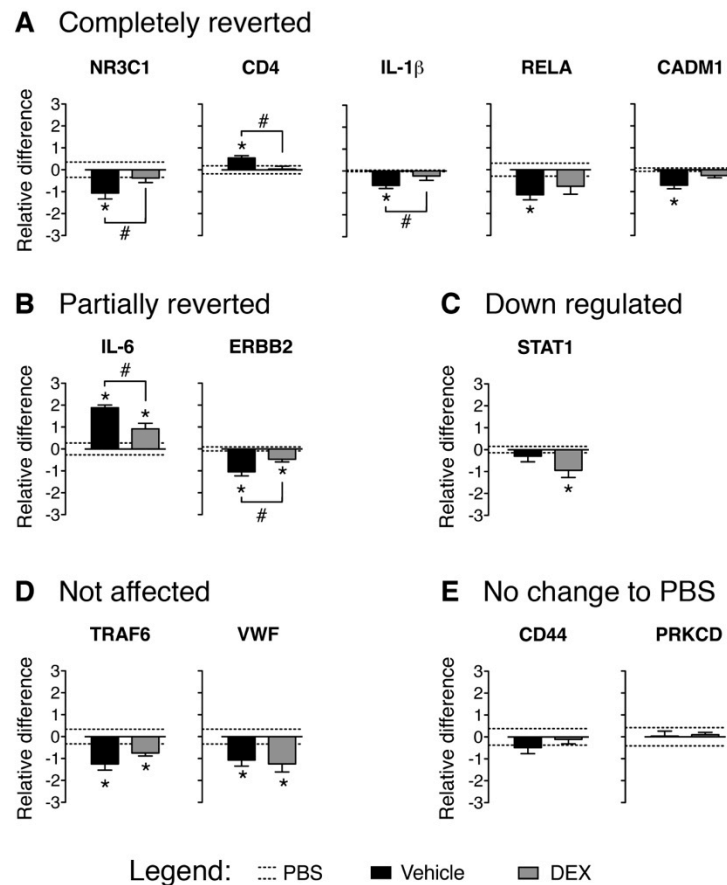


**Figure 8. Expression of super-connectors in acute allergic asthma after dexamethasone (DEX) treatment.** Total lung RNA was extracted from mice intranasally challenged with PBS (controls) and mice that received vehicle or dexamethasone before and after ovalbumin challenge to induce allergic asthma. Samples were collected at 72h after allergen challenge and super-connector expression was determined with quantitative PCR. Super-connectors are grouped according to their change to dexamethasone treatment into (A) completely reverted, (B) partially reverted, (C) further down regulated, (D) not affected with dexamethasone treatment, and (E) not changed in comparison to PBS controls. Data are presented as mean  $\log_2$  fold changes of gene expression relative to control (PBS) mice and are pooled from 2 independent experiments (n=6). \*  $p < 0.05$  compared with PBS challenged mice; #  $p < 0.05$  compared with vehicle-treated group (unpaired  $t$ -test).

## References

1. Chapman DG, Tully JE, Nolin JD, Janssen-Heininger YM, Irvin CG. Animal models of allergic airways disease: where are we and where to next? *J Cell Biochem* 2014;115:2055–2064.
2. Camateros P, Kanagaratham C, Henri J, Sladek R, Hudson TJ, Radzi- och D. Modulation of the allergic asthma transcriptome following resiquimod treatment. *Physiological Genomics* 2009;38:303–318.
3. Karp CL, Grupe A, Schadt E, Ewart SL, Keane-Moore M, Cuomo PJ, Köhl J, Wahl L, Kuperman D, Germer S, Aud D, Peltz G, Wills-Karp M. Identification of complement factor 5 as a susceptibility locus for exper- imental allergic asthma. *Nat Immunol* 2000;1:221–226.
4. Tumes DJ, Connolly A, Dent LA. Expression of survivin in lung eosino- phils is associated with pathology in a mouse model of allergic asthma. *International Immunology* 2009;21:633–644.
5. Di Valentin E, Crahay C, Garbacki N, Hennuy B, Gueders M, Noel A, Foidart JM, Grooten J, Colige A, Piette J, Cataldo D. New asthma bio- markers: lessons from murine models of acute and chronic asthma. *AJP: Lung Cellular and Molecular Physiology* 2008;296:L185–L197.
6. Stevens T, Krantz QT, Linak WP, Hester S, Gilmour MI. Increased Transcription of Immune and Metabolic Pathways in Naive and Allergic Mice Exposed to Diesel Exhaust. *Toxicological Sciences* 2007;102:359–370.
7. Tolgyesi G, Molnar V, Semsei AF, Kiszkel P, Ungvari I, Pocza P, Wiener Z, Komlosi ZI, Kunos L, Galffy G, Losonczy G, Seres I, Falus A, Szalai C. Gene expression profiling of experimental asthma reveals a possible role of paraoxonase-1 in the disease. *International Immunology* 2009;21:967–975.
8. Zimmermann N, King NE, Laporte J, Yang M, Mishra A, Pope SM, Mun- tel EE, Witte DP, Pegg AA, Foster PS, Hamid Q, Rothenberg ME. Diss- ection of experimental asthma with DNA microarray analysis identifies arginase in asthma pathogenesis. *J Clin Invest* 2003;111:1863–1874.
9. King NE, Zimmermann N, Pope SM, Fulkerson PC, Nikolaidis NM, Mishra A, Witte DP, Rothenberg ME. Expression and regulation of a di-

- sintegrin and metalloproteinase (ADAM) 8 in experimental asthma. *American Journal of Respiratory Cell and Molecular Biology* 2004;31:257–265.
10. Tachdjian R, Mathias C, Khatib AI S, Bryce PJ, Kim HS, Blaeser F, O'Connor BD, Rzymkiewicz D, Chen A, Holtzman MJ, Hershey GK, Garn H, Harb H, Renz H, Oettgen HC, Chatila TA. Pathogenicity of a disease-associated human IL-4 receptor allele in experimental asthma. *Journal of Experimental Medicine* 2009;206:2191–2204.
  11. Zimmermann N, Mishra A, King NE, Fulkerson PC, Doepker MP, Nikolaidis NM, Kindinger LE, Moulton EA, Aronow BJ, Rothenberg ME. Transcript signatures in experimental asthma: identification of STAT6-dependent and -independent pathways. *J Immunol* 2004;172:1815–1824.
  12. Pfeiffer T, Hoffmann R. Temporal patterns of genes in scientific publications. *PNAS* 2007;104:12052–12056.
  13. Su AI, Hogenesch JB. Power-law-like distributions in biomedical publications and research funding. *Genome Biol* 2007;8:404.
  14. Hoffmann R, Valencia A. Life cycles of successful genes. *Trends Genet* 2003;19:79–81.
  15. Pandey AK, Lu L, Wang X, Homayouni R, Williams RW. Functionally enigmatic genes: a case study of the brain ignorome. In: Ouzounis CA, editor. *PLoS ONE* 2014;9:e88889.
  16. Stupka E. The emergence of genomics in mouse asthma models. *Drug Discovery Today - Disease Models* 2009;6:119–127.
  17. Lu X, Jain VV, Finn PW, Perkins DL. Hubs in biological interaction networks exhibit low changes in expression in experimental asthma. *Mol Syst Biol* 2007. p. 98.
  18. Wang T, Moreno-Vinasco L, Huang Y, Lang GD, Linares JD, Goonewardena SN, Grabavoy A, Samet JM, Geyh AS, Breyse PN, Lussier YA, Natarajan V, Garcia JGN. Murine Lung Responses to Ambient Particulate Matter: Genomic Analysis and Influence on Airway Hyperresponsiveness. *Environ Health Perspect* 2008;116:1500–1508.
  19. Sehmi R, Wood LJ, Watson R, Foley R, Hamid Q, O'Byrne PM, Denburg JA. Allergen-induced increases in IL-5 receptor alpha-subunit ex-

- pression on bone marrow-derived CD34+ cells from asthmatic subjects. A novel marker of progenitor cell commitment towards eosinophilic differentiation. *J Clin Invest* 1997;100:2466–2475.
20. Dorman SC, Efthimiadis A, Babirad I, Watson RM, Denburg JA, Hargreave FE, O'Byrne PM, Sehmi R. Sputum CD34+IL-5Ralpha+ cells increase after allergen: evidence for in situ eosinophilopoiesis. *Am J Respir Crit Care Med* 2004;169:573–577.
  21. Mazzarella G, Grella E, D'Auria D, Paciocco G, Perna F, Petillo O, Peluso G. Phenotypic features of alveolar monocytes/macrophages and IL-8 gene activation by IL-1 and TNF-alpha in asthmatic patients. *Allergy* 2000;55 Suppl 61:36–41.
  22. Bentley JK, Popova AP, Bozyk PD, Linn MJ, Baek AE, Lei J, Goldsmith AM, Hershenson MB. Ovalbumin sensitization and challenge increases the number of lung cells possessing a mesenchymal stromal cell phenotype. *Respir Res* 2010;11:127.
  23. Scheiermann C, Kunisaki Y, Frenette PS. Circadian control of the immune system. *Nature Publishing Group* 2013;13:190–198.
  24. Curtis AM, Bellet MM, Sassone-Corsi P, O'Neill LAJ. Circadian clock proteins and immunity. *Immunity* 2014;40:178–186.
  25. Bates EE, Dieu MC, Ravel O, Zurawski SM, Patel S, Bridon JM, Ait-Yahia S, Vega F, Banchereau J, Lebecque S. CD40L activation of dendritic cells down-regulates DORA, a novel member of the immunoglobulin superfamily. *Mol Immunol* 1998;35:513–524.
  26. Daniel H, Kottra G. The proton oligopeptide cotransporter family SLC15 in physiology and pharmacology. *Pflugers Arch* 2004;447:610–618.
  27. Aoki N, Kimura Y, Kimura S, Nagato T, Azumi M, Kobayashi H, Sato K, Tateno M. Expression and functional role of MDL-1 (CLEC5A) in mouse myeloid lineage cells. *Journal of Leukocyte Biology* 2009;85:508–517.
  28. Chen S-T, Liu R-S, Wu M-F, Lin Y-L, Chen S-Y, Tan DT-W, Chou T-Y, Tsai I-S, Li L, Hsieh S-L. CLEC5A regulates Japanese encephalitis virus-induced neuroinflammation and lethality. In: Walker CM, editor. *PLoS Pathog* 2012;8:e1002655.
  29. Chen S-T, Lin Y-L, Huang M-T, Wu M-F, Cheng S-C, Lei H-Y, Lee C-K, Chiou T-W, Wong C-H, Hsieh S-L. CLEC5A is critical for dengue-virus-

- induced lethal disease. *Nature* 2008;453:672–676.
30. Halwani R, Al-Muhsen S, Al-Jahdali H, Hamid Q. Role of transforming growth factor- $\beta$  in airway remodeling in asthma. *American Journal of Respiratory Cell and Molecular Biology* 2011;44:127–133.
  31. Moiseeva EP, Roach KM, Leyland ML, Bradding P. CADM1 is a key receptor mediating human mast cell adhesion to human lung fibroblasts and airway smooth muscle cells. In: Taube C, editor. *PLoS ONE* 2013;8:e61579.
  32. Steinberg SF. Distinctive activation mechanisms and functions for protein kinase Cdelta. *Biochem J* 2004;384:449–459.
  33. Hillgruber C, Steingraber AK, Pöppelmann B, Denis CV, Ware J, Vestweber D, Nieswandt B, Schneider SW, Goerge T. Blocking von Willebrand factor for treatment of cutaneous inflammation. *J Invest Dermatol* 2014;134:77–86.
  34. Gutierrez C, Schiff R. HER2: biology, detection, and clinical implications. *Arch Pathol Lab Med* 2011;135:55–62.
  35. Lu X, Jain VV, Finn PW, Perkins DL. Hubs in biological interaction networks exhibit low changes in expression in experimental asthma. *Mol Syst Biol* 2007. p. 98.
  36. Niu N, Manickam V, Kalari KR, Moon I, Pelleymounter LL, Eckloff BW, Wieben ED, Schaid DJ, Wang L. Human glucocorticoid receptor alpha gene (NR3C1) pharmacogenomics: gene resequencing and functional genomics. *J Clin Endocrinol Metab* 2009;94:3072–3084.
  37. Hu X, Li W-P, Meng C, Ivashkiv LB. Inhibition of IFN-gamma signaling by glucocorticoids. *J Immunol* 2003;170:4833–4839.
  38. Wurmbach E, González-Maeso J, Yuen T, Ebersole BJ, Mastaitis JW, Mobbs CV, Sealfon SC. Validated genomic approach to study differentially expressed genes in complex tissues. *Neurochem Res* 2002;27:1027–1033.
  39. Draghici S, Khatri P, Eklund AC, Szallasi Z. Reliability and reproducibility issues in DNA microarray measurements. *Trends Genet* 2006;22:101–109.
  40. Novershtern N, Itzhaki Z, Manor O, Friedman N, Kaminski N. A functional and regulatory map of asthma. *American Journal of Respiratory Cell*

- and Molecular Biology* 2008;38:324–336.
41. Hoffmann R, Valencia A. Life cycles of successful genes. *Trends Genet* 2003;19:79–81.
  42. Smolensky MH, Lemmer B, Reinberg AE. Chronobiology and chronotherapy of allergic rhinitis and bronchial asthma. *Adv Drug Deliv Rev* 2007;59:852–882.
  43. Ingram JL, Kraft M. IL-13 in asthma and allergic disease: asthma phenotypes and targeted therapies. *J Allergy Clin Immunol* 2012;130:829–42– quiz 843–4.
  44. Kelly-Welch AE, Hanson EM, Boothby MR, Keegan AD. Interleukin-4 and interleukin-13 signaling connections maps. *Science* 2003;300:1527–1528.
  45. Jilma B, Cvitko T, Winter-Fabry A, Petroczi K, Quehenberger P, Blann AD. High dose dexamethasone increases circulating P-selectin and von Willebrand factor levels in healthy men. *Thromb Haemost* 2005;94:797–801.
  46. Brotman DJ, Girod JP, Posch A, Jani JT, Patel JV, Gupta M, Lip GYH, Reddy S, Kickler TS. Effects of short-term glucocorticoids on hemostatic factors in healthy volunteers. *Thromb Res* 2006;118:247–252.
  47. Sun H, Gong Y, Qiu J, Chen Y, Ding F, Zhao Q. TRAF6 inhibition rescues dexamethasone-induced muscle atrophy. *Int J Mol Sci* 2014;15:11126–11141.
  48. Martinez FD, Vercelli D. Asthma. *Lancet* 2013;382:1360–1372.

Revealing the acute asthma ignorome: characterization and validation of uninvestigated gene networks

Michela Riba, Jose Manuel Garcia Manteiga, Berislav Bosnjak, Davide Cittaro, Pavol Mikolka, Connie Le, Michelle M. Epstein and Elia Stupka

Online Data Supplement

Supplementary materials and methods

Supplementary tables

Supplementary figures

Supplementalry references

## Supplementary materials and methods

### *Multi-dataset bioinformatics analysis*

To overcome the limitations of direct comparison of the results obtained by other laboratories with their own differing analysis pipelines, we retrieved the raw data from the GEO database (E1) and re-analyzed them using a common pipeline for signal normalization and extraction of differentially expressed genes with limma and Affy Bioconductor libraries (E2). Raw data were normalized using robust multi-array average [RMA; (E3)]. In each experiment, genes with expression values lower than the first quartile of the entire distribution of values were considered as non-expressed and hence removed from the analysis. We applied parametric moderated  $t$ -statistics, implemented in limma library, to identify differentially expressed genes between asthmatic and control samples. Each differential expression analysis was conducted separately for each experiment. Significantly up and down regulated genes were selected using an adjusted  $p$ -value threshold of 0.05 (Benjamini-Hochberg correction (E4)).

The resulting gene lists were then utilized for our multi-dataset bioinformatics analysis that combines two approaches: a top-down, biological process enrichment driven approach, from now on called 'pathway-driven', and a bottom-up, 'gene-driven' approach. The former strategy is based on the selection of common asthma-specific pathways from a combination of enriched biological terms found across individual studies. In the latter strategy, a list of differentially expressed genes has been created across all individual datasets, normalizing the size of the list to balance the different statistical power of each experimental design. Results from each single approach have been merged in a comprehensive list of genes. Human orthologs of such genes were used to query a network of interactions and investigated in terms of topological structure using STRINGdb Bioconductor library (E5) and Cytoscape (E6). The details of each strategy are described below.

### *Pathway-driven strategy*

We performed GO.BP (Gene Ontology Biological Process) term enrichment analysis using the lists of differentially expressed genes derived from each microarray comparison, selected at a stringency of adjusted  $p$ -value  $< 0.05$ , using NCBI DAVID online tool (E7). 76 GO.BP were selected according to the following criteria: ease score  $< 0.01$ , presence in at least 2 studies, fold enrichment  $> 2$ ; categories which were also enriched in the background of mouse transcriptome alone were filtered out. We calculated semantic similarity among enriched terms using GO.SemSim Bioconductor library (E8). Similarities were used to build clusters of semantically related terms, including regulation of morphogenesis, T-cell selection, antigen processing and presentation, response to external stimuli, immune signaling, and leukocyte-mediated response (Supplementary figure E10). Differentially expressed genes referring to enriched GO.BPs were retained to form a non-redundant list of interesting targets ( $n=493$ ), namely “pathway-driven” list.

### *Gene-driven strategy*

To obtain a list of differentially expressed genes (DGEs) based on a ‘gene-driven approach’, we performed a two-step analysis: normalized union of DGEs and Rank Product of DGEs.

### *Normalized Union of DGEs*

The genes obtained from the limma differential expression analysis were ranked from highest to lowest significance for all 10 comparisons performed (A to J). The comparison which produced the smallest list of genes was used to define a cut-off for the remaining comparisons performed to produce 10 lists of genes of the same size, all containing highly significant genes (adjusted  $p$ -value  $< 0.05$ ). This approach was used to ensure, on the one hand a stringent approach for the inclusion of genes, and on the other hand to obtain a balanced contribution of each study for the downstream analysis. We then performed a non-redundant merge of these 10 lists.

### *Rank Product of DGEs*

We used a non-parametric approach to analyze the 10 studies together based on the Rank Product using the RankProd Bioconductor library (E9). This approach makes it possible for datasets generated at different laboratories or from different environments to be combined for study and it has been previously used with success for meta-analyses of gene expression data (E10). RankProd uses the rank product non-parametric method to identify up- or down-regulated genes in one condition against another condition, based on consistent fold change across experiments, rather than  $t$  statistics. In our comparison of asthmatic vs. control samples, Rank Product detected genes that were consistently highly ranked in a number of lists, *i.e.*, genes that were consistently found among the most strongly up- or down-regulated genes in a number of replicate experiments [see (E9) for further details]. The RankProd Bioconductor package was used to calculate rank product statistics on data coming from the 10 different lists in this study. We derived a list of up-regulated and a list of down-regulated genes. We then ranked these based on their meta-analysis Rank Product FDR ( $pdf$ ) and identified a  $pdf$  cutoff which would allow us to retain the same number of genes obtained in the normalized union approach, with the same up- and down-regulated proportions, to balance the contribution of both approaches. We combined the list of genes from the normalized union step ( $t$ -statistics) with the genes coming from the Rank Product step (non-parametric) and produced an intersection containing genes that were identified by both statistical approaches, leading to a highly stringent and robust set of differentially expressed genes which ranked highly both in terms of  $t$ -statistics and fold-change rank product.

### *Gene Annotation*

For each gene in our list, we performed a literature search in PubMed to identify publications associated to asthma as keyword in the title or abstract. We used NCBI Entrez Gene search engine [(E11); <http://www.ncbi.nlm.nih.gov/gene/>] on EntrezId terms for either mouse genes or their human orthologs (see below). We used a ruby script to retrieve NCBI publication numbers using either “Asthma” or “Immunity OR Inflammation” in the Title/Abstract of the papers and the number of resulting publications was

used to annotate each gene (date of publication number retrieval, 28<sup>th</sup> of November 2014; see Supplementary Table E2). To validate 550 genes that had 0 publications for “asthma”, we performed additional searches in PubMed using the gene abbreviation as a keyword. For 444 genes, we confirmed 0 publications records for “asthma” and for the remaining 106 genes, the publication number was manually curated to retrieve a final list of 493 genes, whose function was not related to “asthma”. An overlap of our asthma signature with known as asthma-related annotated genes was calculated using the Comparative Toxicogenomics Database (CTD) via the enrichment ToppGene Suite (E12) and with Malacards (E13) through GeneCards [(E14), <http://www.genecards.org/>]. GeneCards allergic asthma-related genes were retrieved through the advanced search “allergic asthma” as keyword in February 2014.

#### *Network analysis and network cluster annotation*

Pathway-driven and gene-driven lists were merged into a final union list. We compiled a list of corresponding human orthologs: First, BioMart was used to automatically map the human orthologs from the gene symbols ([www.biomart.org](http://www.biomart.org)). Second, for those genes without any annotated ortholog using BioMart, a combined search using Ensembl and MGI databases was undertaken ([www.ensembl.org](http://www.ensembl.org) and <http://www.informatics.jax.org/>). For those mouse genes that showed more than one potential human ortholog, all genes were retrieved. We used a full list of human orthologs to query STRING interaction network using STRINGdb library in Bioconductor. We performed a topological analysis using STRINGdb library again, searching for clusters of densely connected genes: a group of nodes having denser relations with each other compared with the rest of the network. STRINGdb integrated igraph (E15) functions for this purpose. Clusters with at least 5 genes were entitled for further analysis.

#### *Functional annotation of genes within 7 clusters*

For each cluster, we identified three sets of genes: hub genes, peripheral genes and super-connectors. Hubs were defined as the top 10% of the genes in the each cluster ranked by betweenness centrality parameter in descending

order. Peripheral nodes were defined as 1-degree nodes connected to a clique (a maximal complete subgraph where all vertices are connected). Super-connectors were defined as genes connecting more than 5 clusters.

Each cluster was further analyzed using the online tool EnrichR (E16). We analyzed enrichments for the human orthologs in the following gene sets: Gene Ontology Biological Process (GO.BP), KEGG Pathways and Human\_Atlas. Gene sets with  $p < 0.05$  were considered significant. We also extracted expression values for each gene from the BioGPS (E17) dataset within 17 different tissues that could be represented in asthmatic lungs (<http://biogps.org/downloads/>): 12 related to leukocytes and 5 related to lung tissues. We used pheatmap R library [R package version 0.7.7. <http://CRAN.R-project.org/package=pheatmap>] to produce clustered heatmaps for genes in each cluster characterized in the network analysis (Supplementary Figures E3-E7).

#### *Calculation of relative connection strength between clusters and domains*

To assess the connectivity between different clusters as well as between biological domains, we processed the raw counts of genes and connections in each cluster and each domain. Briefly, we obtained a “connectivity ratio” for each cluster by dividing the number of connections found in each cluster by the square of the number of genes present in that cluster. We then used this “connectivity ratio” to normalize the number of connections of a cluster with another specific cluster by the connectivity ratio of the originating cluster. Finally, to obtain biological domain connectivity scores, we used the average of the connectivity scores of all clusters found within the biological domain.

#### *Acute allergic asthma model*

In all experiments, we used 8-10 week old female BALB/c mice (Charles River, Sulzfeld, Germany) provided with OVA-free food (SSNIFF, Soest, Germany) and autoclaved water *ad libitum*. All experimental protocols complied with the requirements of the Animal Care Committee of the Austrian Ministry of Science. All mice were immunized with 10  $\mu$ g of ovalbumin (Sigma Chemical Co., St. Louis, MO) in 200  $\mu$ l of PBS phosphate buffered saline (PBS) int-

raperitoneally (i.p.) on days 0 and 21 and then intranasally challenged on day 32 with (i) 100 µg of ovalbumin in 50 µl of PBS or (ii) 50 µl of PBS (Supplementary Figure 8A).

#### *Dexamethasone treatment protocol*

For treatment, we administered dexamethasone (Sigma) at the dose of 1 mg/kg, 30 minutes before and 24 and 48h after ovalbumin challenge. Dexamethasone was first dissolved in DMSO (Sigma) and then diluted with PBS to a final concentration of 0.1 mg/ml (final concentration of DMSO was 5%). Control mice received intraperitoneal administration of PBS in the same treatment schedule. All solutions were administered to the mice in 10 ml/kg.

#### *Airway hyperresponsiveness*

At 24h after OVA challenge, we measured airway resistance and dynamic compliance in anesthetized and ventilated animals by Resistance and Compliance System (Buxco Electronics Ltd., Troy, NY, USA). Briefly, PBS, followed by increasing concentrations of methacholine (Sigma), was nebulized for 3 min and lung function was recorded and calculated using FinePoint software (Buxco Electronics Ltd.).

#### *Airway inflammation*

Seventy-two hours after intranasal OVA challenge, the lungs were washed with total volume of 1 ml of PBS to collect bronchoalveolar lavage fluid (BAL). The total number of cells in BAL was enumerated in an improved Neubauer hemocytometer and cytocentrifuged preparations (Cytospin-4, Thermo Shandon Corporation, Pittsburg, PA, USA) were stained with the Kwik-Diff (Thermo Fisher Scientific Inc., Pittsburgh, PA, USA) to determine the percentage of inflammatory cells by morphological examination of at least 300 cells.

#### *Lung inflammation and mucus hypersecretion*

Lungs were dissected after bronchoalveolar lavage and fixed in paraformaldehyde. Paraplast-embedded lung sections of 3 µm were stained with hematoxylin and eosin (H&E) for morphological evaluation and with periodic acid-Schiff stain (PAS) for enumeration of mucopolysaccharide positive cells.

Intensity of inflammation on the H&E stained slides was graded according to our semi-quantitative scoring system as described previously (E18). The number of mucus-containing cells per millimeter of basement membrane was determined with ProgRes CapturePro Software (Jenoptik, Jena, Germany).

#### *Serum OVA-specific immunoglobulin*

The measurement of OVA-specific IgG1 and IgE titers in sera was done by in-house ELISA as described before (E18).

#### *mRNA extraction and quantitative PCR*

Separate groups of mice were used for lung mRNA extraction at 24 or 72h after intranasal challenge with PBS or OVA. Briefly, total RNA was isolated using RNeasy Mini Kit (Qiagen, Germantown, MD, USA) and the integrity of isolated RNA was confirmed using an Agilent 2100 Bioanalyzer and Agilent RNA 6000 Nano Assay Kit (Agilent Technologies, Pao Alto, CA, USA). After reverse-transcription with the Superscript III first-strand cDNA synthesis supermix kit (Invitrogen, Carlsbad, CA, USA), gene expression was analyzed using the SYBR green method for quantitative polymerase chain reaction (qPCR) on StepOnePlus real time PCR system (Applied Biosystems, Foster City, CA, USA). Collected data were analyzed the  $\Delta\Delta CT$  method for which the geometric mean of threshold cycle (CT) values for hypoxanthine-guanine phosphoribosyltransferase (HPRT),  $\beta$ -actin and glyceraldehyde 3-phosphate dehydrogenase (GAPDH) was used as an endogenous control and mean of CT values from recovered mice was used as a reference sample. The list of primers (Invitrogen or Microsynth, Balgach, Switzerland) can be found in Supplementary table E1.

#### *Correlation of microarray and qPCR data*

Data from selected 59 genes with divergent fold changes were analyzed with qPCR and correlated to average microarray expression across 10 divergent microarray comparisons (A-J) used in this study. To include gene into analysis, its expression had to be detectable in control and asthmatic mice with qPCR; i.e. genes with Ct value of 40 in any group were excluded from analysis.

### *Statistical analysis*

To compare airway hyperresponsiveness data, area under curve was calculated for each experimental animal on the graph of resistance or compliance (y axis) vs. the methacholine concentration (mg/ml; x axis). Before analysis, the values for the calculated area under curve for resistance and compliance, the airway inflammation data, as well as the mucus-positive cell counts in the lungs were log-transformed to equalize variances. Those data were analyzed with Student's *t*-test (for experiments with control and asthmatic mice) or with one-way ANOVA followed by Tukey's multiple comparison test (in experiments with dexamethasone treatment). Scores for lung inflammation were analyzed with Chi-squared test for trend. Pearson *r* correlation was used to analyze microarray and qPCR data correlation. Unpaired *t*-test was used to compare differences in gene expression determined with qPCR between control and asthmatic mice as well as vehicle-treated and dexamethasone-treated OVA-challenged mice. All analyses were done using GraphPad InStat v.5.0 (GraphPad Software Inc., San Diego, CA, USA) and *p*-values were considered significant at 0.05 threshold.

## Supplementary tables

**Supplementary table E1.** List of primers (5' -> 3') used for chemokine expression analysis. Primer sequences were mainly selected from PrimerBank (<http://pga.mgh.harvard.edu/primerbank/>).

Gene	NCBI Gene ID	Forward primer	Reverse primer
HPRT	15452	TTGCTCGAGATGTGATGAAGGA	AAAGTTGAGAGATCATCTCCACCAA
$\beta$ -Actin	11461	GTGACGTTGACATCCGTAAAGA	GCCGGACTCATCGTACTCC
GAPDH	14433	ACCCAGAAGACTGTGGATGG	CACATTGGGGGTAGGAACAC
ALAS1	11655	TCGCCGATGCCATTCTTATC	GGCCCCAACTTCCATCATCT
ALPL	11647	GTGACTACCACTCGGGTGAAC	CTCTGGTGGCATCTCGTTATC
BAMBI	68010	CATTGCTGGCGGACTGATCTT	CTTGCCCTTCTTGGAAATGGT
CADM1	54725	GAACCAGCAGTTCACGATTCT	AGCAAGCATAGCATGGCAAAC
CD44	12505	TCTGCCATCTAGCACTAAGAGC	GTCTGGGTATTGAAAGGTGTAGC
CLEC5A	23845	TTATTGGTTTGGTACGTCAGCC	TGGTCCTGATTGGTAACATTGC
CTSS	13040	TAGAGGCAGACGCTTCCTATC	CGGGAGCTGAATGTACCTTGA
CXCL10	15945	CCAAGTGCTGCCGTCATTTTC	GGCTCGCAGGGATGATTTCAA
CXCL9	17329	GGAGTTCGAGGAACCCTAGTG	GGGATTTGTAGTGGATCGTGC
DCK	13178	TGGCAAGCTCAAAGATGCAGA	AGAAGCGAAAATGTACCTGTAC
ENPP1	18605	GAGTGTCAGCAGAGTTTGAAT	CACCCAGGTGTGCAAATACT
ERBB2	13866	GAGACAGAGCTAAGGAAGCTGA	ACGGGGATTTTCACGTTCTCC
HCLS1	15163	GGCCACGAGTATGTTGCTGAT	CCCTCTCAACTCCATATTTGCC
IFN $\gamma$	15978	ATGAACGCTACACACTGCATC	CCATCCTTTTGCCAGTTCCTC
IGSF6	80719	TAGAAGTGGACTACGGTTCT-	GTCTGCCTCATTCTGCATCC
IL13	16163	GGATATTGCATGGCCTCTGTAAC	AACAGTTGCTTTGTGTAGCTGA
IL1 $\beta$	16176	TTCAGGCAGGCAGTATCACTC	GAAGGTCCACGGGAAAGACAC
IL4	16189	ACTTGAGAGAGATCATCGGCA	AGCTCCATGAGAACACTAGAGTT
IL5	16191	CTCTGTTGACAAGCAAT-	TCTTCAGTATGTCTAGCCCCTG
IL6	16193	TAGTCCTTCCACCCCAATTTCC	TTGGTCCTTAGCCACTCCTTC
KLF4	16600	ATCCTTTCCAACCTCGCTAACCC	CGGATCGGATAGCTGAAGCTG
LCK	16818	AACTTCGTGGCGAAAAGCAAAC	CTGACCGACAGGGAAAAGGAC
MAD2L1	56150	GTGGGAAGAATCGGGACCG	CAGTCATTGACAGGGGTTTTGT
MUC5AC	17833	GTGGTTTGACTGACTTCCC	CTCCTCTCGGTGACAGAGTCT
MUC5B	74180	AAGCTGCCCTACAGTCGTG	GACTAGGCGGATGCTGATTTT
NME1	18102	AGGAGCACTACACTGACCTGA	GGTTGGTCTCTCCAAGCATCA
NR1D1	217166	GCTCAGCGTCATAATGAAGCG	GGCCGAATATACGTGGGT
NR3C1	14815	CCGGGTCCCCAGGTAAAGA	TGTCCGGTAAAATAAGAGGCTTG
PARD3	93742	ACATGCTGATACCGATTGGA	CACTGAAAGGCACTACATGGATT
PER2	18627	CAGGTTGAGGGCATTACCTCC	AGGCGTCTTCTTACAGTGAA
PER3	18628	TCAAGACGTGAGGGCGTTCTA	CATTCATACTGCGAGGCTCTTT

PLEK	56193	TTCAGAGGGGTTATCATCAAGCA	CCCAGCAGGATCATAGTAGTGC
PPARA	19013	TACTGCCGTTTTCAACAAGTGC	AGGTCGTGTTACAGGTAAGA
PRKCD	18753	TGGGGGTGACCTGATGTTC	CCAGCACCAACAATACCTGTAA
PRKCI	18759	CCACACTTTTCAAGCCAAACG	TGCACTTGATCCTTGTCGTC
RELA	19697	AGCGCGGGGACTATGACTT	GCCCGGTTATCAAAAATCGGAT
RORA	19883	GATGACCTCAGCACCTATATG-	CGGGTTTGATCCCATTGATGTC
RRM2	20135	GGAAGCTCTGAAACCCGATGA	ACTTCTTGGCTAAATCGCTCC
SIGLEC5	233186	TGCACAGAAAATCGACACAGG	TCAGAGCTATCACAAGCACAGA
STAT1	20846	GCTGCCTATGATGTCTCGTTT	TGCTTTTCCGTATGTTGTGCT
TFF2	21785	CCTTGGTGTTTCCACCCACTT	AGCAGCAGTTTCCACTGGC
TGFBI	21810	TGTCCTGGATAT-	GGTGGTCGATCCCACAACCT
TIMP1	21857	GCAACTCGGACCTGGTCATAA	CGGCCCGTGATGAGAACT
TK1	21877	AAGCTGCCTACACGAAGAGG	CGGCACACGGAGTGATACTT
TMEM17	72512	CTACATTGGGTACTTGC GGTT	GCACCACTGAGCATGTTGTTATG
TRAF6	22034	AAAGCGAGAGATTCTTTCCCTG	ACTGGGGACAATCACTAGAGC
TYROBP	22177	GAGTGACACTTTCCCAAGATGC	CCTTGACCTCGGGAGACCA
VWF	22371	CTTCTGTACGCCTCAGCTATG	GCCGTTGTAATTCCACACAAG





# Supplementary table E2. Continued.

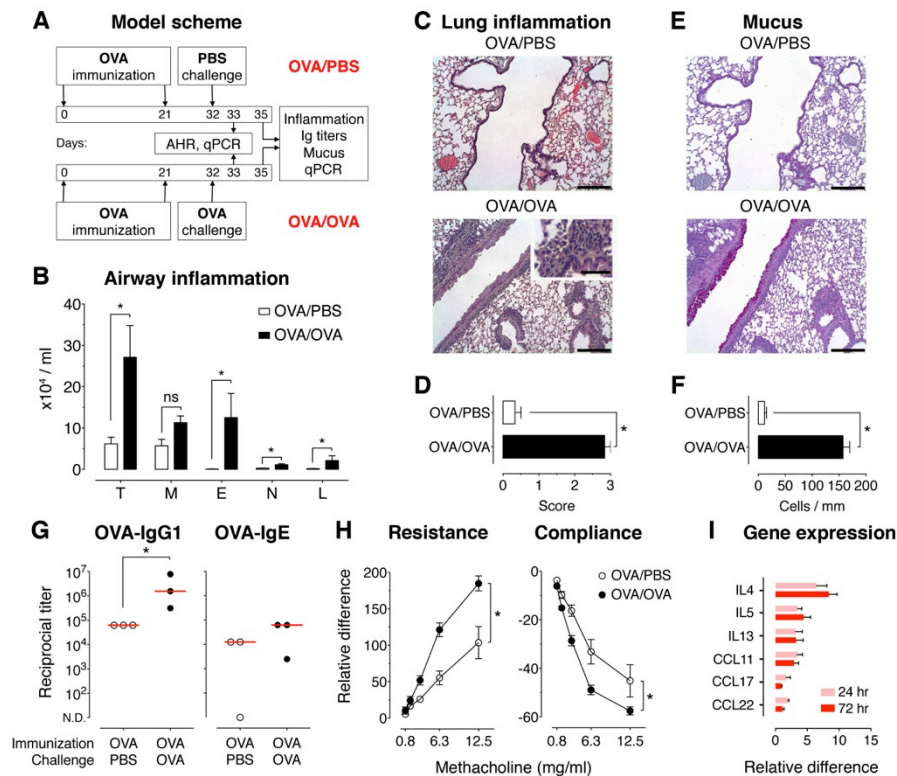
G0p7	GB9	0.204	0.094	1.586	1.588	nan	nan	0.809	0.217	1.07	0.315	-0.433	1A	NO	NO	NO	0	0
G0p8	GB9	-0.34	0.054	1.816	1.14	0.471	0.298	0.258	1.024	1.112	-0.479	1A	NO	NO	NO	0	1	2
G0c	GC6	0.316	0.255	0.665	0.64	1.11	0.484	0	0.139	0.445	0.853	1A	NO	NO	NO	0	0	5
G0a	G0A	0.232	0.287	0.11	0.4027	0.67	0.549	0.021	0.621	0.375	0.693	1A	NO	NO	NO	0	0	7
G0r	G0R	-0.289	-0.287	-0.703	0.31	-0.94	-0.88	-0.217	-0.354	-0.27	-0.187	1A	NO	NO	NO	0	0	3
G0p1	GLP1	0.514	0.424	1.512	0.985	1.197	0.637	0.468	0.138	0.197	0.856	1B	NO	NO	NO	0	0	0
G0p2	GLP2	0.461	0.4015	0.51	0.57	0.317	0.832	0.507	0.789	0.392	0.165	1A	NO	NO	NO	0	0	11
G0c4	GLC4	0.026	0.255	1.807	0.333	0.356	0.918	0.074	1.067	1.001	0.644	1A	NO	NO	NO	0	0	1
G0m1889	C11a9p6	0.391	0.43	0.001	0.009	0.333	1.017	0.724	1.067	0.393	0.644	1A	NO	NO	NO	0	0	0
G0m6	GM6A	-0.429	-0.013	-0.807	-0.608	-0.88	-0.3	-0.288	-0.007	-0.199	-0.207	1A	NO	NO	NO	0	0	0
G0m6b	GM6B	0.455	-0.277	2.102	2.065	1.505	0.058	0.535	-0.077	0.699	2.091	3A	NO	NO	NO	0	0	6
G0p125	GM125	0.025	-0.184	-0.761	0.56	-0.342	-0.545	-0.331	0.554	0.04	0.065	1A	NO	NO	NO	0	0	0
G0p101	GM101	0.421	-0.288	-0.931	-0.135	-0.506	-0.335	-0.377	-0.231	-0.354	-0.201	1A	NO	NO	NO	1	0	2
G0p101	GM101	-0.2017	-0.264	-0.247	-0.5033	-0.085	-0.264	-0.462	-0.521	-0.044	-0.355	1A	NO	NO	NO	0	0	0
G0p1	GW1	0.11	0.106	0.588	0.167	0.7	0.033	0.195	-0.131	0.12	0.587	1A	NO	NO	NO	5	5	24
G0p1	GW1	-0.2481	0.01	-0.295	0.13	-0.84	-0.443	-0.236	0.42	-0.246	0.616	1A	NO	NO	NO	1	1	4
G0p14	GW14	0.336	-0.204	-0.513	-0.215	-0.625	-0.307	-0.646	-0.441	-0.177	-0.64	1A	NO	NO	NO	1	0	1
G0p1	GW1	-0.7778	-0.609	0.05	-0.8031	-0.024	-0.528	-0.31	-0.318	0.371	-0.312	1A	NO	NO	NO	1	0	1
G0p2	GW2	0.002	-0.394	-1.249	-0.64	-0.963	-0.572	-0.943	-0.009	-0.196	-0.678	1A	NO	NO	NO	0	0	0
G0p3	GW3	-0.1403	-0.2035	-1.563	-0.895	-1.15	-0.805	-0.507	-0.482	0.022	-0.38	1A	YES	NO	NO	0	0	0
G0m1	GW1	0.2682	-0.295	-1.802	-0.488	-1.12	-0.442	-0.295	-0.478	0.266	1.201	1A	NO	NO	NO	0	0	0
G0m1	GW1	0.999	0.651	0.646	0.4805	0.73	0.541	0.058	0.42	0.094	0.595	1A	NO	NO	NO	3	4	0
G0c143	GW143	0.028	-0.304	-0.803	-0.587	-0.72	-0.733	-0.319	-0.007	0.199	-0.207	1A	NO	NO	NO	0	0	0
G0c143	GW143	-0.1285	-0.195	-0.776	-0.4785	-0.825	-0.5	-0.143	-0.44	-0.05	0.025	1A	NO	NO	NO	4	1	0
G0c143	GW143	0.0318	0.291	1.209	0.709	1.028	0.294	0.339	0.034	0.04	0.804	1A	NO	NO	NO	0	0	0
H2_Aaa	H2A-DNA1	0.078	0.028	1.585	0.973	1.075	0.819	0.342	0.365	0.618	0.742	1A	NO	NO	NO	1	1	37
H2_Daa	H2A-DNA2	0.096	0.023	1.701	0.6027	0.88	0.895	0.266	0.386	0.29	0.901	1A	NO	NO	NO	1	1	5
H2_Aaa	H2A-DNA	-0.005	0.24	1.075	0.8805	0.825	0.491	0.178	0.118	0.618	0.525	1A	NO	NO	NO	8	5	37
H2_Daa	H2A-DNA	-0.0433	0.043	1.8003	0.895	1.065	0.265	0.066	0.388	0.299	0.817	1A	NO	NO	NO	4	0	1
H2_Caa	H2A-DNA5	0.06	0.03	1.715	0.697	0.882	0.832	0.296	0.273	0.528	0.641	1A	NO	NO	NO	0	0	0
H2_Daa	H2A-DNA	0.078	0.029	1.674	0.607	1.038	0.596	0.267	0.299	0.106	-0.077	1A	NO	NO	NO	10	10	41
H2_Caa	H2A-DNA	0.06	0.03	1.715	0.697	0.882	0.832	0.296	0.273	0.528	0.641	1A	NO	NO	NO	0	0	0
H2_Daa	H2A-DNA	0.078	0.029	1.674	0.607	1.038	0.596	0.267	0.299	0.106	-0.077	1A	NO	NO	NO	10	10	41
H2_Qaa	H2A-DNA	0.078	0.029	1.674	0.607	1.038	0.596	0.267	0.299	0.106	-0.077	1A	NO	NO	NO	10	10	41
H2_Qaa	H2A-DNA	0.078	0.029	1.674	0.607	1.038	0.596	0.267	0.299	0.106	-0.077	1A	NO	NO	NO	10	10	41
H2_Qaa	H2A-DNA	0.078	0.029	1.674	0.607	1.038	0.596	0.267	0.299	0.106	-0.077	1A	NO	NO	NO	10	10	41
H2_Qaa	H2A-DNA	0.078	0.029	1.674	0.607	1.038	0.596	0.267	0.299	0.106	-0.077	1A	NO	NO	NO	10	10	41
H2_Qaa	H2A-DNA	0.078	0.029	1.674	0.607	1.038	0.596	0.267	0.299	0.106	-0.077	1A	NO	NO	NO	10	10	41
H2_Qaa	H2A-DNA	0.078	0.029	1.674	0.607	1.038	0.596	0.267	0.299	0.106	-0.077	1A	NO	NO	NO	10	10	41
H2_Qaa	H2A-DNA	0.078	0.029	1.674	0.607	1.038	0.596	0.267	0.299	0.106	-0.077	1A	NO	NO	NO	10	10	41
H2_Qaa	H2A-DNA	0.078	0.029	1.674	0.607	1.038	0.596	0.267	0.299	0.106	-0.077	1A	NO	NO	NO	10	10	41
H2_Qaa	H2A-DNA	0.078	0.029	1.674	0.607	1.038	0.596	0.267	0.299	0.106	-0.077	1A	NO	NO	NO	10	10	41
H2_Qaa	H2A-DNA	0.078	0.029	1.674	0.607	1.038	0.596	0.267	0.299	0.106	-0.077	1A	NO	NO	NO	10	10	41
H2_Qaa	H2A-DNA	0.078	0.029	1.674	0.607	1.038	0.596	0.267	0.299	0.106	-0.077	1A	NO	NO	NO	10	10	41
H2_Qaa	H2A-DNA	0.078	0.029	1.674	0.607	1.038	0.596	0.267	0.299	0.106	-0.077	1A	NO	NO	NO	10	10	41
H2_Qaa	H2A-DNA	0.078	0.029	1.674	0.607	1.038	0.596	0.267	0.299	0.106	-0.077	1A	NO	NO	NO	10	10	41
H2_Qaa	H2A-DNA	0.078	0.029	1.674	0.607	1.038	0.596	0.267	0.299	0.106	-0.077	1A	NO	NO	NO	10	10	41
H2_Qaa	H2A-DNA	0.078	0.029	1.674	0.607	1.038	0.596	0.267	0.299	0.106	-0.077	1A	NO	NO	NO	10	10	41
H2_Qaa	H2A-DNA	0.078	0.029	1.674	0.607	1.038	0.596	0.267	0.299	0.106	-0.077	1A	NO	NO	NO	10	10	41
H2_Qaa	H2A-DNA	0.078	0.029	1.674	0.607	1.038	0.596	0.267	0.299	0.106	-0.077	1A	NO	NO	NO	10	10	41
H2_Qaa	H2A-DNA	0.078	0.029	1.674	0.607	1.038	0.596	0.267	0.299	0.106	-0.077	1A	NO	NO	NO	10	10	41
H2_Qaa	H2A-DNA	0.078	0.029	1.674	0.607	1.038	0.596	0.267	0.299	0.106	-0.077	1A	NO	NO	NO	10	10	41
H2_Qaa	H2A-DNA	0.078	0.029	1.674	0.607	1.038	0.596	0.267	0.299	0.106	-0.077	1A	NO	NO	NO	10	10	41
H2_Qaa	H2A-DNA	0.078	0.029	1.674	0.607	1.038	0.596	0.267	0.299	0.106	-0.077	1A	NO	NO	NO	10	10	41
H2_Qaa	H2A-DNA	0.078	0.029	1.674	0.607	1.038	0.596	0.267	0.299	0.106	-0.077	1A	NO	NO	NO	10	10	41
H2_Qaa	H2A-DNA	0.078	0.029	1.674	0.607	1.038	0.596	0.267	0.299	0.106	-0.077	1A	NO	NO	NO	10	10	41
H2_Qaa	H2A-DNA	0.078	0.029	1.674	0.607	1.038	0.596	0.267	0.299	0.106	-0.077	1A	NO	NO	NO	10	10	41
H2_Qaa	H2A-DNA	0.078	0.029	1.674	0.607	1.038	0.596	0.267	0.299	0.106	-0.077	1A	NO	NO	NO	10	10	41
H2_Qaa	H2A-DNA	0.078	0.029	1.674	0.607	1.038	0.596	0.267	0.299	0.106	-0.077	1A	NO	NO	NO	10	10	41
H2_Qaa	H2A-DNA	0.078	0.029	1.674	0.607	1.038	0.596	0.267	0.299	0.106	-0.077	1A	NO	NO	NO	10	10	41
H2_Qaa	H2A-DNA	0.078	0.029	1.674	0.607	1.038	0.596	0.267	0.299	0.106	-0.077	1A	NO	NO	NO	10	10	41
H2_Qaa	H2A-DNA	0.078	0.029	1.674	0.607	1.038	0.596	0.267	0.299	0.106	-0.077	1A	NO	NO	NO	10	10	41
H2_Qaa	H2A-DNA	0.078	0.029	1.674	0.607	1.038	0.596	0.267	0.299	0.106	-0.077	1A	NO	NO	NO	10	10	41
H2_Qaa	H2A-DNA	0.078	0.029	1.674	0.607	1.038	0.596	0.267	0.299	0.106	-0.077	1A	NO	NO	NO	10	10	41
H2_Qaa	H2A-DNA	0.078	0.029	1.674	0.607	1.038	0.596	0.267	0.299	0.106	-0.077	1A	NO	NO	NO	10	10	41
H2_Qaa	H2A-DNA	0.078	0.029	1.674	0.607	1.038	0.596	0.267	0.299	0.106	-0.077	1A	NO	NO	NO	10	10	41
H2_Qaa	H2A-DNA	0.078	0.029	1.674	0.607	1.038	0.596	0.267	0.299	0.106	-0.077	1A	NO	NO	NO	10	10	41
H2_Qaa	H2A-DNA	0.078	0.029	1.674	0.607	1.038	0.596	0.267	0.299	0.106	-0.077	1A	NO	NO	NO	10	10	41
H2_Qaa	H2A-DNA	0.078	0.029	1.674	0.607	1.038	0.596	0.267	0.299	0.106	-0.077	1A	NO	NO	NO	10	10	41
H2_Qaa	H2A-DNA	0.078	0.029	1.674	0.607	1.038	0.596	0.267	0.299	0.106	-0.077	1A	NO	NO	NO	10	10	41
H2_Qaa	H2A-DNA	0.078	0.029	1.674	0.607	1.038	0.596	0.267	0.299	0.106	-0.077	1A	NO	NO	NO	10	10	41
H2_Qaa	H2A-DNA	0.078	0.029	1.674	0.607	1.038	0.596	0.267	0.299	0.106	-0.077	1A	NO	NO	NO	10	10	41
H2_Qaa	H2A-DNA	0.078	0.029	1.674	0.607	1.038	0.596	0.267	0.299	0.106	-0.077	1A	NO	NO	NO	10	10	41
H2_Qaa	H2A-DNA	0.078	0.029	1.674	0.607	1.038	0.596	0.267	0.299	0.106	-0.077	1A	NO					



# Supplementary table E2. Continued.

SDZ02	SDZ11	1	0.616	1.136	0.535	1.523	0.205	0.008	0.333	0.35	1.088**	NO	NO	NO	0	0	
Sdp	SDPR	-0.287	-0.187	-0.277	-0.737	-1.175	-0.888	-0.494	-0.78	-0.286	-0.343	NO	YES	NO	0	0	
SD111	SD112	0.176	0.205	0.184	0.245	0.371	0.273	0.599	0.534	0.548	-0.020**	NO	NO	NO	0	0	
SD113	SD114	-0.351	-0.182	-0.702	-0.496	-1.435	-1.054	-0.207	-0.593	-0.044	-0.216	2	NO	NO	0	0	
SD115	SD116	0.174	0.103	0.131	0.005	0.021	1.514	1.144	1.006	0.458	0.101	14	NO	NO	0	0	
SD117	SD118	0.154	0.206	1.095	0.711	0.489	0.724	0.809	0.222	0.501	0.496	14	NO	NO	0	0	
SD119	SD120	0.302	-0.067	-0.251	-0.537	-0.732	-0.217	-0.139	-0.498	-0.213	-0.203	14	NO	NO	0	0	
SD121	SD122	-0.535	-0.255	-0.62	-0.485	-0.866	-0.091	0.111	-0.259	-0.129	-0.301	14	NO	NO	0	0	
SD123	SD124	0.145	0.205	0.761	0.192	0.333	0.873	0.366	0.623	0.301	0.395	14	NO	NO	0	0	
SD125	SD126	-0.041	0.141	1.095	1.182	0.756	1.081	0.756	0.494	0.574	0.125	14	NO	NO	0	0	
SD127	SD128	1.207	0.187	-0.260	-0.279	0.483	1.048	1.205	1.164	0.021	0.313	14	NO	NO	0	0	
SD129	SD130	1.141	1.302	1.238	1.624	1.756	2.887	1.411	2.846	2.621	1.471	14	NO	NO	0	0	
SD131	SD132	0.496	0.191	0.140	0.127	nan	nan	nan	nan	nan	nan	14	NO	NO	0	0	
SD133	SD134	1.499	1.144	1.402	0.199	1.624	0.725	1.778	1.037	1.063	0.264	14	NO	NO	0	0	
SD135	SD136	0.134	0.202	nan	-0.115	nan	nan	nan	nan	nan	nan	14	NO	NO	0	0	
SD137	SD138	0.379	1.103	0.878	0.8	0.908	0.544	0.518	0.428	0.449	0.687	14	NO	NO	0	0	
SD139	SD140	0.179	0.086	0.702	0.958	0.744	0.076	0.382	0.084	-0.459	0.708	14	NO	NO	0	0	
SD141	SD142	0.182	0.465	0.791	0.956	0.209	nan	nan	nan	nan	nan	4	NO	NO	0	0	
SD143	SD144	0.707	0.392	1.079	1.464	0.485	nan	nan	nan	nan	nan	4	NO	NO	0	0	
SD145	SD146	0.130	0.025	0.028	0.239	0.42	0.772	0.067	0.636	0.263	0.305	14	NO	NO	0	0	
SD147	SD148	0.478	0.067	1.149	0.617	0.505	0.42	0.235	-0.245	0.454	0.436**	NO	NO	NO	0	0	
SD149	SD150	-0.187	0.012	0.762	0.465	0.886	1.061	0.908	0.407	0.465	0.178	14	NO	NO	0	0	
SD151	SD152	0.065	0.562	0.647	0.156	0.145	0.08	-0.113	0.004	-0.193	-1.466	14	NO	YES	NO	0	0
SD153	SD154	0.299	0.192	1.298	1.788	0.737	0.506	0.512	0.352	0.213	0.478	14	NO	NO	0	0	
SD155	SD156	0.194	0.141	1.591	0.936	0.803	1.206	1.704	0.803	0.803	0.178	14	NO	NO	0	0	
SD157	SD158	0.303	0.054	0.508	0.533	0.807	0.281	-0.002	0.619	0.637	0.71**	NO	NO	NO	0	0	
SD159	SD160	0.408	0.408	0.408	0.408	0.408	0.408	0.408	0.408	0.408	0.408	NO	NO	NO	0	0	
SD161	SD162	0.185	0.136	0.267	0.583	0.607	0.882	0.265	0.932	0.432	0.309	14	NO	NO	0	0	
SD163	SD164	0.124	0.168	0.081	0.023	1.248	2.489	0.605	0.447	0.461	0.307	14	NO	NO	0	0	
SD165	SD166	0.044	0.287	0.513	0.855	0.622	0.184	0.566	0.067	0.352	0.955**	NO	NO	NO	0	0	
SD167	SD168	-0.197	-0.188	-1.875	-0.221	-0.633	-0.122	-0.202	-0.059	-0.153	-1.105	14	NO	NO	0	0	
SD169	SD170	0.566	0.174	0.2115	0.393	0.144	1.921	1	1.127	0.307	0.1108	14	NO	NO	0	0	
SD171	SD172	0.217	0.506	0.769	0.264	0.45	0.752	0.478	0.654	0.281	0.646**	NO	NO	NO	0	0	
SD173	SD174	2.105	1.174	1.805	0.945	1.332	1.079	1.272	0.909	1.022	0.025	14	NO	NO	0	0	
SD175	SD176	0.612	1.038	2.407	0.504	2.448	0.002	0.016	1.097	0.761	4.789	14	NO	NO	0	0	
SD177	SD178	0.144	1.561	0.486	0.486	0.208	0.112	0.355	0.376	0.268	0.129**	NO	NO	NO	0	0	
SD179	SD180	0.992	0.726	1.168	1.173	1.257	0.937	0.743	0.757	0.007	1.435**	NO	NO	NO	0	0	
SD181	SD182	0.548	0.191	0.827	0.179	0.986	0.239	0.101	1.123	0.544	0.511**	NO	NO	NO	0	0	
SD183	SD184	0.139	0.542	1.106	1.126	0.534	1.386	0.952	0.747	0.339	0.324**	NO	NO	NO	0	0	
SD185	SD186	0.101	0.138	0.11	0.416	0.058	-0.04	0.244	0.055	1.115	0.364	0.062**	NO	NO	NO	0	0
SD187	SD188	-0.157	-0.185	-0.128	0.137	-0.068	0.054	-0.239	-0.376	-0.019	-0.333	14	NO	NO	0	0	
SD189	SD190	0.107	0.281	1.056	0.79	0.778	0.99	0.645	0.714	0.17	0.415	14	NO	NO	0	0	
SD191	SD192	-0.202	-0.151	-0.661	-0.719	-1.191	-2.018	-0.471	-0.787	-0.191	-0.106	4	NO	NO	0	0	
SD193	SD194	0.026	0.005	0.135	0.023	0.148	0.042	0.144	0.042	0.144	0.124	4	NO	NO	0	0	
SD195	SD196	0.173	0.116	0.763	0.417	0.127	0.008	0.284	-0.278	0.101	-0.393	4	NO	NO	0	0	
SD197	SD198	0.148	0.168	0.081	0.023	1.248	2.489	0.605	0.447	0.461	0.307	4	NO	NO	0	0	
SD199	SD200	0.112	0.145	0.6065	0.1945	0.456	0.009	0.282	0.78	0.309	0.201**	NO	NO	NO	0	0	
SD201	SD202	0.108	0.095	0.146	0.146	0.146	0.146	0.146	0.146	0.146	0.146	NO	NO	NO	0	0	
SD203	SD204	0.1785	0.39	0.183	0.0025	0.1745	1.174	0.173	1.403	0.175	0.265	14	NO	NO	0	0	
SD205	SD206	0.141	0.214	0.214	0.214	0.214	0.214	0.214	0.214	0.214	0.214	NO	NO	NO	0	0	
SD207	SD208	0.047	0.557	0.181	0.0177	0.174	2.566	1.228	1.517	0.637	0.438	14	NO	NO	0	0	
SD209	SD210	0.249	0.117	0.107	0.425	0.135	0.801	0.298	1.052	0.143	0.467	14	NO	NO	0	0	
SD211	SD212	0.1465	-0.174	-0.215	0.112	-0.469	0.218	-0.132	-0.141	-0.141	-0.212	4	NO	NO	0	0	
SD213	SD214	-0.2025	-0.205	-0.3945	-0.4025	-0.607	-1.180	-0.109	-0.550	-0.444	-0.212	14	NO	NO	0	0	
SD215	SD216	0.271	-0.005	0.147	0.068	0.217	0.429	0.235	0.409	0.262	0.214	NO	NO	NO	0	0	
SD217	SD218	0.138	0.482	-0.013	0.495	-0.222	-0.092	-0.171	0.655	0.311	0.538	14	NO	NO	0	0	
SD219	SD220	0.148	0.148	0.491	0.172	1.111	0.484	0.312	0.11	-0.242	-0.1865**	NO	NO	NO	0	0	
SD221	SD222	nan	nan	0.212	0.534	0.431	nan	nan	nan	nan	0.714	14	NO	NO	0	0	
SD223	SD224	1.103	0.941	1.741	0.321	0.646	nan	nan	nan	nan	0.137	4	NO	NO	0	0	
SD225	SD226	-0.187	-0.0495	-0.085	-0.0315	-0.568	2.104	0.227	0.543	-0.172	-0.0885	14	NO	NO	0	0	
SD227	SD228	-0.0335	0.1745	0.8395	0.4435	0.802	nan	nan	nan	nan	-0.0705	14	NO	NO	0	0	
SD229	SD230	-0.154	-0.196	-0.119	-0.102	nan	nan	nan	nan	nan	nan	NO	YES	NO	0	0	
SD231	SD232	0.189	0.189	0.117	0.102	0.147	0.159	0.109	0.109	0.109	0.109	NO	YES	NO	0	0	
SD233	SD234	-0.278	-0.202	-0.193	-0.623	-0.742	-0.474	-0.476	-0.61	-0.346	-0.294	14	NO	NO	0	0	
SD235	SD236	0.205	0.205	0.205	0.205	0.205	0.205	0.205	0.205	0.205	0.205	NO	NO	NO	0	0	
SD237	SD238	0.185	0.031	0.528	0.176	0.838	1.482	1.091	0.983	0.489	0.248	14	NO	NO	0	0	
SD239	SD240	0.148	0.148	0.148	0.148	0.148	0.148	0.148	0.148	0.148	0.148	NO	NO	NO	0	0	
SD241	SD242	-0.125	0.0095	-0.275	-0.264	-0.498	-0.215	-0.54	-0.3	-0.824	0.035	14	NO	NO	0	0	
SD243	SD244	0.108	0.088	0.088	0.088	0.088	0.088	0.088	0.088	0.088	0.088	NO	NO	NO	0	0	
SD245	SD246	-0.079	0.2335	1.008	1.217	0.0875	0.01	0.364	0.688	0.777	-1.045	14	YES	NO	0	0	
SD247	SD248	0.115	0.115	0.115	0.115	0.115	0.115	0.115	0.115	0.115	0.115	NO	YES	NO	0	0	
SD249	SD250	0.025	-0.025	-0.128	-0.1765	-0.138	-0.118	-0.111	-0.014	-0.103	0.038	14	NO	NO	0	0	
SD251	SD252	0.061	0.124	-0.154	-0.144	-0.422	-0.948	-0.462	-0.637	-0.06	0.077	NO	NO	NO	0	0	
SD253	SD254	0.1805	0.1805	0.1805	0.1805	0.1805	0.1805	0.1805	0.1805	0.1805	0.1805	NO	NO	NO	0	0	
SD255	SD256	0.4085	0.321	1.125	1.266	0.72	2.528	1.465	1.897	0.79	1.113**	NO	NO	NO	0	0	
SD257	SD258	-0.305	-0.1085	-0.205	-0.2005	-0.109	-0.102	-0.206	-0.204	0.146	0.108**	NO	NO	NO	0	0	
SD259	SD260	0.156	-0.156	-0.0615	0.7983	0.613	nan	nan	nan	nan	nan	4	NO	NO	0	0	
SD261	SD262	-0.192	-0.192	-0.192	-0.192	-0.192	-0.192	-0.192	-0.192	-0.192	-0.192	4	NO	NO	0	0	
SD263	SD264	0.1875	0.1875	0.1875	0.1875	0.1875	0.1875	0.1875	0.1875	0.1875	0.1875	NO	NO	NO	0	0	
SD265	SD266	0.136	0.136	0.136	0.136	0.136	0.136	0.136	0.136	0.136	0.136	NO	NO	NO	0	0	
SD267	SD268	-0.217	0.013	0.507	0.149	0.055	0.566	0.169	0.408	0.459	0.248**	NO					

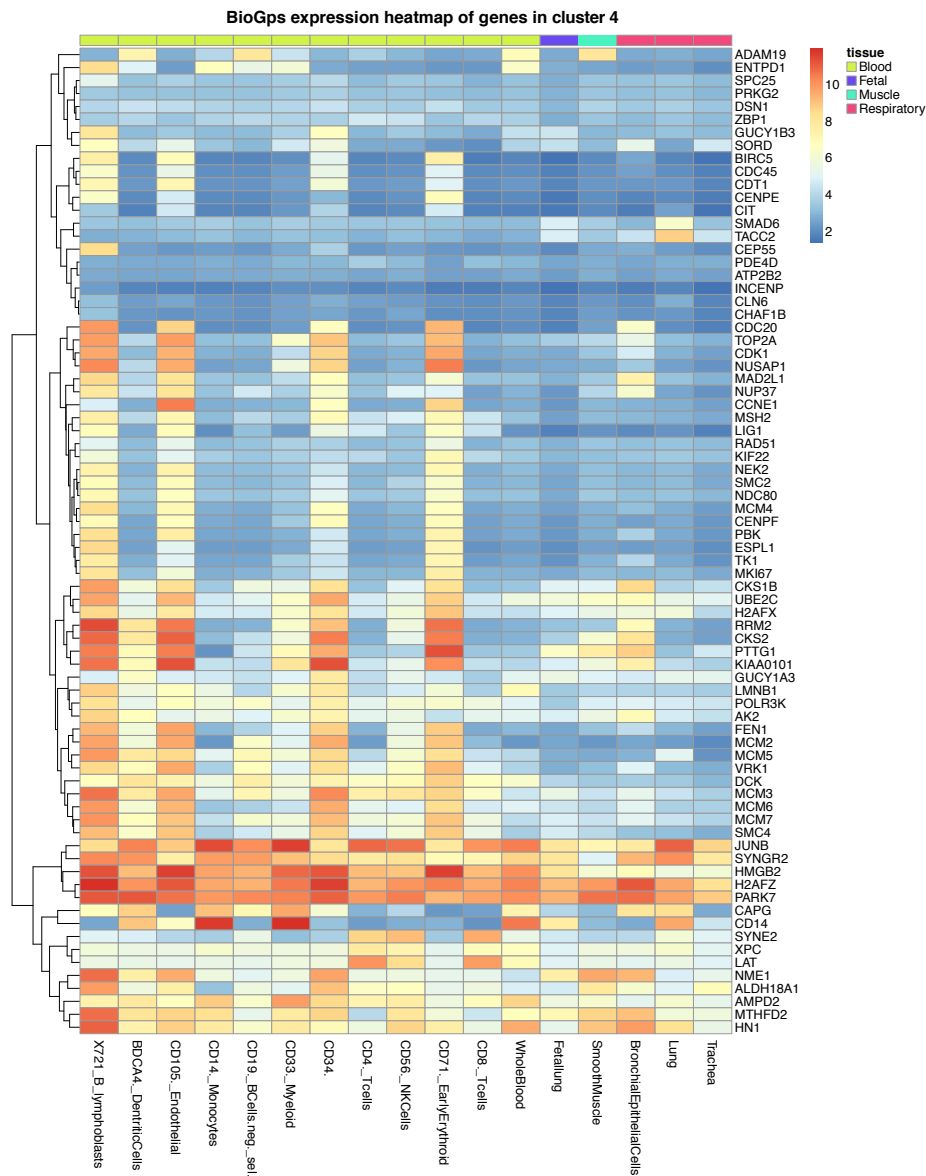
## Supplementary Figures



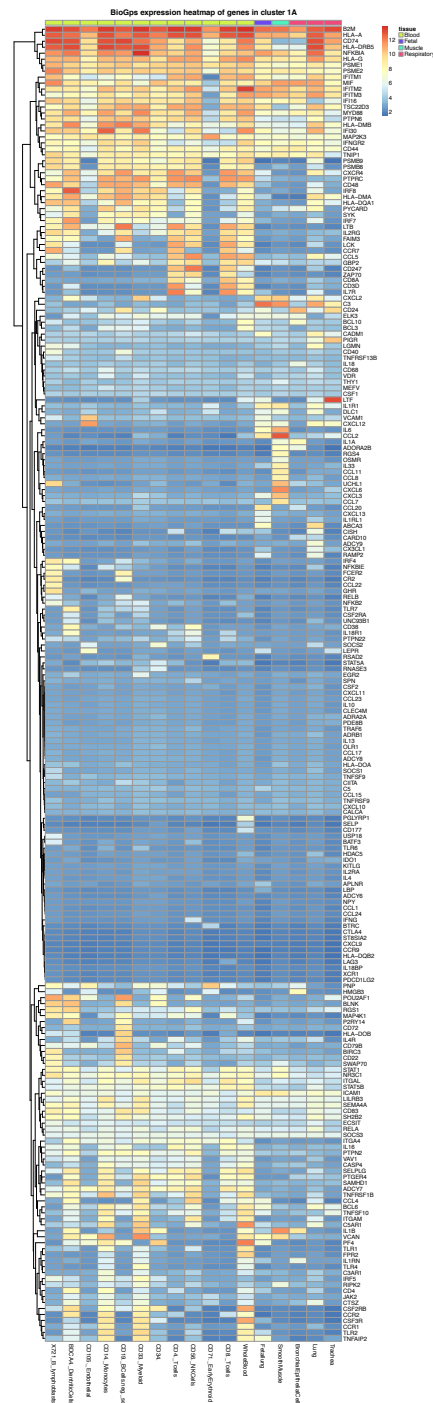
**Supplementary Figure E1.** Ovalbumin (OVA) immunized and challenged mice have increased airway and lung inflammation, mucus hypersecretion, serum allergen-specific IgG1 and IgE titers, airway hyperresponsiveness, and type-2 related cytokine and chemokine gene expression in the lungs compared to control animals. (A) Schematic representation of acute allergic asthma model. (B) Total and differential cell counts in bronchoalveolar lavage fluid. T – total cells, M – macrophages, E – eosinophils, N – neutrophils, L – lymphocytes. (C) Representative photomicrographs of H&E stained lung sections. Inset shows eosinophils in inflammatory infiltrates in asthmatic mice. Scale bars: 200  $\mu$ m (inset 50  $\mu$ m), original objective: 10x (inset 40x). (D) Grades for lung inflammation; for description please refer to material and methods. (E) Representative photomicrographs of Periodic-acid Schiff (PAS) stained lung sections showing fuchsia-stained mucus in epithelial goblet cells of asthmatic animals. Scale bar: 200  $\mu$ m; original objective: 10x. (F) Number of mucus-positive cells per millimeter of basement membrane. (G) Serum titers of OVA-specific IgG1 and IgE. (H) Airway resistance and dynamic compliance in response to methacholine presented as relative difference to base-

line values measured after PBS nebulization. (I) Increased mRNA expression of selected type-2 immune response cytokines and chemokines in whole lungs at 24 and 72h after OVA challenge. Data are expressed as relative difference to corresponding PBS challenged mice. Data in A-G and I are shown as mean  $\pm$  SEM and are representative from at least 2 independent experiments ( $n = 3$ ). Data in H show summary for at least 5 mice per group and are shown as mean  $\pm$  SEM. (B-H) \*  $p < 0.05$  unpaired Student's  $t$ -test.

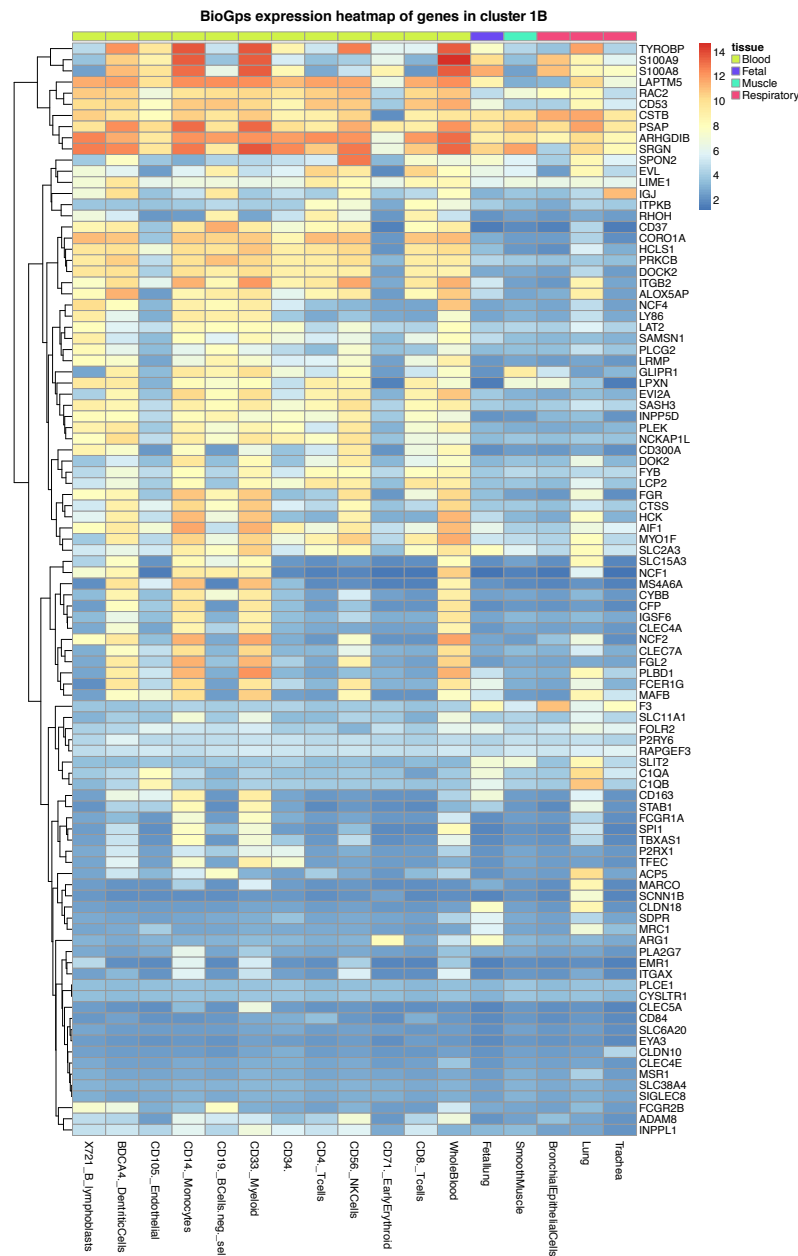




**Supplementary Figure E3.** BioGPS expression heatmap of cluster 4 genes indicates enrichment for genes highly overexpressed in B lymphoblasts, CD105<sup>+</sup> Endothelial cells, CD34<sup>+</sup> cells and CD71<sup>+</sup> early erythroid cells. Data are shown as expression levels normalized in log scale within selected set of 17 different tissues (12 leukocytes and 5 present in whole lungs). Euclidean distance was used for clustering genes.

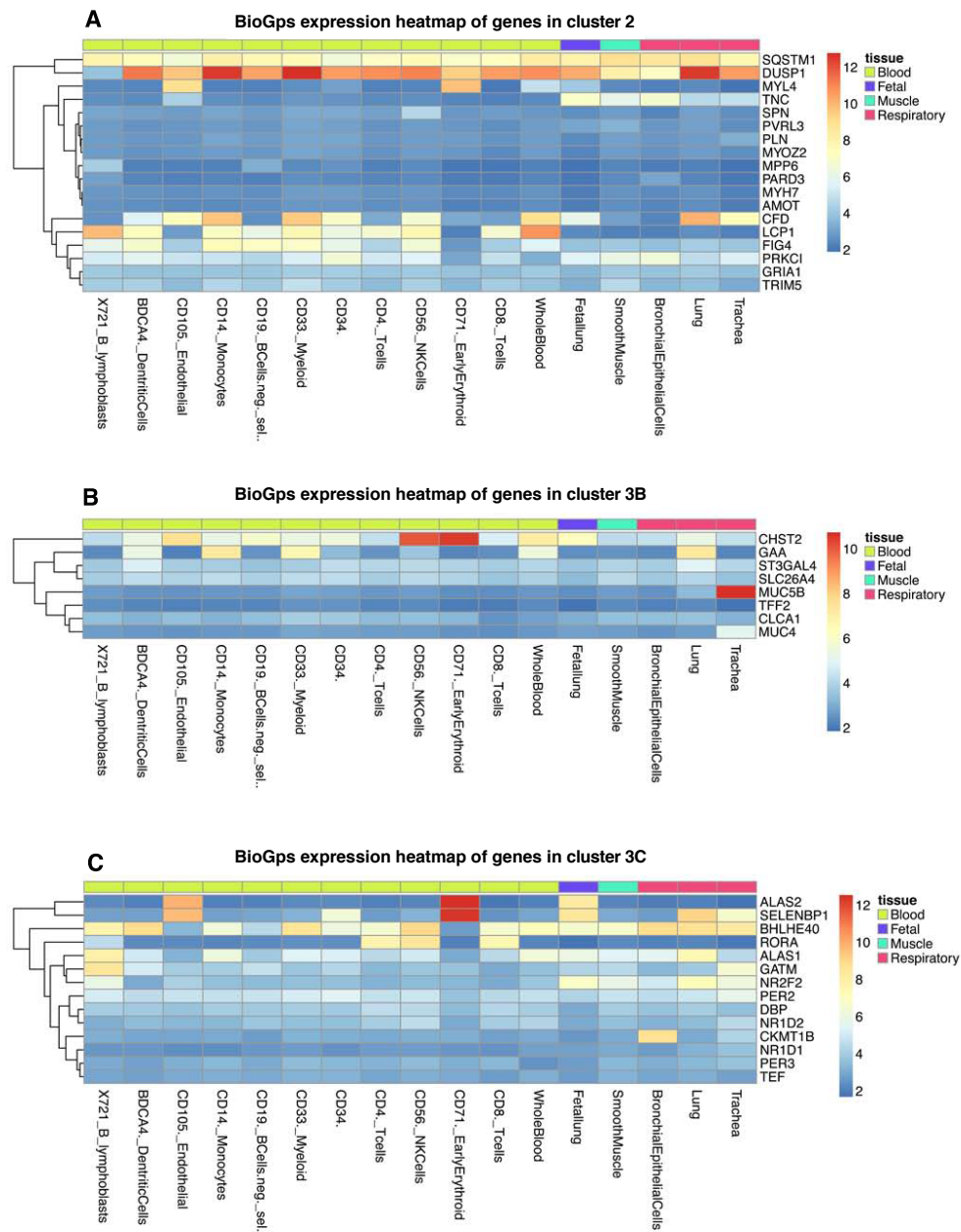


**Supplementary Figure E4.** BioGPS expression heatmap of cluster 1A genes indicates enrichment for genes overexpressed in leukocytes compared to the lung tissues, indicating that genes in cluster 1A are mainly involved in inflammation. Data are shown as expression levels normalized in log scale within selected set of 17 different tissues (12 leukocytes and 5 present in whole lungs). Euclidean distance was used for clustering genes.

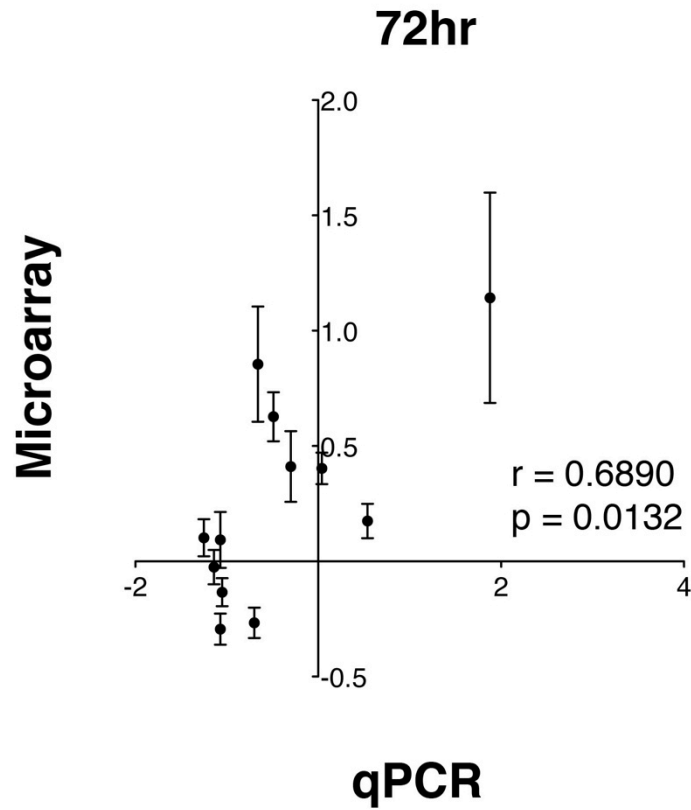


**Supplementary Figure E5.** BioGPS expression heatmap of cluster 1B genes indicates enrichment for genes overexpressed in the lung tissues compared to leukocytes, suggesting that those genes are involved in lung tissue response to allergic inflammation. Data are shown as expression levels normalized in log scale within selected set of 17 different tissues (12 leukocytes and 5 present in whole lungs). Euclidean distance was used for clustering genes.

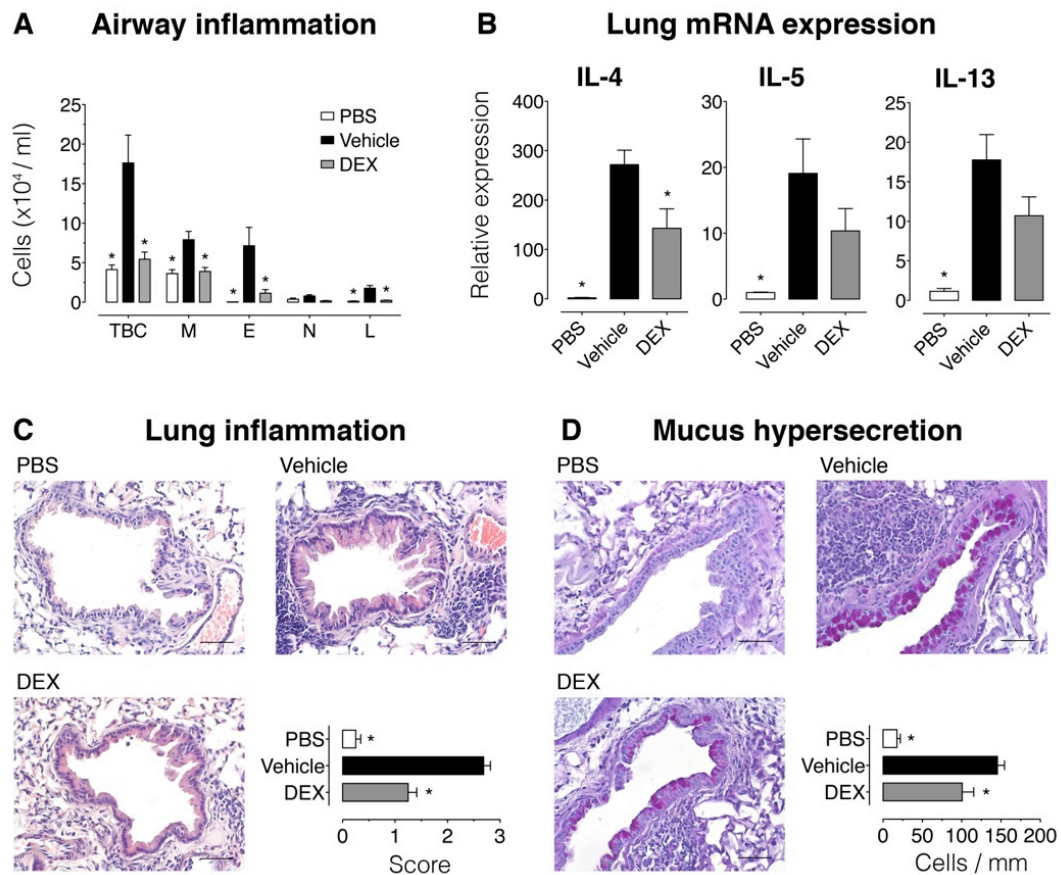




**Supplementary Figure E7.** BioGPS expression heatmap of (A) cluster 2, (B) cluster 3B and (C) cluster 3C genes. No specific tissue was found enriched in these clusters, probably due to low number of genes in each cluster. Data are shown as expression levels normalized in log scale within selected set of 17 different tissues (12 leukocytes and 5 present in whole lungs). Euclidean distance was used for clustering genes.



**Supplementary Figure E8.** Microarray data for 12 super-connector genes from 10 comparisons of control and asthmatic mice correlate to quantitative PCR data from our independent mouse asthma model. For qPCR, OVA-sensitized BALB/c mice received PBS (controls) or OVA challenge 72h before extraction of total lung RNA. Pearson  $r$  coefficients and  $p$  values for each correlation are indicated.



**Supplementary Figure E9.** Dexamethasone significantly inhibits airway and lung inflammation, mucus hypersecretion and lung cytokine mRNA expression. (A) Total and differential cell counts in bronchoalveolar lavage fluid of control (PBS challenged), vehicle and dexamethasone (DEX) treated mice 72h after the last aerosol challenge. T – total cells, M – macrophages, E – eosinophils, N – neutrophils, L – lymphocytes. (B) Dexamethasone treatment suppressed IL-4, IL-5, and IL-13 mRNA expression in whole lungs at 72h after OVA challenge. Data are expressed as relative difference to corresponding PBS challenged mice. (C) Representative photomicrographs of H&E stained lung sections (scale bars: 50  $\mu$ m, original objective: 40x). Control animals (PBS) have normal lung physiology, while dense eosinophilic inflammatory infiltrates in vehicle-treated mice and are reduced in dexamethasone (DEX) treated group. Grades for lung inflammation were done according to the description in material and methods. (D) Representative photomicrographs of Periodic-acid Schiff (PAS) stained lung sections with fuchsia-stained mucus in epithelial goblet cells (scale bars: 50  $\mu$ m, original objective: 40x) and numbers of mucus-positive cells per millimeter of basement membrane. Data are

shown as mean  $\pm$  SEM and are pooled from 2 independent experiments ( $n = 6$ ). \*  $p < 0.05$  vs. vehicle treated group, one-way ANOVA followed by Tukey's multiple comparison test.



## Supplementary references

- E1. Edgar R, Domrachev M, Lash AE. Gene Expression Omnibus: NCBI gene expression and hybridization array data repository. *Nucleic Acids Res* 2002;30:207–210.
- E2. Gentleman RC, Carey VJ, Bates DM, Bolstad B, Dettling M, Dudoit S, Ellis B, Gautier L, Ge Y, Gentry J, Hornik K, Hothorn T, Huber W, Iacus S, Irizarry R, Leisch F, Li C, Maechler M, Rossini AJ, Sawitzki G, Smith C, Smyth G, Tierney L, Yang JYH, Zhang J. Bioconductor: open software development for computational biology and bioinformatics. *Genome Biol* 2004;5:R80.
- E3. Irizarry RA, Hobbs B, Collin F, Beazer-Barclay YD, Antonellis KJ, Scherf U, Speed TP. Exploration, normalization, and summaries of high density oligonucleotide array probe level data. *Biostatistics* 2003;4:249–264.
- E4. Benjamini Y, Hochberg Y. Controlling the false discovery rate: a practical and powerful approach to multiple testing. *Journal of the Royal Statistical Society Series B Methodological* 1995;57:289–300.
- E5. Franceschini A, Szklarczyk D, Frankild S, Kuhn M, Simonovic M, Roth A, Lin J, Minguez P, Bork P, Mering von C, Jensen LJ. STRING v9.1: protein-protein interaction networks, with increased coverage and integration. *Nucleic Acids Res* 2013;41:D808–15.
- E6. Saito R, Smoot ME, Ono K, Ruscheinski J, Wang P-L, Lotia S, Pico AR, Bader GD, Ideker T. A travel guide to Cytoscape plugins. *Nat Methods* 2012;9:1069–1076.
- E7. Dennis G, Sherman BT, Hosack DA, Yang J, Gao W, Lane HC, Lempicki RA. DAVID: Database for Annotation, Visualization, and Integrated Discovery. *Genome Biol* 2003;4:P3.
- E8. Yu G, Li F, Qin Y, Bo X, Wu Y, Wang S. GOSemSim: an R package for measuring semantic similarity among GO terms and gene products. *Bioinformatics* 2010;26:976–978.
- E9. Hong F, Breitling R, McEntee CW, Wittner BS, Nemhauser JL, Chory J. RankProd: a bioconductor package for detecting differentially expressed genes in meta-analysis. *Bioinformatics* 2006;22:2825–2827.
- E10. Hong F, Breitling R. A comparison of meta-analysis methods for detec-

- ting differentially expressed genes in microarray experiments. *Bioinformatics* 2008;24:374–382.
- E11. Maglott D, Ostell J, Pruitt KD, Tatusova T. Entrez Gene: gene-centered information at NCBI. *Nucleic Acids Res* 2011;39:D52–7.
- E12. Chen J, Bardes EE, Aronow BJ, Jegga AG. ToppGene Suite for gene list enrichment analysis and candidate gene prioritization. *Nucleic Acids Res* 2009;37:W305–11.
- E13. Rappaport N, Twik M, Nativ N, Stelzer G, Bahir I, Stein TI, Safran M, Lancet D. MalaCards: A Comprehensive Automatically-Mined Database of Human Diseases. *Curr Protoc Bioinformatics* 2014;47:1.24.1–1.24.19.
- E14. Stelzer G, Dalah I, Stein TI, Satanower Y, Rosen N, Nativ N, Oz-Levi D, Olender T, Belinky F, Bahir I, Krug H, Perco P, Mayer B, Kolker E, Safran M, Lancet D. In-silico human genomics with GeneCards. *Hum Genomics* 2011;5:709–717.
- E15. Csardi G, Nepusz T. The igraph software package for complex network research. *InterJournal, Complex Systems* 2015;1695.
- E16. Chen EY, Tan CM, Kou Y, Duan Q, Wang Z, Meirelles GV, Clark NR, Ma'ayan A. Enrichr: interactive and collaborative HTML5 gene list enrichment analysis tool. *BMC Bioinformatics* 2013;14:128.
- E17. Wu C, Orozco C, Boyer J, Leglise M, Goodale J, Batalov S, Hodge CL, Haase J, Janes J, Huss JW, Su AI. BioGPS: an extensible and customizable portal for querying and organizing gene annotation resources. *Genome Biol* 2009;10:R130.
- E18. Bosnjak B, Tilp C, Tomsic C, Dekan G, Pieper MP, Erb KJ, Epstein MM. Tiotropium bromide inhibits relapsing allergic asthma in BALB/c mice. *Pulmonary Pharmacology & Therapeutics* 2014;27:44–51.

### 3.2. Publication 1

#### **Dendritic polyglycerolsulfate near infrared fluorescent (NIRF) dye conjugate for non-invasively monitoring of inflammation in an allergic asthma mouse model**

Stefania Biffi<sup>1,2,\*</sup>, Simeone Dal Monego<sup>3,\*</sup>, Christian Dullin<sup>4</sup>, Chiara Garrovo<sup>1,2</sup>, Berislav Bosnjak<sup>5</sup>, Kai Licha<sup>6</sup>, Pia Welker<sup>6</sup>, Michelle M. Epstein<sup>5</sup>, Frauke Alves<sup>7</sup>

<sup>1</sup> *Cluster in Biomedicine (CBM srl), Optical Imaging Laboratory, Trieste, Italy*

<sup>2</sup> *Institute for Maternal and Child Health, IRCCS Burlo Garofolo, Trieste, Italy,*

<sup>3</sup> *Cluster in Biomedicine (CBM srl), Bioinformatics, Trieste, Italy,*

<sup>4</sup> *Department of Diagnostic Radiology, University Medical Center Göttingen, Göttingen, Germany,*

<sup>5</sup> *Department of Dermatology, Division of Immunology, Allergy and Infectious Diseases, Experimental Allergy, Medical University of Vienna, Vienna, Austria,*

<sup>6</sup> *Mivenion GmbH, Berlin, Germany,*

<sup>7</sup> *Department of Hematology and Oncology, University Medical Center, Göttingen, Germany*

**Published in: PLoS ONE 2013; 8(2): e57150.**

**doi:10.1371/journal.pone.0057150**

\* *These authors contributed equally to this work.*

# Dendritic Polyglycerolsulfate Near Infrared Fluorescent (NIRF) Dye Conjugate for Non-Invasively Monitoring of Inflammation in an Allergic Asthma Mouse Model

Stefania Biffi<sup>1,2,\*</sup>, Simeone Dal Monego<sup>3,9</sup>, Christian Dullin<sup>4</sup>, Chiara Garrovo<sup>1,2</sup>, Berislav Bosnjak<sup>5</sup>, Kai Licha<sup>6</sup>, Pia Welker<sup>6</sup>, Michelle M. Epstein<sup>5</sup>, Frauke Alves<sup>7</sup>

**1** Cluster in Biomedicine (CBM srl), Optical Imaging Laboratory, Trieste, Italy, **2** Institute for Maternal and Child Health, IRCCS Burlo Garofolo, Trieste, Italy, **3** Cluster in Biomedicine (CBM srl), Bioinformatics, Trieste, Italy, **4** Department of Diagnostic Radiology, University Medical Center Göttingen, Göttingen, Germany, **5** Department of Dermatology, Division of Immunology, Allergy and Infectious Diseases, Experimental Allergy, Medical University of Vienna, Vienna, Austria, **6** Mivenion GmbH, Berlin, Germany, **7** Department of Hematology and Oncology, University Medical Center Göttingen, Germany

## Abstract

**Background:** Non-invasive *in vivo* imaging strategies are of high demand for longitudinal monitoring of inflammation during disease progression. In this study we present an imaging approach using near infrared fluorescence (NIRF) imaging in combination with a polyanionic macromolecular conjugate as a dedicated probe, known to target L- and P-selectin and C3/C5 complement factors.

**Methodology/Principal Findings:** We investigated the suitability of dendritic polyglycerol sulfates (dPGS), conjugated with a hydrophilic version of the indocyanine green label with 6 sulfonate groups (6S-ICG) to monitor sites of inflammation using an experimental mouse model of allergic asthma. Accumulation of the NIRF-conjugated dPGS (dPGS-NIRF) in the inflamed lungs was analyzed *in* and *ex vivo* in comparison with the free NIRF dye using optical imaging. Commercially available smart probes activated by matrix metalloproteinase's (MMP) and cathepsins were used as a comparative control. The fluorescence intensity ratio between lung areas of asthmatic and healthy mice was four times higher for the dPGS in comparison to the free dye *in vivo* at four hrs post intravenous administration. No significant difference in fluorescence intensity between healthy and asthmatic mice was observed 24 hrs post injection for dPGS-NIRF. At this time point *ex-vivo* scans of asthmatic mice confirmed that the fluorescence within the lungs was reduced to approximately 30% of the intensity observed at 4 hrs post injection.

**Conclusions/Significance:** Compared with smart-probes resulting in a high fluorescence level at 24 hrs post injection optical imaging with dPGS-NIRF conjugates is characterized by fast uptake of the probe at inflammatory sites and represents a novel approach to monitor lung inflammation as demonstrated in mice with allergic asthma.

**Citation:** Biffi S, Dal Monego S, Dullin C, Garrovo C, Bosnjak B, et al. (2013) Dendritic Polyglycerolsulfate Near Infrared Fluorescent (NIRF) Dye Conjugate for Non-Invasively Monitoring of Inflammation in an Allergic Asthma Mouse Model. PLoS ONE 8(2): e57150. doi:10.1371/journal.pone.0057150

**Editor:** Henrik Einwaechter, Klinikum rechts der Isar der TU München, Germany

**Received:** January 27, 2012; **Accepted:** January 21, 2013; **Published:** February 21, 2013

**Copyright:** © 2013 Biffi et al. This is an open-access article distributed under the terms of the Creative Commons Attribution License, which permits unrestricted use, distribution, and reproduction in any medium, provided the original author and source are credited.

**Funding:** The funders (European Commission through an FP7- IAPP Marie Curie Action - (GA 230739)) had no role in study design, data collection and analysis, decision to publish, or preparation of the manuscript.

**Competing Interests:** Stefania Biffi, Simeone dal Monego and Chiara Garrovo are employees of Cluster in Biomedicine (CBM Srl). CBM offers services in different research areas, spanning from genomics and bioinformatics, to optical imaging and advanced microscopy. CBM is also actively involved in research collaborations within the framework of european and national projects, as well as project management and grant writing support. Kai Licha and Pia Welker are employees of Mivenion GmbH. Mivenion is a life-science company focusing on personalized medicine for patients with inflammatory and autoimmune diseases. A network of academia and industry partners is supporting Mivenion. This does not alter the authors' adherence to all the PLOS ONE policies on sharing data and materials. The authors from Academia (Goettingen and Vienna) have declared that no competing interests exist.

\* E-mail: stefania.biffi@cbm.fvg.it

<sup>9</sup> These authors contributed equally to this work.

## Introduction

Currently, NIRF imaging is a common technology in preclinical studies that obtains functional information *in vivo* over time for assessment of antibody binding, protein expression, enzyme activities, cell tracking etc. [1–3]. Optical imaging provides relatively inexpensive and non-harmful methods and is preferred over other imaging methods used in preclinical research and drug development, such as PET and SPECT that are more complex to perform. However, the penetration depth of typically up to 4 cm

in the near infrared range (NIR) limits its clinical application to endoscopic techniques and structures beneath the skin or fluorescence guided surgery [4]. Crucial for the success of *in vivo* NIRF imaging will be the development of dedicated NIRF probes for distinct targets of molecular events characterizing different diseases. So far, these probes, based on their mechanisms of target-detection can be divided into four groups: passive probes to image areas with increased blood supply [5], target-specific fluorescent probes which are directed against molecular and/or disease-specific markers [6], fluorescent labels to track injected fluores-

cence stained cells [7], and application of smart probes activated by enzymes for the detection of molecular events [8].

NIRF imaging in lung disease models has remained challenging due to the high scattering nature of the lung and its comparable deep location. Recent application of novel non-invasive imaging technologies in mouse models of asthma has enabled functional and longitudinal *in vivo* monitoring of disease, validation of novel biomarkers, and direct tracking of immune cells within tissues. Novel methods for *in vivo* monitoring of lung inflammation in mice include the utilization of smart-probes activated by MMPs or cathepsin, enzymes known to be involved in lung inflammation [9–11].

Airway inflammation is a central component of asthma that consists of edema, cellular infiltration, particularly of eosinophils, neutrophils, activated T lymphocytes and mast cells, increased airway secretions, and deposition of excess collagen. Therefore mouse models of asthma present attractive tools for evaluating probes suitable for *in vivo* molecular imaging of lung inflammation [12,13].

Using a model of allergen-induced lung inflammation, we applied fluorescence imaging in combination with near-infrared (NIR) fluorescently-labeled dendritic polyglycerol sulfates (dPGS), a class of compounds that selectively bind to mediators of inflammatory processes such as L- and P-selectin and C3/C5 complement factors [14,15]. The role of selectin-ligand interactions in allergic asthma is well established, making them an attractive target for visualization of inflammation [16–19]. For example, reduced airway hyperresponsiveness in asthma in L-Selectin-deficient mice has been reported [19]. Furthermore, studies show that dPGS is transported into inflammatory cells e.g. in activated mononuclear cells [20,21]. Generally, dPGS consists of a highly branched (dendritic) polyglycerol core, which due to the large amount of hydroxyl end groups enables high functionalization. In our case, sulfate groups were generated from the hydroxyl groups, thereby creating the highly charged, polyanionic dPGS compound (Figure 1). dPGS acts via a multivalent binding mechanism mimicking naturally occurring selectin ligands [20], with a clearly demonstrated dependence of the binding affinity from molecular weight and degree of sulfation [15,21]. Sulfation of the hydroxyl groups in the polymer established a multivalent polyanionic entity with high affinity for L- and P-selectin [22]. Anti-inflammatory property of dPGS in much higher concentrations has been reported to occur as a result of a multivalent interaction enabled by the multitude of sulfate groups. For instance, binding of dPGS to L-selectin on leukocytes and P-selectin on inflamed vascular endothelium reduces leukocyte extravasation by shielding the adhesion molecule [22]. Additionally, inhibition of C5a generation inhibits leukocyte chemotaxis [14,22].

The compound used herein has a core molecular weight of about 6000 Da, imparting high binding affinity of the respective polysulfate [21] and at the same time having a reasonable molecular weight range for sufficient distribution and excretion [20], as well as chemical derivatization in order to conjugate NIRF dyes to the polymeric entity. The aim of the present study was to assess the capacity of dPGS conjugated with a near infrared fluorescent (NIRF) dye related to indocyanine green (dPGS-NIRF) to detect inflammatory sites in lungs by NIRF optical imaging analysis in a mouse model of asthma and to compare dPGS-NIRF to the commercially available smart-probes MMPsense and ProSense.

## Results

### OVA-immunization and challenge-induced allergic inflammation and extensive mucus hypersecretion in the lungs, and elevated serum OVA-specific IgG1

Allergic asthma inflammation and mucus hypersecretion in mice was induced by two intraperitoneal injections and subsequent intranasal challenges with OVA. Figure 2 illustrates lung histology from H&E and PAS-stained lung sections of asthmatic and healthy control mice. H&E staining revealed that no inflammatory infiltrates were present in lungs from healthy mice (Figure 2A). In contrast, immunized mice had dense inflammatory infiltrates containing predominantly eosinophils, as well as macrophages and lymphocytes surrounding blood vessels, and large and small airways (Figure 2B). The extent of allergic inflammation was evaluated by assessing the total surface area and location of leukocyte infiltration in lung sections (Figure 2C). Mice with allergic inflammation have histological scores of  $5.2 \pm 0.4$  (dPGS-NIRF group) and  $4.4 \pm 0.3$  (dye group) compared to healthy controls with  $0.5 \pm 0.3$  (dPGS-NIRF group) to  $0.8 \pm 0.3$  (dye group), demonstrating that diseased mice have lung inflammation affecting more than two thirds of the examined lung sections with infiltrates present in the hilum extending to the lung periphery.

To assess mucus hypersecretion, adjacent lungs sections were stained with PAS. As expected, only rare mucus producing cells were detected in the central airways of healthy control mice (Figure 2D), whereas numerous mucus producing cells were observed in asthmatic mice (Figure 2E). Histological evaluation revealed that asthmatic mice have histological scores for mucus overproduction of  $2.8 \pm 0.4$  (dPGS-NIRF group) and  $2.5 \pm 0.5$  (dye group) compared to healthy controls with  $0.3 \pm 0.3$  (dPGS-NIRF group) to  $0.2 \pm 0.3$  (dye group) (Figure 2F), indicating that mucus hypersecretion extended to the periphery of the diseased lungs.

We also tested serum OVA-specific Th2-isotype antibody titres. While no OVA-specific antibodies in sera were detected before immunization with OVA, high titres ( $\geq 1:7812500$ ) of OVA-specific IgG1 were detected in all OVA-sensitized and challenged mice (results not shown), further supporting presence of allergic immune responses in both investigated groups.

### Allergic asthma can be successfully visualized by combination of dPGS-NIRF probe and *in vivo* optical imaging

To visualize allergic inflammation *in vivo*, we injected dPGS-NIRF and the control dye i.v. into the tail vein at 72 hrs after last OVA challenge, when we expected that allergic inflammation in the lung is at its peak. Asthmatic and healthy mice were imaged at 4 and 24 hrs post dPGS-NIRF or unconjugated NIRF dye injection as control.

Figures 3 and 4 illustrate the distribution of the control dye and dPGS-NIRF, respectively, after 4 hrs in the thoracic area of asthmatic in comparison to healthy mice. A slight increase of fluorescent signal was recorded after injection of control dye in asthmatic mice in comparison to healthy mice (Figure 3A). In order to localize the dPGS-NIRF probe within inflamed lung region we applied fluorescence microscopy in combination with immunofluorescence staining of macrophages by the use of an antibody against F4/80, a 160 kDa cell surface glycoprotein that is widely expressed on mature tissue macrophages. As shown in Figure 3B a higher amount of macrophages was clearly detectable in lungs of asthmatic mice in comparison to healthy controls. The Control dye was not detected in lung sections of asthmatic mice using fluorescence microscopy (Figure 3B). In contrast, higher

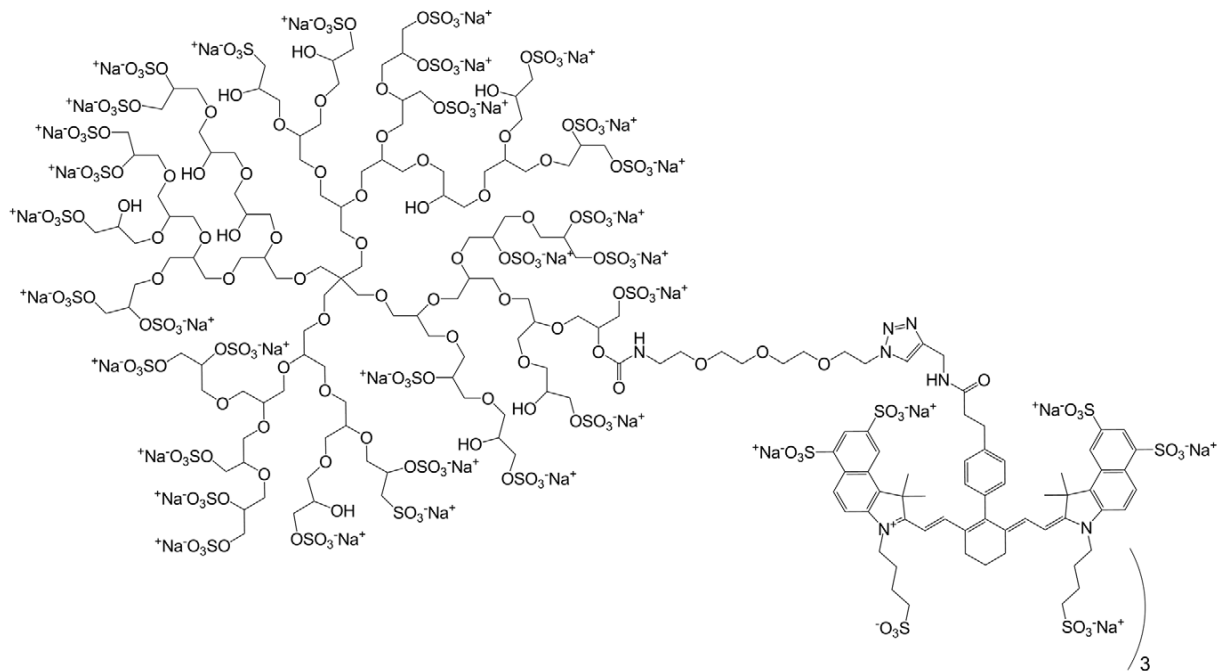


**Figure 1. Chemical structure of dPGS-NIRF.** The chemical structure indicates the linker structure and connection to the dye (approx. 3 dyes per polymer). Please note that the polymer is not depicted in original molecular weight, but is shown only as principle sketch.  
doi:10.1371/journal.pone.0057150.g001

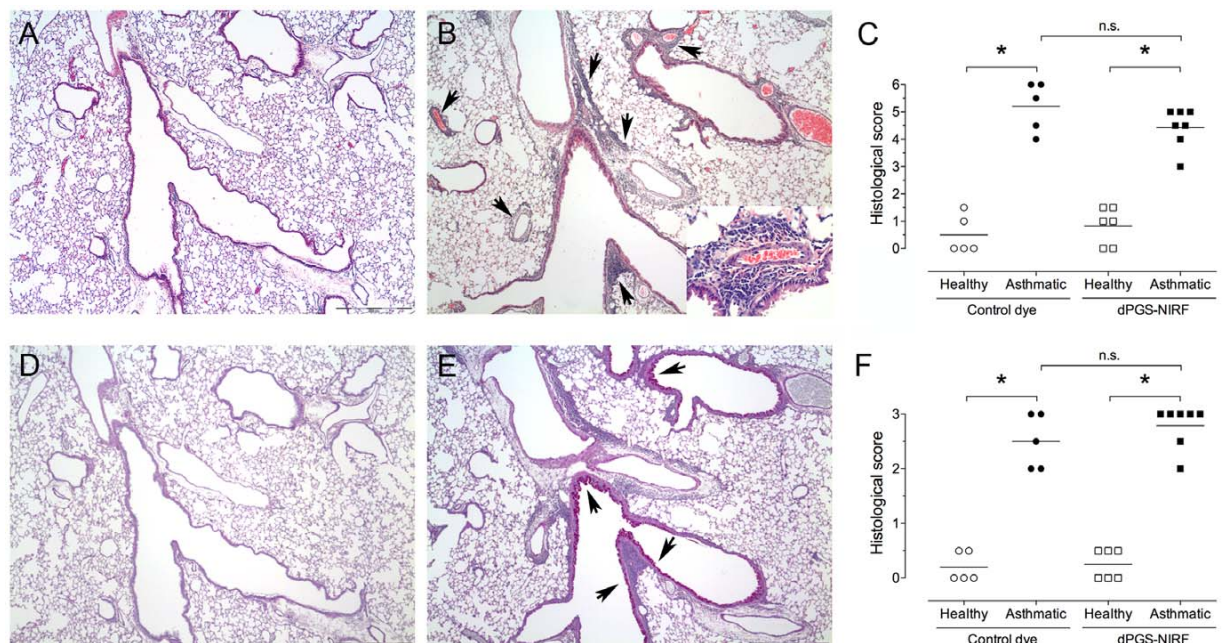


**Figure 2. Allergic inflammation and mucus hypersecretion in the lungs of asthmatic, but not control mice.** Lungs were harvested 76 hrs after the final ovalbumin (OVA) challenge meaning 4 hrs post i.v. probe injection. Representative H&E (A and B) and PAS (D and E) stained photomicrographs of lungs from healthy (A and D) or asthmatic mice (B and E) are shown (magnification 40 $\times$ , inset 400 $\times$ ). (B) Arrows indicate inflammation, and in (E) arrows indicate mucus hypersecretion. Allergic inflammation (C) and mucus hypersecretion (F) scores in H&E and PAS stained lung sections, respectively, of healthy (open symbols) or asthmatic mice (filled symbols). Each symbol represents individual mice (n=5–6 for healthy groups and n=5–7 for asthmatic groups), and line represents group mean. One-way ANOVA followed by Tukey's multiple comparison test (\* $P < 0.05$ ) was used to compare differences between groups.  
doi:10.1371/journal.pone.0057150.g002

fluorescence intensity was detected in the thoracic region of asthmatic mice 4 hrs post dPGS-NIRF probe injection (Figure 4A). Moreover, fluorescence microscopy of lung sections of asthmatic mice confirmed dPGS-NIRF probe localization in areas where F4/80 stained macrophages could be detected, which demonstrated that dPGS-NIRF accumulates especially in the inflamed region of lungs of the pathological model (Figure 4B).

Fluorescence signals obtained with *in vivo* imaging were quantified and intensity ratios were calculated as described in the Material and Methods. As depicted in Figure 5A, at 4 hrs post injection of control dye, we observed a slight increase in fluorescence signal in asthmatic mice when compared to healthy mice (increase in average  $RI_{Dye}(4h) \sim 11\%$ , p-value = 0.047), most probably due to an increase in the vascular flow in the inflamed lungs. In contrast, dPGS-NIRF increased the fluorescence signal in the thorax of asthmatic mice dramatically, as seen by an average  $RI_{dPGS}(4h) \sim 44\%$  with p-value = 0.004. Moreover, a direct comparison of the contrast (RI) between dPGS-NIRF and free dye in the asthmatic mice revealed a 30% higher  $RI_{dPGS}(4h)$  than  $RI_{Dye}(4h)$  (p-value = 0.005) at this time point. At 24 hrs post dPGS-NIRF injection, fluorescence signals over the lung areas of healthy and asthmatic mice were not longer distinguishable (average  $RI_{dPGS}(24h)$  difference  $\sim 8\%$ , p-value = 0.162) (Figure 5B). *In vitro* analysis of serum binding of ICG as well as of 6S-ICG demonstrate that ICG completely binds to serum proteins (23), whereas less than 40% of 6S-ICG was bound to serum proteins (data not shown).

#### Ex vivo optical imaging confirmed the *in vivo* results

To confirm the *in vivo* imaging findings immediately after the last imaging, we imaged the lungs ex-vivo using an Optix MX2 system. Ex-vivo imaging avoids autofluorescence of other organs and absorption and scattering within the body and fur. This increases both specificity and sensitivity of probe detection. In accordance to the *in vivo* results, we found a significant difference between the fluorescence intensity within the lungs of asthmatic

and healthy mice 4 hrs post injection of the dPGS-NIRF conjugate (difference of  $RI_{dPGS}^{ex-vivo}(4h) \sim 65\%$ , p-value = 0.009), but not control dye (difference of  $RI_{Dye}^{ex-vivo}(4h) \sim 18\%$ , p-value = 0.127) (Figure 6A and 6B). At 24 hrs post administration of dPGS-NIRF, the observed fluorescence intensity over the lungs was reduced to about 30% of the intensity measured 4 hrs post injection. Moreover, the difference in fluorescence intensity between healthy and asthmatic mice dropped down to  $\sim 10\%$  and was not significant (difference of  $RI_{dPGS}^{ex-vivo}(24h) \sim 10\%$ , p-value = 0.323) (Figure 6B).

#### Comparison of dPGS-NIRF with commercially available smart-probes

Commercially available smart-probes ProSense and MMPsense, activated by cathepsins and MMPs, respectively, were used for imaging lung inflammation [9]. Both smart-probes were injected at 72 hrs after the last OVA challenge and imaged after 24 hrs, according to probe manufacturer's recommendations. The intensity difference from the thoracic region between healthy and asthmatic mice was  $\sim 27\%$  (p-value = 0.013) after administration of ProSense and  $\sim 83\%$  after injection of MMPsense but with no statistical significance (p-value = 0.093) (Table 1).

#### Discussion

In this study, we present a novel approach for functional *in-vivo* imaging utilizing a dendritic polyglycerolsulfate conjugated to a NIRF dye related to ICG (dPGS-NIRF) in combination with optical imaging to monitor sites of inflammation in the lung by applying an experimental model of allergic asthma [12].

We successfully demonstrated that the applied dPGS-NIRF probe accumulates to inflammatory sites within the lung already 4 hrs after probe administration. The results show a significant four times stronger contrast of the fluorescence intensity of the dPGS-NIRF probe compared to the free dye in lungs of asthmatic in comparison to healthy mice. At this time point fluorescence

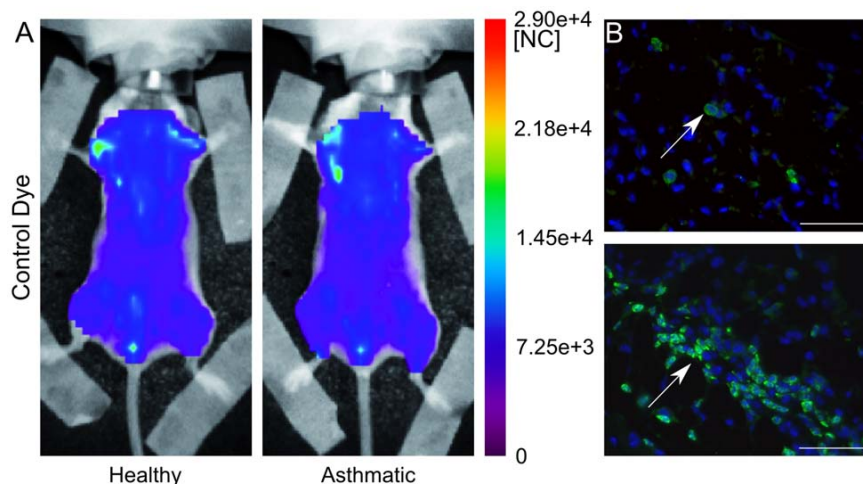


**Figure 3. In vivo distribution of free dye (indocyanine green) 4 hours post probe injection and 76 hours post last OVA challenge.** Panel A: whole body fluorescence intensity distribution of a representative healthy and asthmatic mouse displayed in normalized counts [NC]. Panel B: Fluorescence microscopy images of F4/80 stained macrophages and DAPI stained cell nuclei of lungs isolated from asthmatic and healthy mice injected with the NIRF labeled control dye and sacrificed 4 hrs post injection demonstrate no fluorescent control dye. F4/80 expression on macrophages are depicted in green, cell nucleus in blue, control dye was not detected (bar = 50  $\mu$ m). In the healthy model few macrophages have been detected with respect to the asthmatic mouse, where cluster of cells are visible (see white arrows indicating macrophages). In both samples no unconjugated NIRF dye 6S-ICG has been visualized.  
doi:10.1371/journal.pone.0057150.g003

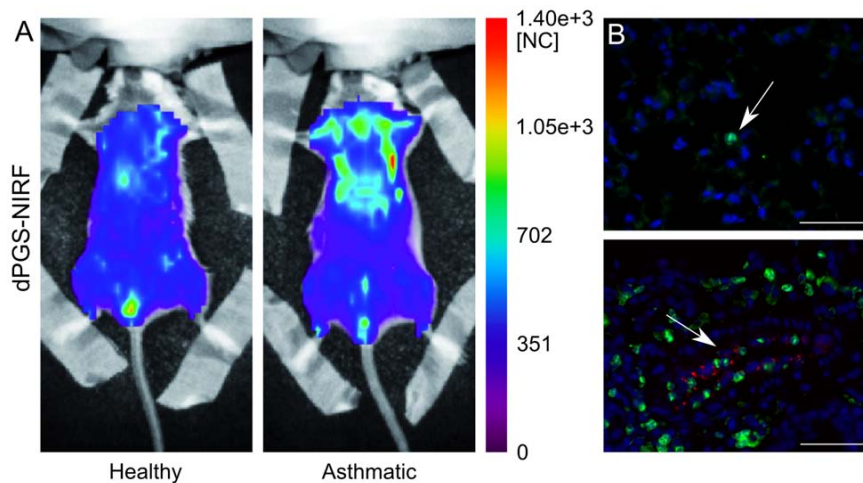


**Figure 4. In vivo distribution of dPGS-NIRF 4 hours post probe injection and 76 post last OVA challenge.** Panel A: whole body fluorescence intensity distribution in a representative healthy and asthmatic mouse displayed in normalized counts [NC]. Stronger fluorescence intensity over the lung area of the asthmatic mouse can be seen. Panel B Fluorescence microscopy images of F4/80 stained macrophages and DAPI stained cell nuclei of lungs isolated from asthmatic and healthy mice injected with dPGS-NIRF and sacrificed 4 hrs post injection. F4/80 expression on macrophages are depicted in green, cell nucleus in blue, dPGS-NIRF displayed in red (bar = 50  $\mu$ m). In the healthy model, few macrophages and no probe localization have been detected. In the asthmatic mouse, cluster of macrophages are detectable (see white arrows) and the dPGS-NIRF probe was visualized in the same region of macrophages.  
doi:10.1371/journal.pone.0057150.g004

microscopy confirmed the localization of the dPGS-NIRF probe within the inflamed lungs in areas where F4/80 stained macrophages could be detected and histology demonstrated the presence of inflammatory infiltrates in more than two thirds of the examined lung sections. Therefore, dPGS-NIRF is suitable to monitor inflamed lungs by NIRF imaging.

Furthermore, at 4 hrs post injection, the calculated  $RI_{ex}(4h)$  was significantly lower in asthmatic lungs after administration of free dye. These results indicate that a specific target in the model appears to be involved. dPGS-NIRF exerts high-affinity binding to

positively charged protein motifs e.g. P- and L-selectin as well as to C3/C5 complement factors [22]. The selectivity is demonstrated by the very low affinity for E-selectin compared to P and L-selectin, which dPGS bind to with nanomolar affinity *in vitro* [20,22]. Furthermore, dPGS accumulates in inflamed tissue by a not yet understood cellular uptake mechanism into macrophages and endothelial cells, but not into lymphocytes. This was shown for example by fluorescence microscopy of liver tissue specimens after dPGS-NIRF application that depicted accumulation in rat liver macrophages (Kupffer cells) and of A549 tumor cells as well

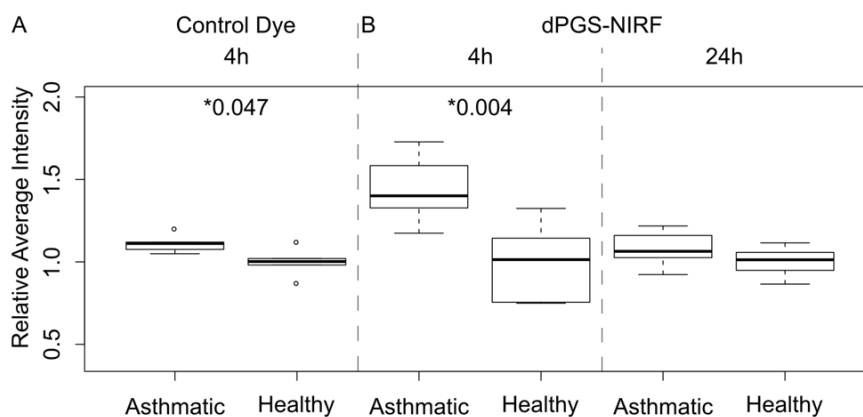


**Figure 5. Quantification of in vivo imaging results of dPGS-NIRF and pure dye.** Box plots of ratios of average fluorescence intensity over the lung area compared with the mean value of each control group respectively are reported for asthmatic and healthy mice. Mice treated with free dye 4 hrs post injection showed a slight increase in fluorescence signal in asthmatic mice (n = 5) when compared to healthy mice (n = 5; increase in average ~11%, p-value = 0.047, panel A). Mice treated with dPGS-NIRF probe 4 hrs post injection (healthy n = 6, asthmatic n = 6) showed an increased fluorescence signal in the thorax in asthmatic mice (increase in average ~44% with p-value = 0.004, panel B left side). At 24 hrs post injection fluorescence signals over the lung areas of healthy (n = 5) and asthmatic mice (n = 10) shown no difference (difference ~8%, p-value = 0.162, panel B right side). Both control dye and dPGS-NIRF probe were injected 72 hrs after last aerosol challenge. Note, intensity ratios were used to compare probes with different brightness, therefore the box plots are depicted in the same scale.  
doi:10.1371/journal.pone.0057150.g005

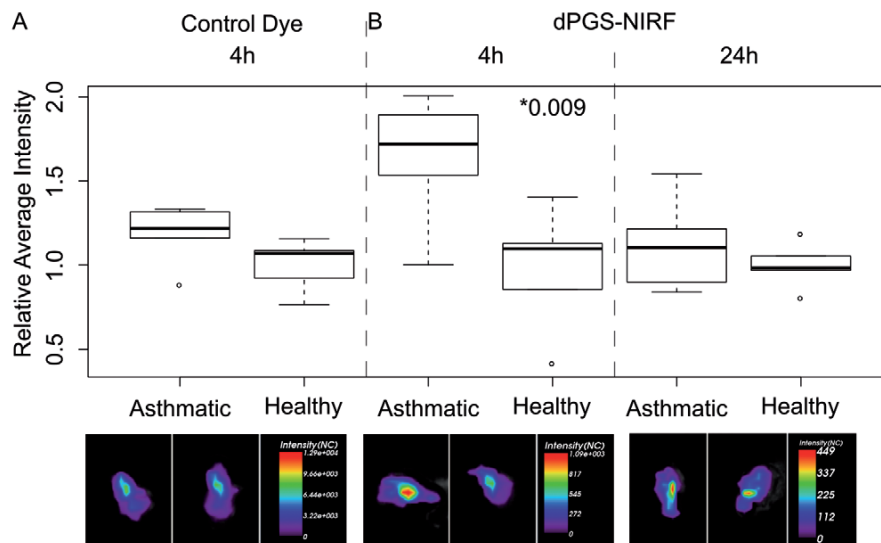


**Figure 6. Ex vivo imaging results of dPGS-NIRF and pure dye.** Box plots of ratios of average fluorescence intensity over the explanted lungs compared with the mean value of each control group respectively are reported for asthmatic and healthy mice treated with free dye 4 hrs post injection (panel A), and treated with dPGS-NIRF probe 4 hrs (panel B left side) and 24 hrs (panel B right side) post injection. The corresponding fluorescence intensity images of representative lungs are given at the bottom of each box plot. A significant difference between the fluorescence intensity within the lungs of asthmatic ( $n=5$ ) and healthy mice ( $n=5$ ) was observed 4 hrs post injection of the dPGS-NIRF conjugate (difference of  $\sim 65\%$ ,  $p$ -value = 0.009), but not of the control dye (healthy  $n=5$ , asthmatic  $n=5$ ; difference of  $\sim 18\%$ ,  $p$ -value = 0.127). Both control dye and dPGS-NIRF probe were injected 72 hrs after last aerosol challenge. Note, intensity ratios were used to compare probes with different brightness, therefore the box plots are depicted in the same scale. doi:10.1371/journal.pone.0057150.g006

as of activated, LPS-stimulated mononuclear cells, both demonstrating accumulation of dPGS [22].

The underlying chemical structure of the polymer in published studies [22] is based on a polyglycerol core of 6000 Da, whereas different dyes were attached to the polymer, such as a visible cyanine dye or a NIRF dye in a ratio of approx. 1 dye per polymer, yielding identical selectin-binding properties. The conjugate used herein employs the same polymer, but a more hydrophilic indocyanine dye with 6 sulfonate groups (6S-ICG) added to the fluorophore structure. Coupling to the dPGS could be achieved at a dye-to-polymer ratio of 3 without signs of aggregation known to be induced by more lipophilic indocyanine dyes in bioconjugates, as described in [20].

Previously, studies show also inflammation-specific imaging with dPGS-NIRF in an animal model of collagen induced rheumatoid arthritis using the preceding conjugate with a lipophilic indocyanine green label. Comparable to our study, the authors demonstrated a fast and selective uptake of the probe with a 3.5 fold higher fluorescence difference between healthy and diseased

joints and a signal peak at 1 hr after probe administration. Together with a rough estimation of a blood half-life of shorter than 1 hr by employing the eye fluorescence as a provisional solution to monitor blood kinetics, they postulate targeting mechanisms not yet fully understood [20] whereby dPGS-NIRF binds to mediators of inflammation.

Interestingly, the high contrast between the fluorescence intensity of dPGS-NIRF in the asthmatic and healthy groups was not observed after 24 hrs. This might be explained in part by shedding of P- and L-selectins from the cell surface after binding of dPGS-NIRF [23]. Bound dPGS-NIRF probes will be removed from the cells resulting in the reduction of fluorescence intensity to background after 24 hrs.

The MMPsense and ProSense probes, which are activated in the presence of inflammation-associated enzymes such as cathepsin and MMPs that are present in the lungs during allergen challenge are successfully used by others, for example to detect lung inflammation and rapidly screen for new drug effects [9–11] as well as to visualize colon adenomas [8]. Similar to our study,

**Table 1.** Calculated average fluorescence intensity ratios  $RI_{ex}(t)$  between healthy and asthmatic mice after injection of control dye, dPGS-NIRF, or two commercially available probes: ProSense and MMPsense.

	Control Dye	dPGS-NIRF	ProSense	MMPsense
measurement time (hours)	4	4	24	24
<i>in vivo</i>	1.11 ± 0.06 (0.047)	1.45 ± 0.20 (0.004)	1.08 ± 0.10 (0.162)	1.27 ± 0.02 (0.013)
<i>ex vivo</i>	1.18 ± 0.18 (0.127)	1.65 ± 0.35 (0.009)	1.10 ± 0.22 (0.323)	n.d.

Results are shown as mean calculated average fluorescence intensity ratios  $\pm$  standard deviation, while statistical significance between each pair of control and asthmatic mice is given by  $p$ -value for the Welch-T-Test in brackets. Legend: n.d. – not done.

doi:10.1371/journal.pone.0057150.t001

Cortez-Retamozo et al. demonstrated fluorescence differences between asthmatic lungs and healthy controls by applying the same amount of MMPsense or ProSense however by using fiberoptic bronchoscopy and fluorescence molecular tomography (FMT) [9]. Others also reported that the *in vivo* profile of cysteine protease activation was depicted by FMT in a mouse model of acute airway inflammation by LPS-induction [10,11].

These smart probes exhibit slower kinetics due to their activation mechanism, demonstrating maximal fluorescence intensity within the lungs about 24 hrs after probe injection [9]. The application of these enzymatically activated probes is often hampered by the fact that despite a dramatic increase of their fluorescence intensity over inflammatory areas, the activated probes do not remain at the site of interest for very long and instead produce a strong liver signal due to their excretion pathway.

In conclusion, we present a novel *in vivo* NIRF imaging probe for detection of inflammatory reactions within the lungs of mice, as demonstrated in mice with allergic inflammation, by utilizing a dendritic polyglycerolsulfate NIRF dye conjugate known to bind to selectins and complement factors. The greater fluorescence intensity of dPGS-NIRF in inflammation of mice with allergic asthma in combination with rapid kinetics makes dPGS-NIRF a powerful probe candidate to monitor inflammation processes and responses to therapy in experimental mouse models of lung disease.

## Materials and Methods

### Mice

Female BALB/c mice (4- to 6-weeks old) were purchased from Charles River and maintained with ad libitum food and water. All the experimental procedures were performed in compliance with the guidelines of European (86/609/EEC) and Italian (D.L.116/92) as well as German laws and were approved by the Italian Ministry of University and Research and the Administration of the University Animal Facility, Trieste, as well as by the administration of Lower Saxony, Germany.

### Synthesis of a dendritic polyglycerol sulfates NIR dye conjugate probe (dPGS-NIRF)

dPGS was synthesized by anionic polymerization of glycidol and subsequent sulfation using SO<sub>3</sub>/pyridinium complex according to Türk and colleagues [14]. Conjugation of dPGS to an NIRF dye (based on indocyanine green chromophore; derivative with reactive group for conjugation) are described [20] elsewhere. Briefly, the polyglycerol intermediate was reacted with an aliphatic linker chain followed by the sulfation reaction. To this linker, a novel NIRF dye (6S-ICG propargyl; mivenion GmbH) was conjugated followed by high-performance liquid chromatography (HPLC) purification yielding dPGS-NIRF with a mean dye-to-polymer ratio of 3 and an average molecular weight of 19000 Da. The degree of sulfonation was 85% (elementary analysis) and the polydispersity index (PDI) within 1.6–1.8 (measured for the polyglycerol intermediate using GPC). The dye used herein is a hydrophilic version of the previously described indocyanine green label, with 4 additional sulfonate groups in the molecule resulting in a 6-fold sulfonated entity of maximal hydrophilicity for this type of NIR fluorophore. The chemical structure is depicted in Figure 1. Absorption maxima in PBS were 710 and 795 nm, fluorescence emission maximum 810 nm. Unconjugated NIRF dye (6S-ICG molecular weight ~1700 g/mol, free carboxylic acid instead of linkage to polymer) served as control probe in the *in vivo* experiments.

### Mouse Model of Acute Allergic Asthma

Mice were sensitized intraperitoneally (i.p.) at day 0 and day 21 with 10 µg ovalbumin (OVA) dissolved in 200 µl PBS. At day 28 and day 29 mice were treated intranasal (i.n.) with a solution of 100 µg OVA/50 µl PBS/mouse. Healthy age and gender matched BALB/c mice served as controls. Histology of H&E stained lung sections was performed at 76 hrs post last challenge

### Optical Imaging Scan

48 mice were examined by optical imaging (Table 2). Mice were shaved over the lung area prior to the scanning procedure in order to reduce scattering of the signal from fur. Throughout all imaging sessions, mice were anesthetized with vaporized isoflurane at 1.8–2 volume % as described [2]. The anesthetized mice were placed inside an Optix MX2 acquisition system (Advanced Research Technologies, Montreal, Canada) and gently fixed on a heated block (37°C) for the entire duration of data acquisition.

All *in vivo* analyses were preceded by native scans of the mice prior to NIRF probe injection to provide a base line for later analysis. At 72 hrs after the last OVA challenge, mice were injected intravenously (i.v.) via the tail with 100 µl of one of the following: dPGS-NIRF (2.6 nmol, polymer/dye = 1/3), free NIRF dye (3.6 nmol), 100 µl (5 nmol) of either MMPsense (MMPsense®, Perkin Elmer) or ProSense (ProSense®, Perkin Elmer), all dissolved in 0.9% NaCl. The amount of injected dPGS-NIRF and NIRF solutions was calculated based on the weaker fluorescence signal of dye in the conjugate than in the unconjugated control dye. Exact numbers of animals in each group are shown in Table 2.

### *In vivo* and *ex vivo* Optical Imaging

Animals with acute asthma and wild type controls were scanned at 4 and 24 hrs post i.v. dPGS-NIRF or NIRF dye administration. For the MMPsense and ProSense, scans were performed 24 hrs after probe administration. According to the supplier (PerkinElmer), this time point constitutes the peak activation of these probes [9]. All *in vivo* data was acquired by using the small-animal time-domain Optix MX2 preclinical NIRF-imager (Advanced Research Technologies, Montreal, CA), equipped with four pulsed laser diodes and a time correlated single photon counting detector [24]. This system works in reflection mode applying a raster acquisition scheme, measuring and analyzing fluorescence response to pulsed excitation for each excitation spot by creating fluorescence photon time of flight histograms. In all imaging experiments applying the dPGS-NIRF and control dye, a 785 nm pulsed laser diode with a repetition frequency of 80 MHz was used whereas for the MMPsense and ProSense studies a 670 nm pulsed laser diode with a repetition frequency of 80 MHz was applied. Fluorescence emission was accordingly collected with an 800 nm long pass filter for dPGS-NIRF and control dye and a 700 nm long pass filter for both MMPsense and ProSense to block the excitation light. Two-dimensional regions of interest (ROIs) were selected, and laser power, integration time (repetition time of the excitation per raster point), and scan step size were optimized according to the emitted signal. Prior to probe application, mice were scanned to obtain background images. These background signal intensities recorded with the baseline image for each animal before the injection of the probe was subtracted from each post injection image. At the end of the last imaging session, 4 and 24 hrs after dPGS-NIRF/NIRF dye i.v. injection, animals were sacrificed and *ex vivo* optical imaging of the explanted lungs was performed. To calculate the total lung fluorescence intensity (I<sub>lung</sub>) in each scan, fluorescence intensities were normalized with the laser power used for excitation and summed up in ROI's

**Table 2.** Experimental design of optical imaging biodistribution study.

	Control Dye	dPGS-NIRF	ProSense	MMPSense
<b>Measurement time (hours)</b>	4	4	24	24
<b>Healthy mice (number)</b>	5	6	5	2
<b>Asthmatic mice (number)</b>	5	6	10	3

doi:10.1371/journal.pone.0057150.t002

encompassing the whole organ. Lungs were then preserved in formalin for histological analysis.

### Image processing

Image analysis was done using OptiView (2.02.00), the proprietary software developed for the Optix device. All data sets of mice receiving dPGS-NIRF, free NIRF dye control as well MMPSense and ProSense were normalized for different excitation laser power and variations of the used integration time and therefore expressed in normalized counts [NC], an arbitrary unit. Average fluorescence intensity was calculated within a region of interest covering the whole lung for every sample (x) and time point (t) as  $\bar{I}(x,t)$  and subtracted by the base line intensity within the same region  $\bar{I}_{bg}(x)$ . To remove the influence of different brightness of all applied probes, ratios  $RI_{ex}(x,t)$  between the average intensity of the sample (x) and the mean average intensity of the control group for each experiment (ex) and time point (t) were calculated and denominated as  $RI_{ex}(x,t)$ .

$$RI_{ex}(x,t) = \frac{\bar{I}(x,t) - \bar{I}_{bg}(x)}{N_{ctrl}^{-1} \sum \bar{I}(x,t)} \quad (1)$$

$RI_{ex}(x,t)$  can be interpreted as contrast or probability to distinguish asthma mice from controls at certain time points and was therefore used for comparison of the different studies and statistical calculations.

### Histological analysis of lung inflammation

Following *ex vivo* image analysis performed 76 hrs after the last ovalbumin challenge, tissue samples were fixed in 10% buffered formalin and embedded in paraffin. To evaluate allergic lung inflammation, 3  $\mu$ m thick lung sections containing main stem bronchi were stained with hematoxylin and eosin (H&E). A blinded grading of the slides was done to evaluate the intensity and extent of inflammation according to our semi-quantitative scoring system. For intensity of inflammation: 0 – no inflammatory infiltrates; 1 – inflammatory infiltrates in central airways; 2 – inflammatory infiltrates extending to middle third of lung parenchyma; and 3 – inflammatory infiltrates extending to periphery of the lungs. For extent of inflammation: 0 – no inflammatory infiltrates; 1 – inflammatory infiltrates present in one third of lung surface; 2 – inflammatory infiltrates spreading up to two thirds of lung surface; 3 – inflammatory infiltrates present in more than two thirds of lung surface. Data are presented as histological score calculated as the sum of intensity and extent of inflammation for each sample. For detection of mucus-containing cells in lung tissue, adjacent 3  $\mu$ m sections containing main stem bronchi from each lung specimen were stained with periodic acid-Schiff (PAS) and counter stained with hematoxylin. Slides were examined blinded for the treatment and mucus overproduction

was scored as: Grade 0 – no mucus producing cells in airways; Grade 1 – few mucus producing cells in central airways; Grade 2 – mucus producing cells detected in middle airways; and Grade 3 – mucus producing cells extending to respiratory bronchioles. In borderline cases, an intermediate grade was used (0.5; 1.5 or 2.5), extending the scoring to a total of seven grades.

### Serum OVA-specific immunoglobulin

For the measurement of OVA-specific immunoglobulin (Ig) G1, ELISA plates were coated with OVA at 10  $\mu$ g/ml overnight at 4°C. The plates were washed and blocked with 2% bovine serum albumin in PBS with 0.05% Tween 20 for 2 hrs at RT. Then sera were titrated onto the plates and incubated for 24 hrs at 4°C before washing. Plates were incubated for an additional 2 hrs at 4°C with biotinylated anti-IgG1 (Southern biotechnology associates Inc., Birmingham, AL, USA) detection mAb, followed by incubation with streptavidin horseradish peroxidase (Southern biotechnology) for 1 h at RT. Plates were washed and incubated with TMB substrate solution (100  $\mu$ l/well, BD OptEIAMT, Becton Dickinson Biosciences) for 10 min at RT. The reaction was stopped with 100  $\mu$ l of 0.18 M H<sub>2</sub>SO<sub>4</sub> and the plates were measured at 450 nm.

### In vitro analysis of serum binding

The serum binding of 6S-ICG was determined in vitro by incubation with pooled human serum (PAA) with dye concentration of 5  $\mu$ g/ml [25]. The sample was placed in a Centriprep micropartition unit NWML 30 kDa (Milipore, Billerica, USA), and centrifuged at 5000 g for 20 min. The protein-bound 6S-ICG and the free dye in the ultrafiltrate was quantified spectrophotometrically (Beckman Coulter, USA).

### Fluorescence microscopy

Detection of injected dPGS-NIRF probe or unconjugated NIRF dye 6S-ICG in lungs of control and asthmatic mice was carried out by fluorescence microscopy. In order to correlate NIRF fluorescence signals from the probes to inflammatory sites, lungs were counterstained with anti-mouse F4/80 antibody. detecting macrophages Two-micrometer-thick sections were cut from paraffin blocks, the slides were first processed for avidin/biotin and protein blocking steps using xylol and decreasing alcohol concentration for deparaffination and rehydration and later incubated with the primary antibody rat anti-mouse F4/80 (AbD Serotec, Oxford, UK), dilution factor 1:100 at 4°C overnight. After the incubation with the primary antibody, the samples were incubated with secondary biotinylated antibody goat anti-rat (BioLegend, San Diego, USA), dilution factor 1:200 at RT for 1 hour, and then with streptavidin- Alexa 555 (Molecular Probes, Life Technologies Corporation, USA) dilution factor 1:400 at RT for 1 hour. DAPI was diluted in the mounting media and used as nuclear counterstaining. Fluorescence was analyzed with a Zeiss Axiovert 200 M inverted microscope (Carl Zeiss,

Germany) equipped with a xenon lamp and a high sensitivity ORCA-AG digital camera (Hamamatsu, Japan). Data were acquired with AxioVs40 software (Carl Zeiss). Filter settings were as followed: DAPI: Ex: BP 365/25 (+/-12.5); FT 395; Em: BP 445/50 (+/-25); Cy7: BP 708/75 (+/-37.5); FT 757; BP 809/81 (+/-40.5); Alexa555: BP 546/12 ( $\pm$ 6); FT 580 and LP 590 filter. Subsequent analyses were performed using the java-based image processing program ImageJ.

### Statistical Analysis

Statistical verification of the differences of  $RI_{ex}(x,t)$  between asthmatic and control mice for each experiment and time point was done using an unpaired Welch Two Sample t-test implemented in the PAST statistic software [26]. A p-value of less than 0.05 was considered significant.

Histological scores between groups were compared using One-way ANOVA followed by Tukey's multiple comparison test.

### References

- Biffi S, Garrovo C, Macor P, Tripodo C, Zorzet S, et al. (2008) *In vivo* biodistribution and lifetime analysis of cy5.5-conjugated rituximab in mice bearing lymphoid tumor xenograft using time-domain near-infrared optical imaging. *Mol Imaging* 7: 272–282.
- Agostinis C, Biffi S, Garrovo C, Durigutto P, Lorenzon A, et al. (2011) *In vivo* distribution of  $\beta$ 2 glycoprotein I under various pathophysiological conditions. *Blood* 118(15):4231–8.
- Napp J, Mathejczyk JE, Alves F (2011) Optical imaging *in vivo* with a focus on paediatric disease: technical progress, current preclinical and clinical applications and future perspectives. *Pediatr Radiol* 41: 161–175.
- Hutteman M, Choi HS, Mieog JSD, van der Vorst JR, Ashitate Y, et al. (2011) Clinical translation of *ex vivo* sentinel lymph node mapping for colorectal cancer using invisible near-infrared fluorescence light. *Ann. Surg. Oncol.* 18: 1006–1014.
- Montet X, Figueiredo J-L, Alencar H, Ntziachristos V, Mahmood U, et al. (2007) Tomographic fluorescence imaging of tumor vascular volume in mice. *Radiology* 242: 751–758.
- Dullin C, Zientkowska M, Napp J, Missbach-Guentner J, Krell H-W, et al. (2009) Semiautomatic landmark-based two-dimensional-three-dimensional image fusion in living mice: correlation of near-infrared fluorescence imaging of Cy5.5-labeled antibodies with flat-panel volume computed tomography. *Mol Imaging* 8: 2–14.
- Ushiki T, Kizaka-Kondoh S, Ashihara E, Tanaka S, Masuko M, et al. (2010) Noninvasive tracking of donor cell homing by near-infrared fluorescence imaging shortly after bone marrow transplantation. *PLoS ONE* 5: e11114.
- Clapper ML, Hensley HH, Chang W-CL, Devarajan K, Nguyen MT, et al. (2011) Detection of colorectal adenomas using a bioactivatable probe specific for matrix metalloproteinase activity. *Neoplasia* 13: 685–691.
- Cortez-Retamozo V, Swirski FK, Waterman P, Yuan H, Figueiredo JL, et al. (2008) Real-time assessment of inflammation and treatment response in a mouse model of allergic airway inflammation. *J Clin. Invest.* 118: 4058–4066.
- Ntziachristos V (2009) Optical imaging of molecular signatures in pulmonary inflammation. *Proc Am Thorac Soc* 6: 416–418.
- Haller J, Hyde D, Deliolanis N, de Kleine R, Niedre M, et al. (2008) Visualization of pulmonary inflammation using noninvasive fluorescence molecular imaging. *J Appl. Physiol.* 104: 795–802.
- Epstein MM (2004) Do mouse models of allergic asthma mimic clinical disease? *Int. Arch. Allergy Immunol.* 133: 84–100.
- Jannasch K, Missbach-Guentner J, Alves F (2009) Using *in vivo* imaging for asthma. *Drug Discovery Today: Disease Models* 6: 129–135.
- Türk H, Haag R, Alban S (2004) Dendritic polyglycerol sulfates as new heparin analogues and potent inhibitors of the complement system. *Bioconjug. Chem.* 15: 162–167.
- Weinhart M, Gröger D, Enders S, Dermedde J, Haag R (2011) Synthesis of dendritic polyglycerol anions and their efficiency toward L-selectin inhibition. *Biomacromolecules* 12: 2502–2511.
- Banerjee ER (2011) Triple selectin knockout (ELP<sup>-/-</sup>) mice fail to develop OVA-induced acute asthma phenotype. *J Inflamm (Lond)* 8: 19.
- Tang ML, Fiscus LC (2001) Important roles for L-selectin and ICAM-1 in the development of allergic airway inflammation in asthma. *Pulm Pharmacol Ther* 14: 203–210.
- Keramidas E, Merson TD, Steeber DA, Tedder TF, Tang ML (2001) L-selectin and intercellular adhesion molecule 1 mediate lymphocyte migration to the inflamed airway/lung during an allergic inflammatory response in an animal model of asthma. *J Allergy Clin. Immunol.* 107: 734–738.
- Royce SG, Lee M, Tang MLK (2010) The contribution of L-selectin to airway hyperresponsiveness in chronic allergic airways disease. *J Asthma Allergy* 3: 9–17.
- Licha K, Welker P, Weinhart M, Wegner N, Kern S, et al. (2011) Fluorescence Imaging with Multifunctional Polyglycerol Sulfates: Novel Polymeric near-IR Probes Targeting Inflammation. *Bioconjug. Chem.* 22: 2453–2460.
- Reichert S, Welker P, Calderón M, Khandare J, Mangoldt D, et al. (2011) Size-dependant cellular uptake of dendritic polyglycerol. *Small* 7: 820–829.
- Dermedde J, Rausch A, Weinhart M, Enders S, Tauber R, et al. (2010) Dendritic polyglycerol sulfates as multivalent inhibitors of inflammation. *Proc. Natl. Acad. Sci. U.S.A.* 107: 19679–19684.
- Hafezi-Moghadam A, Thomas KL, Prorock AJ, Huo Y, Ley K (2001) L-selectin shedding regulates leukocyte recruitment. *J Exp. Med.* 193: 863–872.
- Ma G, Gallant P, McIntosh L (2007) Sensitivity characterization of a time-domain fluorescence imager: eXplore Optix. *Appl Opt* 46: 1650–1657.
- Gootz TD, Subashi TA, Lindner DL (1988) Simple spectrophotometric assay for measuring protein binding of penem antibiotics to human serum. *Antimicrobial Agents and Chemotherapy* 32: 159–163.
- Hammer Ø, Harper D, Ryan P (2001) PAST: Paleontological Statistics Software Package for Education and Data Analysis. *Palaentological Association* 22.

GraphPad Prism (v.5.00, GraphPad Software, San Diego, CA) was used for data analysis.

### Acknowledgments

This work was carried out at the University Medical Center Goettingen (Germany) with excellent support of Rosi Streich, Sarah Greco and Andrea Markus. We also want to acknowledge to Joanna Napp who helped in the fluorescence acquisition of the images.

### Author Contributions

Conceived and designed the experiments: FA SB SDM MME BB. Performed the experiments: SB SDM CD CG BB. Analyzed the data: SB SDM CD MME BB. Contributed reagents/materials/analysis tools: KL PW. Wrote the paper: FA MME SB CD SDM.

### 3.3. Publication 2

#### **Tiotropium bromide inhibits relapsing allergic asthma in BALB/c mice**

Berislav Bosnjak<sup>a</sup>, Cornelia Tilp<sup>c</sup>, Christopher Tomsic<sup>c</sup>, Gerhard Dekan<sup>b</sup>, Michael P. Pieper<sup>c</sup>, Klaus J. Erb<sup>c</sup>, Michelle M. Epstein<sup>a</sup>

<sup>a</sup> *Division of Immunology, Allergy and Infectious Diseases, Experimental Allergy, Department of Dermatology, Medical University of Vienna, Vienna, Austria*

<sup>b</sup> *Institute of Clinical Pathology, Medical University of Vienna, Vienna, Austria*

<sup>c</sup> *Department of Pulmonary Disease Research, Boehringer-Ingelheim Pharma, Biberach, Germany*

***Published in: Pulmonary Pharmacology & Therapeutics 2014; 27: 44-51***



ELSEVIER

Contents lists available at ScienceDirect

## Pulmonary Pharmacology &amp; Therapeutics

journal homepage: [www.elsevier.com/locate/ypupt](http://www.elsevier.com/locate/ypupt)

## Tiotropium bromide inhibits relapsing allergic asthma in BALB/c mice<sup>☆</sup>



Berislav Bosnjak<sup>a</sup>, Cornelia Tilp<sup>c</sup>, Christopher Tomsic<sup>c</sup>, Gerhard Dekan<sup>b</sup>,  
Michael P. Pieper<sup>c</sup>, Klaus J. Erb<sup>c</sup>, Michelle M. Epstein<sup>a,\*</sup>

<sup>a</sup> Division of Immunology, Allergy and Infectious Diseases, Experimental Allergy, Department of Dermatology, Medical University of Vienna, Vienna, Austria

<sup>b</sup> Institute of Clinical Pathology, Medical University of Vienna, Vienna, Austria

<sup>c</sup> Department of Pulmonary Disease Research, Boehringer-Ingelheim Pharma, Biberach, Germany

### ARTICLE INFO

#### Article history:

Received 4 April 2013

Received in revised form

19 August 2013

Accepted 23 September 2013

#### Keywords:

Mice

Inbred BALB/c

Allergic lung inflammation

Airway hyperresponsiveness

Experimental allergic asthma

Tiotropium bromide

### ABSTRACT

Recurrent relapses of allergic lung inflammation in asthmatics may lead to airway remodeling and lung damage. We tested the efficacy of tiotropium bromide, a selective long-acting, muscarinic receptor antagonist as an adjunct therapy in relapses of allergic asthma in mice. We compared the effectiveness of local intranasal administration of tiotropium and dexamethasone in acute and relapsing allergic asthma in BALB/c mice. Although tiotropium at low doses is a potent bronchodilator, we tested higher doses to determine effectiveness on inflammation and mucus hypersecretion. A 5-day course of twice daily intranasal tiotropium or dexamethasone (1 mg/kg (b.w.)) suppressed airway eosinophils by over 87% during disease initiation and 88% at relapse compared to vehicle alone. Both drugs were comparable in their capacity to suppress airway and parenchymal inflammation and mucus hypersecretion, though tiotropium was better than dexamethasone at reducing mucus secretion during disease relapse. Despite treatment with either drug, serum antigen-specific IgE or IgG1 antibody titres remained unchanged. Our study indicates that tiotropium at higher doses than required for bronchodilation, effectively suppresses inflammation and mucus hypersecretion in the lungs and airways of mice during the initiation and relapse of asthma. Tiotropium is currently not approved for use in asthma. Clinical studies have to demonstrate the efficacy of tiotropium in this respiratory disease.

© 2013 Elsevier Ltd. All rights reserved.

### 1. Introduction

The importance of eosinophilic inflammation in the lungs of individuals with allergic asthma is underscored by their essential role in allergen-induced airway hyperresponsiveness (AHR) and ultimately airway remodeling in mouse models [12,20]. T helper (Th) 2 cytokines IL-4, IL-5, and IL-13 produced by T lymphocytes are important for eosinophil accumulation and activation [3,6,32]. Once present in the lung, eosinophils produce factors such as cytokines that lead to mucus hypersecretion and airway

remodeling [7,28]. Although it is important to address the long-term adverse effects of chronic eosinophilic lung inflammation in asthmatics, we argue that it is also crucial to recognize the role of eosinophils in recurrent allergen-induced relapses common in individuals with seasonal allergic asthma. Asymptomatic patients between relapses of allergic asthma have lung pathology [25,30,33]. Additionally, mice recovered from one episode of acute allergic asthma have chronic lung inflammation containing allergen-specific Th2 cells without eosinophils and respond vigorously to allergen rechallenge which induces disease relapses [24]. Chronic inflammation, even without eosinophils during asymptomatic remissions and undoubtedly recurrent relapses may lead to airway remodeling.

Anticholinergic drugs, such as tiotropium bromide are important for the treatment of chronic obstructive pulmonary disease, but are generally not used to treat asthma. However, there is clinical evidence revealing that tiotropium, a selective long-acting, muscarinic receptor antagonist treatment reduces relapses in severe asthmatics [27]. The effects of tiotropium on bronchoconstriction are well known [10]. However, its properties

**Abbreviations:** AHR, airway hyperresponsiveness; AUC, area under curve; BAL, bronchoalveolar lavage fluid; OVA, ovalbumin; PBS, phosphate buffered saline; Th, T helper.

<sup>☆</sup> These studies were supported by Department of Pulmonary Disease Research, Boehringer-Ingelheim Pharma, Biberach, Germany.

\* Corresponding author. Medical University of Vienna, Department of Dermatology, DIAID, Experimental Allergy, Waehringer Guertel 18-20, Room 4P9.02, A-1090 Vienna, Austria. Tel.: +431 40160 63012; fax: +431 40160 963012.

E-mail address: [Michelle.Epstein@meduniwien.ac.at](mailto:Michelle.Epstein@meduniwien.ac.at) (M.M. Epstein).

1094-5539/\$ – see front matter © 2013 Elsevier Ltd. All rights reserved.

<http://dx.doi.org/10.1016/j.pupt.2013.09.004>

on inflammation and immunity have not been extensively studied [15,26]. Acetylcholine appears to play a role in the regulation of immune responses [8,11] and the release of pro-inflammatory mediators from airway smooth muscle and epithelial cells [14,18,19]. Moreover, lymphocytes, Th2 cells, eosinophils, alveolar macrophages and mast cells all synthesize and contain acetylcholine (reviewed in Ref. [34]). Furthermore, muscarinic receptors are expressed on T cells, neutrophils, macrophages and mast cells [11] and the muscarinic receptor antagonist, atropine inhibits antibody production, T cell proliferation and leukocyte migration [31]. Additional evidence comes from animal models showing that tiotropium effectively suppresses inflammation in chronic asthma in mice and guinea pig [16,21,22].

In this study, we sought to further analyze the anti-inflammatory properties of tiotropium in a mouse model of relapsing allergic asthma that mimics seasonal allergic disease. Our data suggest that higher doses of tiotropium suppress inflammation and have clinical implications for the prevention of allergic relapses.

## 2. Materials and methods

### 2.1. Mice

Eight week old female BALB/c mice (Charles River, Germany) provided ovalbumin (OVA)-free food (SSNIFF, Soest, Germany) and water *ad libitum* were used in all experiments. All experimental protocols complied with the requirements of the Animal Care Committee of the Austrian Ministry of Science and the ethics committee at Boehringer-Ingelheim, Biberach.

### 2.2. Induction of allergic asthma

Immunization and challenge of mice in models of acute allergic asthma and disease relapse were done as previously described [24]. Briefly, naïve BALB/c mice were compared with mice immunized with 10 µg of OVA (Sigma Chemical Co., St. Louis, MO, USA) intraperitoneally (i.p.) on days 0 and 21 and then challenged 1 week later (or as indicated) with nebulized 1% OVA in phosphate buffered saline

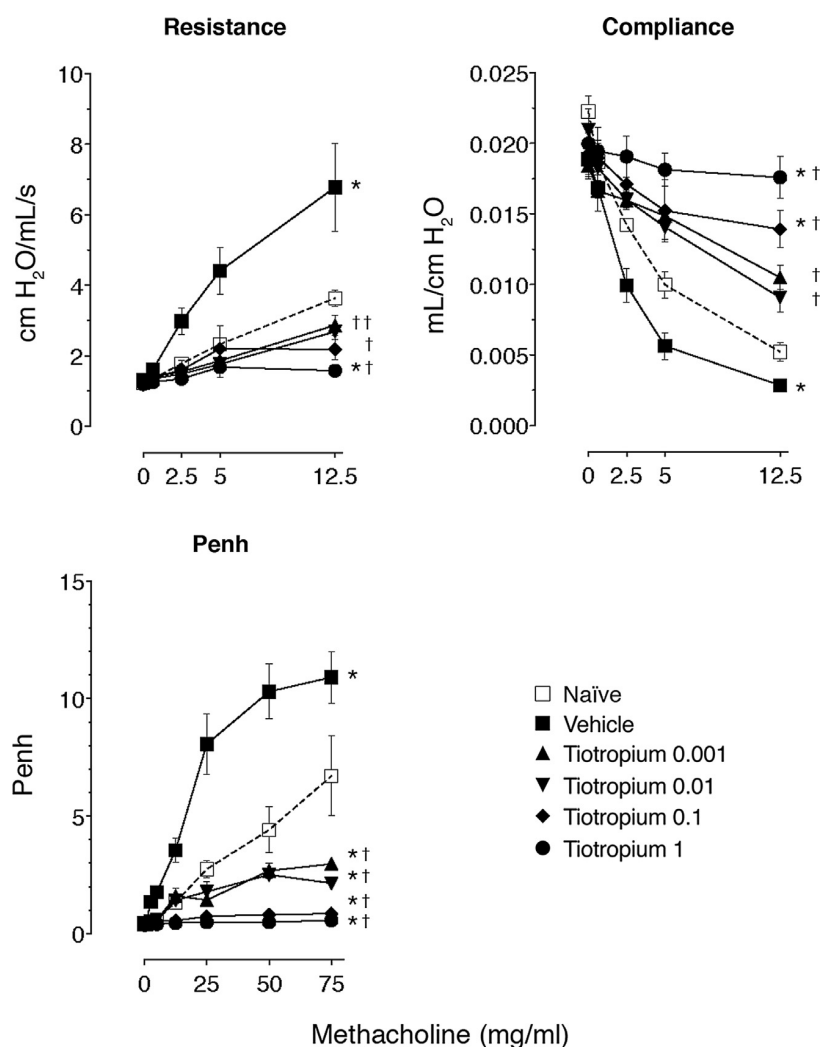


**Fig. 1.** Effect of tiotropium on methacholine-induced airway hyperresponsiveness. Titrated doses of aerosolized methacholine-induced resistance and compliance measured with resistance and compliance system, as well as enhanced pause measured with whole-body plethysmography. Naïve mice, vehicle-treated, and mice treated with titrated doses of tiotropium from 0.001 to 1 mg/kg were compared 72 h after aerosol challenge. Data are expressed as mean  $\pm$  SEM from two independent experiments ( $n = 6-8$ ). One-way ANOVA followed by Dunnett's multiple comparison test of mean AUC; \* $p < 0.05$  is significant for all groups compared to the naïve group and † $p < 0.05$  is significant when compared to the vehicle-treated group.

(PBS) in a Plexiglas chamber by an ultrasonic nebulizer (Aerodyne, Kendall, Neustadt, Germany) for 60 min twice daily on 2 consecutive days (days 28, 29 unless indicated) to induce acute onset disease (acute). For disease relapse, mice with acute disease were rested for at least 90 days and then rechallenged with a 1% OVA nebulization for 60 min twice daily on 2 consecutive days as indicated.

### 2.3. Treatment protocols

For the treatment of AHR, we administered dexamethasone (Sigma Chemical Company, St. Louis, USA) at the dose of 1 mg/kg or tiotropium (Boehringer-Ingelheim Pharma, Biberach, Germany) at the doses of 1, 0.1, 0.01 or 0.001 mg/kg for 5 days, starting 3 days before nebulized OVA challenges in the acute model. For the treatment of other disease parameters before the onset of acute disease and before inducing disease relapse, mice received twice daily intranasal instillations of dexamethasone or tiotropium at the dose of 1 mg/kg for 5 days, starting 3 days before nebulized OVA challenges. For all treatments, we administered the drugs 30 min before aerosol challenges. For each application of 1 mg/kg dose, dexamethasone and tiotropium were dissolved in PBS for a final concentration of 0.5 mg/ml. For 0.1, 0.01 and 0.001 mg/kg doses, tiotropium was dissolved in PBS for a final concentration of 50, 5 and 0.5 µg/ml, respectively. All solutions were administered to the mice in 50 µl.

### 2.4. Airway hyperresponsiveness

We measured airway hyperresponsiveness (AHR) as a change in airway function at 72 h after the last challenge with aerosolized methacholine (Sigma) using two different techniques. In conscious, unrestrained mice, we measured AHR by whole-body plethysmography (Buxco Electronics Ltd., NY, USA). PBS, followed by increasing concentrations of methacholine, was nebulized for 3 min and lung function was recorded and calculated as enhanced pause (Penh), which is a dimensionless unit that correlates with pulmonary resistance. In separate experiments, airway resistance and compliance were measured in anesthetized and ventilated animals by Resistance and Compliance System (Buxco Electronics Ltd.). As for whole-body plethysmography, PBS followed by increasing concentrations of methacholine was nebulized for 3 min and lung function was recorded and calculated using FinePoint software (Buxco Electronics Ltd.).

### 2.5. Airway inflammation

Seventy-two hours after last challenge, mice were terminally anesthetized, tracheostomy was performed and a plastic catheter was clamped into the trachea. The lungs were washed 3 times with PBS in a total volume of 1 ml (0.4, 0.3 and 0.3 ml) to collect bronchoalveolar lavage fluid (BAL). The total number of cells in BAL was enumerated in a Neubauer hemocytometer. The percentage of inflammatory cells was determined by morphological examination of at least 300 cells in cytocentrifuged preparations (Cytospin-4, Shandon Instruments, UK), stained with the Kwik-Diff (Thermo Fisher Scientific Inc., Pittsburgh, PA, USA).

### 2.6. Lung inflammation and mucus hypersecretion

After bronchoalveolar lavage, lungs were dissected and fixed by immersion in 4% paraformaldehyde. Paraplast-embedded lung sections of 3 µm were stained with hematoxylin and eosin (H&E) for morphological evaluation, with Luna stain for eosinophil enumeration [23] and with periodic acid-Schiff stain (PAS) for mucopolysaccharide staining intensity of lung. For scoring of inflammatory cell infiltration, sections containing main stem bronchi from each lung specimen stained with H&E were used. An expert respiratory

pathologist blinded to the treatment groups graded the extent of inflammation in the lungs according to a semi-quantitative scoring system: Grade 0 – no inflammatory infiltrates; Grade 1 – inflammatory infiltrates in central airways; Grade 2 – inflammatory infiltrates extending to middle third of lung parenchyma; and Grade 3 – inflammatory infiltrates extending to the periphery of the lung [24]. For quantification of eosinophil infiltration, eosinophils were counted on 5 random fields in Luna stained sections (400× magnification) containing major airways and vessels (which were selected from low power magnification) and averaged for each lung. For detection of mucus-containing cells in formalin-fixed lung tissue, 4 µm sections containing main stem bronchi from each lung specimen were stained with PAS and counter stained with hematoxylin. The number of mucus-containing cells per millimeter of basement membrane was determined with CellB software (Olympus Europa Holding GmbH, Hamburg, Germany).

### 2.7. Serum OVA-specific immunoglobulin

For the measurement of OVA-specific IgG1 and IgE, ELISA plates were coated with OVA at 10 µg/ml overnight at 4 °C. The plates were washed and blocked with 2% bovine serum albumin in PBS with 0.05% Tween 20 for 2 h at room temperature. Then sera were titrated onto the plates and incubated for 24 h at 4 °C before washing. Plates were incubated for an additional 2 h at 4 °C with biotinylated anti-IgG1 (Southern Biotechnology Associates Inc., Birmingham, AL, USA) or anti-IgE (Becton Dickinson Biosciences, Franklin Lakes, NJ, USA) detection antibodies, followed by incubation with streptavidin horseradish peroxidase (Southern Biotechnology) for 1 h at room temperature. Plates were washed and incubated with TMB substrate solution (100 µl/well, BD OptEIAM,

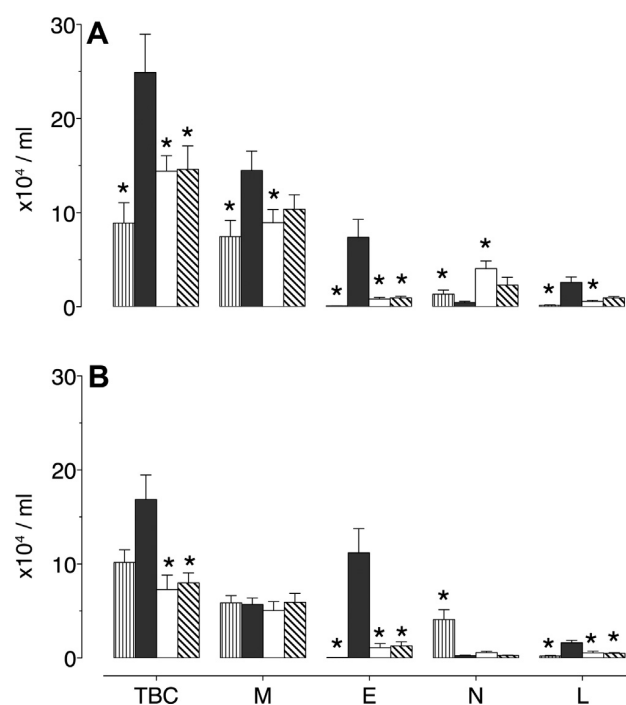


**Fig. 2.** Effect of tiotropium on airway inflammation. Total inflammatory cell count and differential counts in BAL of naive, vehicle, dexamethasone and tiotropium treated mice 72 h after the last aerosol challenge at (A) disease initiation and at (B) disease relapse. Results are expressed as mean cell counts  $\pm$  SEM from two independent experiments ( $n = 6-10$ ). One-way ANOVA followed by Dunnett's multiple comparison test; \* $p < 0.05$  is significant for all groups compared to the naive group and † $p < 0.05$  is significant when compared to the vehicle-treated group. TBC: Total BAL cell count, M: Macrophages, E: Eosinophils, N: Neutrophils, L: Lymphocytes.

Becton Dickinson Biosciences) for 10 min at room temperature. The reaction was stopped with 100  $\mu$ l of 0.18 M H<sub>2</sub>SO<sub>4</sub> and the plates were measured at 450 nm.

### 2.8. Statistical analysis

To compare AHR data, area under curve (AUC) was calculated for each experimental animal on the graph of resistance, compliance or Penh (y axis) vs. the methacholine concentration (mg/ml; x axis). Calculated AUC values from AHR data, airway inflammation data, as well as mucus-positive cell and eosinophil counts in the lungs were log-transformed to equalize variances and analyzed with one-way

ANOVA followed by Dunnett's multiple comparison test. Histology scores for inflammation were analyzed with Chi-squared test for trend. All analyses were done using GraphPad InStat v.5.0 (GraphPad Software Inc.) and *p* values were considered significant at <0.05.

## 3. Results

### 3.1. Tiotropium inhibits airway hyperresponsiveness in allergic asthma

Tiotropium as a muscarinic receptor antagonist in chronic obstructive pulmonary disease inhibits bronchoconstriction. To test

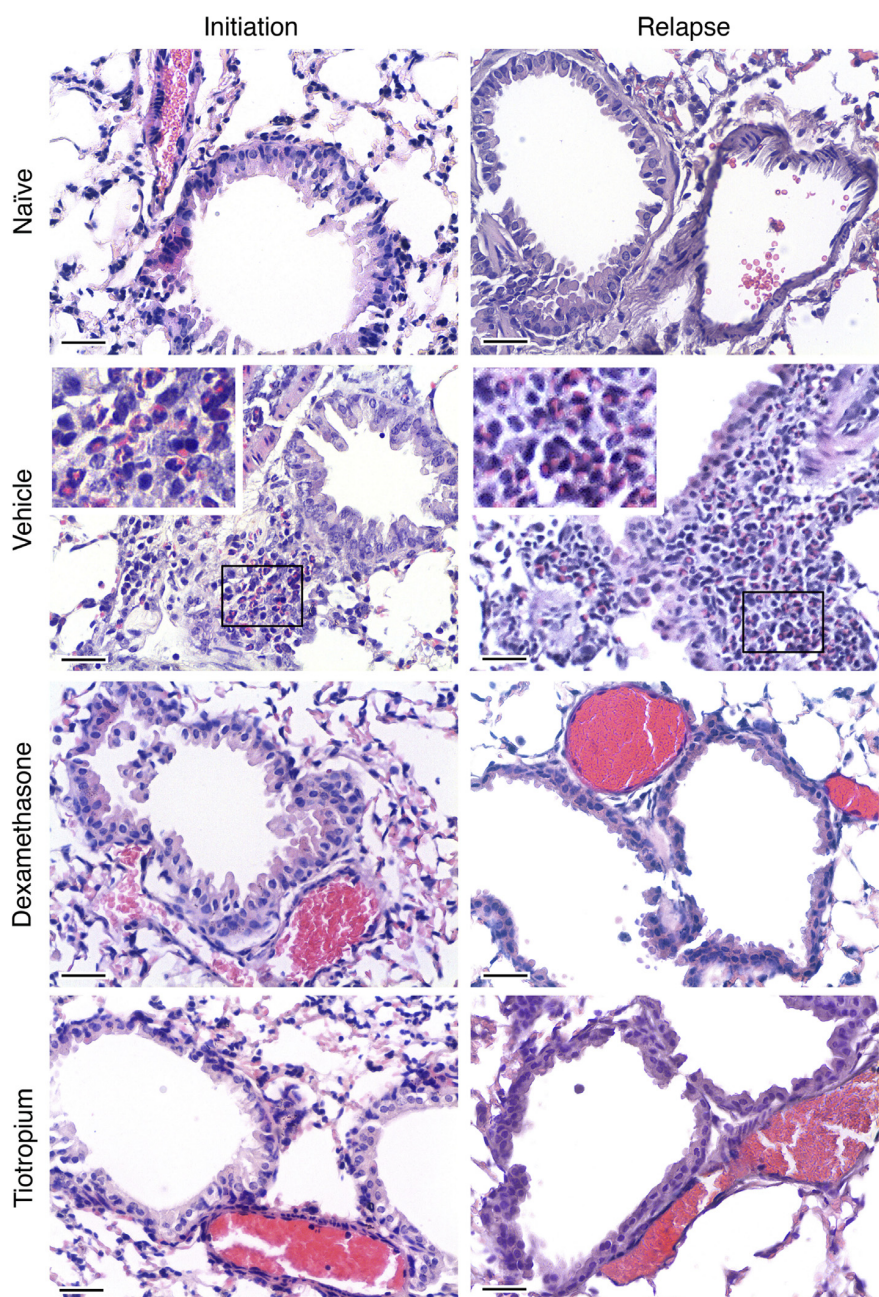


**Fig. 3.** Effect of tiotropium on lung inflammation. Representative photomicrographs of lung tissue on H&E stained sections (bar 100  $\mu$ m) from naïve, vehicle, dexamethasone and tiotropium treated mice 72 h after the last aerosol challenge (*n* = 6–10). Naïve mice have normal tissue without evidence of inflammation. At initiation and relapse, inflammatory infiltrates containing eosinophils (insets) are observed, but are reduced in the lungs of dexamethasone and tiotropium treated mice.

bronchodilator efficacy in acute allergic asthma, we instilled mice with the drugs intranasally for 5 days starting 3 days before the first challenge and then measured methacholine-induced AHR by unrestrained plethysmography. Tiotropium significantly reduced AHR at doses starting at 0.001 mg/kg (Fig. 1). Tiotropium treatment continued to inhibit AHR for 72 h after treatment at all doses, showing a long-acting effect on AHR even at low doses. However, at higher doses of 1 mg/kg, AHR was inhibited for over 1 week and airway eosinophils were suppressed (data not shown). We also measured airway resistance and compliance in anesthetized and ventilated allergen-treated animals and found that tiotropium at the same doses effectively and dose-dependently inhibited airway resistance and compliance (Fig. 1) an effect that was also seen when the mice were treated with dexamethasone (data not shown). Furthermore, in naïve mice tiotropium also reduced methacholine-induced AHR, but not as strongly as seen in the allergen treated mice (data not shown).

### 3.2. Tiotropium has anti-inflammatory effects in allergic asthma

Dexamethasone is one of the most effective anti-inflammatory drugs used in allergic asthma. To address whether tiotropium exhibited similar anti-inflammatory properties, we compared the effect of dexamethasone and tiotropium on inflammatory cell infiltrates in the airways and lungs of mice. At the initiation of allergic asthma, tiotropium and dexamethasone significantly inhibited overall airway inflammation by 41.1% and 42.1%, respectively compared to vehicle controls (Fig. 2). Both treatment regimens significantly inhibited airway eosinophilia from  $7.4 \pm 1.9 \times 10^4$  cells/ml in the vehicle, to  $0.84 \pm 0.17 \times 10^4$  and  $0.9 \pm 0.18 \times 10^4$  cells/ml in dexamethasone and tiotropium treated mice, respectively. Both drugs also significantly reduced the number of lymphocytes. An additional effect of dexamethasone treatment was the reduction of macrophages and increase in neutrophils, a feature not observed with tiotropium treatment. To evaluate the drug efficacy during a relapse of allergic asthma, mice were treated with either tiotropium or dexamethasone just before and at the time of OVA-aerosol rechallenges (Fig. 2). We found that, similar to the effect on acute initiation of disease, tiotropium and dexamethasone inhibited the extent of inflammation in the airways by 52.6% and 56.8%, respectively, and specifically reduced the number of infiltrating eosinophils by 88.4% and 90.2% and lymphocytes by 69.0% and 66.0%, respectively.

Further evaluation of inflammation was achieved by examining H&E stained lung sections (Fig. 3). These lung sections were graded for the severity of inflammation and eosinophils were enumerated in the tissues (Fig. 4). At disease initiation, drug treatment suppressed overall inflammation in the parenchyma by up to 43.2% and eosinophils were reduced by tiotropium by 82.0% and dexamethasone by 85.2% compared to vehicle alone treatment. Tiotropium and dexamethasone also prevented eosinophilic lung inflammation upon OVA-induced disease relapse (Fig. 4). Taken together, these data demonstrate that tiotropium at higher doses than required to inhibit AHR, has anti-inflammatory properties comparable to dexamethasone.

### 3.3. Tiotropium effectively prevents mucus hypersecretion in acute and relapsing allergic asthma

To determine whether tiotropium inhibits mucus production in allergic disease, we evaluated the extent of mucus secretion of goblet cells in bronchial epithelium (Fig. 5). We compared the efficacy of tiotropium with dexamethasone and vehicle treatments and observed that both drugs markedly suppressed mucus overproduction at the initiation of allergic asthma compared to vehicle-treated control mice (Fig. 6). Naïve mice have the occasional mucus

producing goblet cell whereas vehicle-treated mice have their airway epithelia filled with mucus producing cells. In mice with acute allergic asthma, tiotropium reduced the number of mucus-positive cells by 50.3% compared to 56.7% by dexamethasone, indicating that tiotropium is as good as dexamethasone at suppressing mucus production. In experiments in which mice were treated before disease relapse, tiotropium treatment decreased the number of mucus-positive cells by 33.7%, which was greater than dexamethasone which suppressed mucus-positive cell number by 16.6%. These data demonstrate that tiotropium inhibits mucus hypersecretion as well as and even better than dexamethasone in acute and relapsing allergic asthma.

### 3.4. Tiotropium effect on OVA-specific IgE and IgG1

To determine whether B cell immune responses were influenced by treatment, we tested serum OVA-specific antibody titers 5 days after the last aerosol challenge (Fig. 7). We did not detect OVA-specific antibodies in naïve mice, however, vehicle-treated animals had high titres of OVA-specific IgE and IgG1 antibodies. Neither treatment with dexamethasone nor tiotropium reduced antibody titres.

## 4. Discussion

Here, we compared the potential of tiotropium in the prevention of the onset of acute asthma and a subsequent disease

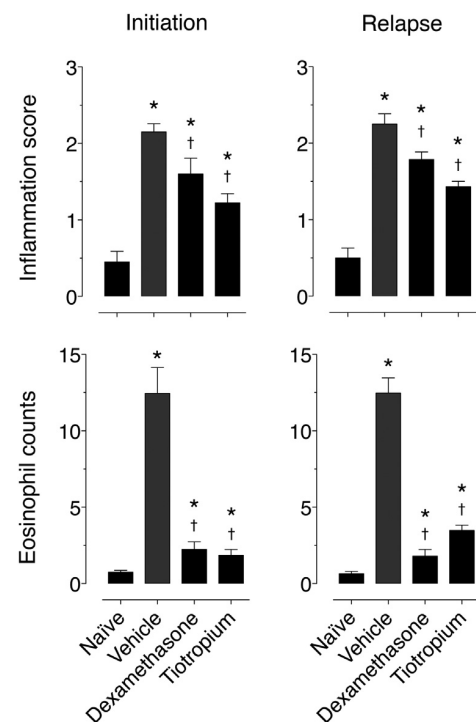


**Fig. 4.** Effect of tiotropium on inflammation and eosinophils in lung parenchyma. Inflammation scores and eosinophil counts in lungs of naïve control mice, vehicle, dexamethasone and tiotropium treated mice before initiation and relapse of asthma. Luna stained lung sections (per 400 $\times$ ) sampled at 72 h after final challenge. Results are expressed as mean inflammation score and eosinophil count per high power field  $\pm$  SEM from two independent experiments ( $n = 6-10$ ). One-way ANOVA followed by Dunnett's multiple comparison test for eosinophil counts and a Chi-square test for trend for inflammation scores. \* $p < 0.05$  compared with naïve group; † $p < 0.05$  compared with vehicle-treated group.

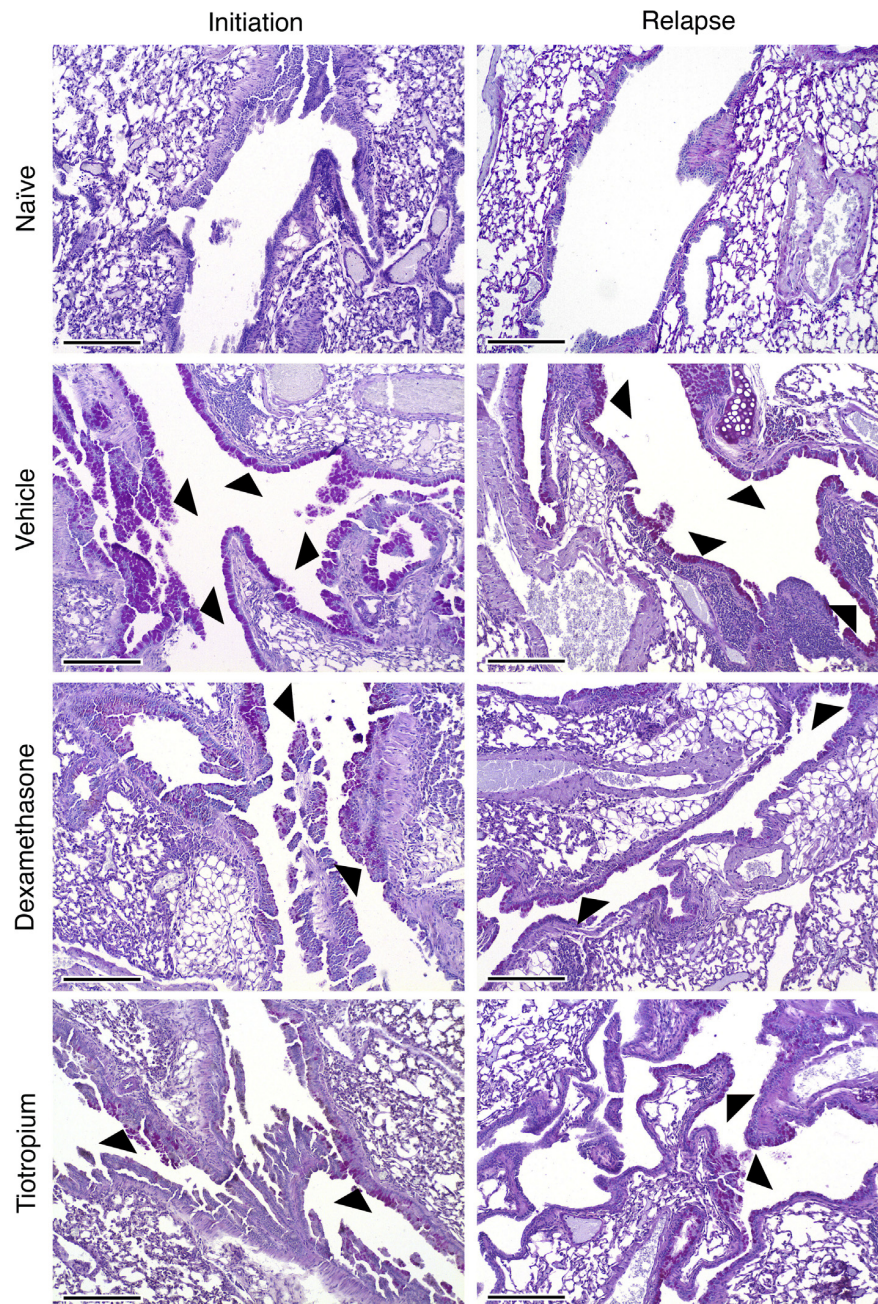


**Fig. 5.** Effect of tiotropium on mucus hypersecretion. Representative photomicrographs of lung tissue on PAS stained sections (bar 200  $\mu\text{m}$ ) from naïve, vehicle, dexamethasone and tiotropium treated mice 72 h after the last aerosol challenge ( $n = 6-10$ ). Naïve mice have normal tissue with very rare mucus-positive cells. At initiation of disease and relapse in the vehicle-treated sections, almost all cells in the epithelium are positive for mucus. At initiation and relapse, mucus-positive cells are observed, but are reduced in the lungs of dexamethasone and tiotropium treated mice. Arrowheads point to the areas of the epithelium with mucus-positive cells.

relapse. We observed a powerful effect on AHR at low doses and at higher doses tiotropium was as effective as dexamethasone at suppressing mucus hypersecretion and eosinophilic lung inflammation. Tiotropium was as effective at preventing the onset of acute disease as it was at preventing disease relapse, suggesting the potential use of tiotropium in patients with seasonal allergic asthma. Our findings support the use of tiotropium as a bronchodilator, mucolytic and anti-inflammatory in the treatment of relapses of allergic asthma.

Tiotropium successfully reduced AHR at very low doses by either decreasing the reactivity of airway smooth muscle or blocking the binding of methacholine to its receptor. There is evidence that non-bronchodilating mechanisms of tiotropium prevent airway hyperreactivity in a guinea pig model of allergic asthma [4]. Antigen-induced hyperreactivity was completely blocked by tiotropium treatment and partially blocked with atropine treatment and that tiotropium blocked bronchoconstriction induced by intravenous acetylcholine but did not inhibit vagally-induced

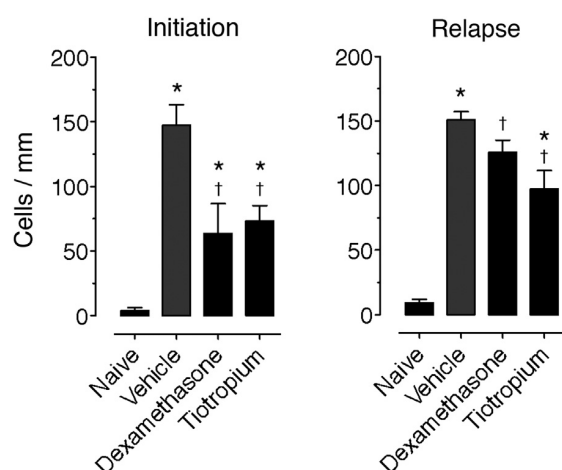


**Fig. 6.** Effect of tiotropium on the extent of mucus hypersecretion. Number of mucus-positive cells per millimeter of basement membrane in naïve control mice, vehicle, dexamethasone and tiotropium treated mice before initiation and relapse. Results are expressed as mean  $\pm$  SEM from two independent experiments ( $n = 6-10$ ). \* $p < 0.05$  compared with naïve group; † $p < 0.05$  compared with vehicle-treated group (Chi-square test for trend).

bronchoconstriction in sensitized controls. These data suggest that tiotropium does not block hyperreactivity by blocking receptors for vagally-released acetylcholine and suggests that tiotropium may work via anti-inflammatory mechanisms because it also inhibited eosinophilia in the lungs and around nerves.

Our findings illustrate that at high doses, tiotropium is as effective an anti-inflammatory as dexamethasone in the initiation and relapse of allergic asthma. Our data support previous reports showing that 4 daily doses of 50  $\mu$ l of 0.1 mM tiotropium given by aerosol over 3 min had anti-inflammatory effects in the airways of mice with acute onset allergic asthma [26] and a study in guinea pigs revealing that tiotropium (1  $\mu$ g/kg) suppresses lung eosinophilia in acute allergic asthma [4]. In contrast, low doses of 50  $\mu$ l of 0.1 nM tiotropium (corresponding to a dose of  $\sim 0.1$   $\mu$ g/kg) given intranasally for 5 days (on the same days that the animals were challenged with allergen) actually increased airway inflammation with an increase in macrophages and eosinophils [15]. Not only do our results

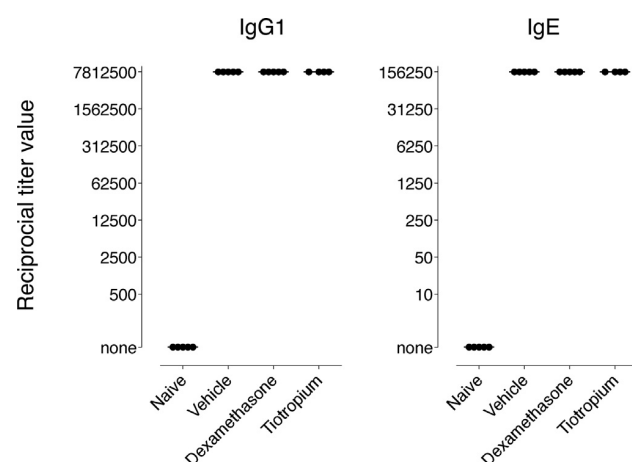


**Fig. 7.** Tiotropium effect on serum OVA-specific antibody at disease initiation. Analysis of serum OVA-specific IgG1 and IgE antibody titres from naïve, vehicle, dexamethasone and tiotropium treated mice 5 days after the last aerosol challenge for the initiation of allergic asthma. Results are shown as reciprocal titres for individual mice (dots) and group mean (line) from two independent experiments ( $n = 4-5$ ). \* $p < 0.05$  compared with naïve group by one-way ANOVA.

with high doses illustrate that acute initiation of eosinophilic airway inflammation is suppressed by tiotropium, but that parenchymal lung inflammation is also significantly suppressed.

Tiotropium and dexamethasone almost completely prevent eosinophil infiltration of the airways at disease relapse. Previous mouse studies reveal that mice recovered from allergic asthma have long-lived memory Th2 cells, macrophages, B cells and dendritic cells residing in chronic infiltrates, but lack eosinophils and neutrophils [24]. These memory cells respond rapidly to allergen rechallenge with recruitment of eosinophils that treatment with both tiotropium and dexamethasone prevent. Although, acute onset eosinophilic airway inflammation and eosinophilia in the parenchyma were prevented, we observed that inflammatory infiltrates in the lungs remain, i.e. the lungs are not like those from naïve mice. Unfortunately, these infiltrates are difficult to eliminate and if maintained, the cells within the infiltrates will continue to respond to allergen rechallenges leading to relapses (M. Epstein, unpublished data). Generally, parenchymal infiltration and airway inflammation correlate. However, we have encountered other situations in which they do not [13]. In this study, parenchymal infiltrates were eliminated while airway inflammation persisted after treatment with dexamethasone. In contrast, tiotropium appears to reduce airway inflammation more rapidly than parenchymal inflammation and seems to target eosinophils earlier than macrophages and lymphocytes, which are the predominant cells within the infiltrates. It is possible that for complete elimination of lung infiltrates, chronic treatment is necessary, even in asymptomatic individuals with infrequent relapses. This is especially relevant in lieu of the studies showing that a longer duration of treatment with low dose tiotropium was effective at reducing inflammation and reduced airway remodeling in chronic models in mice [15,26] and in guinea pigs [2,9].

Clinical evidence of tiotropium treatment reducing the number of relapses in severe asthmatics [27] suggests that tiotropium is beneficial in allergic asthma, yet the mechanisms underlying a potential anti-inflammatory effect remain unclear. There is evidence for a role of muscarinic receptors on immune and inflammatory cells [8,11,31], however, our studies suggest that it is necessary to increase the dose of tiotropium to increase efficacy, at least in mice. Having determined that inflammation is suppressed by treatment with tiotropium, that Th2 cytokines are concomitantly reduced [15,26], and being aware that B cells express muscarinic receptors [34], we anticipated that high doses of tiotropium would inhibit B cell responses resulting in reduced allergen-specific antibody titres. However, we observed no effect of either tiotropium or dexamethasone treatment on antibody production. It is not clear why titres remained unaffected but a possible explanation is that the duration of treatment was too short to observe a change in the titres. In a previous study, no changes in allergen-specific antibody titres were observed in a chronic model with chronic tiotropium treatment [26].

The observed anti-inflammatory mechanism may be related to the bronchodilatory properties of tiotropium. However, preclinical evidence suggests anti-inflammatory properties of tiotropium beyond bronchodilation. Cholinergic stimulation was shown to trigger the release of chemotactic factors in bronchial epithelial cells *in vitro* [5,19]. Supernatant taken from epithelial cells stimulated with acetylcholine induced chemotaxis in primary human eosinophils [19] or neutrophils [5]. This migratory response of neutrophils was absent in experiments where the epithelial cells were pretreated with tiotropium [5]. Neutrophil migration was inhibited directly by an LTB4 antagonist suggesting that this mediator may play a role in cholinergic inflammation. Taken together, these data suggest that tiotropium may also have direct anti-inflammatory effects in our mouse model of allergic

inflammation. Further research is needed to elucidate if and by which mechanism tiotropium causes direct anti-inflammatory effects.

Tiotropium and dexamethasone treatment suppressed mucus secretion by over 50% at the initiation of disease, but they were less effective during a relapse and dexamethasone reduced mucus production half as well as tiotropium. Our results demonstrate that both treatments do not abolish mucus production and this may relate to duration of therapy, however, long-term experiments in mice with chronic treatment reduced mucus from approximately 60 to 40%, but this might be because mucus metaplasia is more severe in chronic disease and therefore, more difficult to treat [26].

Our study indicates that tiotropium at higher doses than required for bronchodilation effectively suppresses inflammation and mucus hypersecretion in the lungs and airways of mice during the initiation and relapse of asthma. Recent studies show that tiotropium is effective as an adjunct in uncontrolled asthma at doses of 5–50 µg daily [1,17,29]. The doses used in the studies are not as high as the doses used in mice. It is likely that in this dose level, the effect is on airway smooth muscle. It is not yet known whether higher doses would further increase effectiveness by reducing inflammation. These studies have not been done. Taken together, our studies in addition to others indicate that tiotropium has anti-inflammatory activity at higher doses and that tiotropium is effective in patients. More studies are needed to understand the mechanism underlying the tiotropium effect in asthma.

#### Authorship contributions

Participated in research design: Bosnjak, Erb, Pieper, Epstein.

Contributed new reagents or analytic tools: none.

Conducted experiments: Bosnjak, Tilp, Tomsic, Dekan.

Performed data analysis: Bosnjak, Erb, Tilp, Tomsic, Dekan, Epstein.

Wrote or contributed to the writing of the manuscript: Bosnjak, Dekan, Pieper, Erb, Epstein.

#### Acknowledgments

The authors would like to thank Drs. Oskar Hoffmann and Peter Stütz for their critical comments.

#### References

- Bateman ED, Kornmann O, Schmidt P, Pivovarova A, Engel M, Fabbri LM. Tiotropium is noninferior to salmeterol in maintaining improved lung function in B16-Arg/Arg patients with asthma. *J Allergy Clin Immunol* 2011;128:315–22.
- Bos IS, Gosens R, Zuidhof AB, Schaafsma D, Halayko AJ, Meurs H, et al. Inhibition of allergen-induced airway remodelling by tiotropium and budesonide: a comparison. *Eur Respir J* 2007;30:653–61.
- Broide DH. Immunologic and inflammatory mechanisms that drive asthma progression to remodeling. *J Allergy Clin Immunol* 2008;121:560–70 quiz 571–2.
- Buels KS, Jacoby DB, Fryer AD. Non-bronchodilating mechanisms of tiotropium prevent airway hyperreactivity in a guinea-pig model of allergic asthma. *Br J Pharmacol* 2012;165:1501–14.
- Buhling F, Lieder N, Kuhlmann UC, Waldburg N, Welte T. Tiotropium suppresses acetylcholine-induced release of chemotactic mediators in vitro. *Respir Med* 2007;101:2386–94.
- Cho JY, Miller M, Baek KJ, Han JW, Nayar J, Lee SY, et al. Inhibition of airway remodeling in IL-5-deficient mice. *J Clin Invest* 2004;113:551–60.
- Flood-Page P, Menzies-Gow A, Phipps S, Ying S, Wangoo A, Ludwig MS, et al. Anti-IL-5 treatment reduces deposition of ECM proteins in the bronchial subepithelial basement membrane of mild atopic asthmatics. *J Clin Invest* 2003;112:1029–36.
- Fujii T, Takada-Takatori Y, Kawashima K. Basic and clinical aspects of non-neuronal acetylcholine: expression of an independent, non-neuronal cholinergic system in lymphocytes and its clinical significance in immunotherapy. *J Pharmacol Sci* 2008;106:186–92.
- Gosens R, Bos IS, Zaagsma J, Meurs H. Protective effects of tiotropium bromide in the progression of airway smooth muscle remodeling. *Am J Respir Crit Care Med* 2005;171:1096–102.
- Gross NJ. Anticholinergic agents in asthma and COPD. *Eur J Pharmacol* 2006;533:36–9.
- Gwilt CR, Donnelly LE, Rogers DF. The non-neuronal cholinergic system in the airways: an unappreciated regulatory role in pulmonary inflammation? *Pharmacol Ther* 2007;115:208–22.
- Humbles AA, Lloyd CM, McMillan SJ, Friend DS, Xanthou G, McKenna EE, et al. A critical role for eosinophils in allergic airways remodeling. *Science* 2004;305:1776–9.
- Jungsuwadee P, Dekan G, Stingl G, Epstein MM. Inhaled dexamethasone differentially attenuates disease relapse and established allergic asthma in mice. *Clin Immunol* 2004;110:13–21.
- Kanefsky J, Lenburg M, Hai CM. Cholinergic receptor and cyclic stretch-mediated inflammatory gene expression in intact ASM. *Am J Respir Cell Mol Biol* 2006;34:417–25.
- Kang JY, Rhee CK, Kim JS, Park CK, Kim SJ, Lee SH, et al. Effect of tiotropium bromide on airway remodeling in a chronic asthma model. *Ann Allergy Asthma Immunol* 2012;109:29–35.
- Karner C, Chong J, Poole P. Tiotropium versus placebo for chronic obstructive pulmonary disease. *Cochrane Database Syst Rev* 2012;7:CD009285.
- Kerstjens HA, Disse B, Schroder-Babo W, Bantje TA, Gahlemann M, Sigmund R, et al. Tiotropium improves lung function in patients with severe uncontrolled asthma: a randomized controlled trial. *J Allergy Clin Immunol* 2011;128:308–14.
- Koyama S, Rennard SI, Robbins RA. Acetylcholine stimulates bronchial epithelial cells to release neutrophil and monocyte chemotactic activity. *Am J Physiol* 1992;262:L466–71.
- Koyama S, Sato E, Nomura H, Kubo K, Nagai S, Izumi T. Acetylcholine and substance P stimulate bronchial epithelial cells to release eosinophil chemotactic activity. *J Appl Physiol* 1998;84:1528–34.
- Lee JJ, Dimina D, Macias MP, Ochkur SI, McGarry MP, O'Neill KR, et al. Defining a link with asthma in mice congenitally deficient in eosinophils. *Science* 2004;305:1773–6.
- Littner MR, Ilowite JS, Tashkin DP, Friedman M, Serby CW, Menjoge SS, et al. Long-acting bronchodilation with once-daily dosing of tiotropium (Spiriva) in stable chronic obstructive pulmonary disease. *Am J Respir Crit Care Med* 2000;161:1136–42.
- Maesen FP, Smeets JJ, Sledsens TJ, Wald FD, Cornelissen PJ. Tiotropium bromide, a new long-acting antimuscarinic bronchodilator: a pharmacodynamic study in patients with chronic obstructive pulmonary disease (COPD). *Dutch Study Group. Eur Respir J* 1995;8:1506–13.
- Meyerholz DK, Griffin MA, Castilow EM, Varga SM. Comparison of histochemical methods for murine eosinophil detection in an RSV vaccine-enhanced inflammation model. *Toxicol Pathol* 2009;37:249–55.
- Mojtabavi N, Dekan G, Stingl G, Epstein MM. Long-lived Th2 memory in experimental allergic asthma. *J Immunol* 2002;169:4788–96.
- Ohruai T, Sekizawa K, Yanai M, Morikawa M, Jin Y, Sasaki H, et al. Partitioning of pulmonary responses to inhaled methacholine in subjects with asymptomatic asthma. *Am Rev Respir Dis* 1992;146:1501–5.
- Ohta S, Oda N, Yokoe T, Tanaka A, Yamamoto Y, Watanabe Y, et al. Effect of tiotropium bromide on airway inflammation and remodeling in a mouse model of asthma. *Clin Exp Allergy* 2010;40:1266–75.
- Park HW, Yang MS, Park CS, Kim TB, Moon HB, Min KU, et al. Additive role of tiotropium in severe asthmatics and Arg16Gly in ADRB2 as a potential marker to predict response. *Allergy* 2009;64:778–83.
- Pascual RM, Peters SP. Airway remodeling contributes to the progressive loss of lung function in asthma: an overview. *J Allergy Clin Immunol* 2005;116:477–86 quiz 487.
- Peters SP, Kunselman SJ, Icitovic N, Moore WC, Pascual R, Ameredes BT, et al. Tiotropium bromide step-up therapy for adults with uncontrolled asthma. *N Engl J Med* 2010;363:1715–26.
- Pijnenburg MW, Hofhuis W, Hop WC, De Jongste JC. Exhaled nitric oxide predicts asthma relapse in children with clinical asthma remission. *Thorax* 2005;60:215–8.
- Razani-Boroujerdi S, Behl M, Hahn FF, Pena-Philippides JC, Hutt J, Sopori ML. Role of muscarinic receptors in the regulation of immune and inflammatory responses. *J Neuroimmunol* 2008;194:83–8.
- Sinaglia F, D'Ambrosio D. Regulation of helper T cell differentiation and recruitment in airway inflammation. *Am J Respir Crit Care Med* 2000;162:S157–60.
- Verini M, Peroni DG, Rossi N, Nicodemo A, De Stradis R, Spagnolo C, et al. Functional assessment of allergic asthmatic children while asymptomatic. *Allergy Asthma Proc* 2006;27:359–64.
- Wessler IK, Kirkpatrick CJ. The non-neuronal cholinergic system: an emerging drug target in the airways. *Pulm Pharmacol Ther* 2001;14:423–34.

## 4. CONCLUDING DISCUSSION

This thesis presented research that (i) led to detection of novel genomic biomarkers involved in disease pathogenesis, (ii) contributed to development of novel imaging approach to monitor lung inflammation and (iii) successfully suppressed all aspects of asthma relapse in mice using novel treatment, tiotropium bromide.

Detailed understanding of gene expression is one of keys for understanding complex biological processes such as asthma (113,114). Moreover, detailed transcriptional profiling of diseases facilitates biomarker and drug discovery enabling target identification and validation, side-effect profiling, pharmacogenomics, biomarker development, clinical trial evaluation and toxicology (68,79,115). In the first manuscript presented in this thesis, we used a powerful bioinformatic analyses to prioritize asthma-related and -ignore genes within the clusters and biological domains and provide important insights into interactions between lung, immune and inflammatory response genes and networks. These data provide important insights into asthma pathogenesis and provides new opportunities for better classification of the disease and development of novel biomarkers and treatment modalities.

Longitudinal monitoring of pathological processes *in vivo* revolutionized the ability to develop new treatments (116). Non-invasive monitoring of cellular and molecular processes not only allows detailed visualization of pathological processes, but also can serve as a biomarker for early indications of efficacy of the treatment response (117). In pulmonary research, improvements of imaging techniques such as PET, SPECT and MRI allowed anatomical, molecular and functional visualization of the lungs in preclinical models (95,118). In publication 1, we developed an imaging approach that combines near infrared fluorescence dye (allowing visualization of mice lungs due to penetration depth of 4 cm) with specificity of probe (dendritic polyglycerol sulfates that bind L- and P-selectins and C3 and C5 complement factors) to non-invasively monitor allergic asthma in mice. The combination of relatively inexpensive and

non-harmful imaging method with specific probe makes this novel imaging approach suitable for monitoring inflammation processes and responses to therapy in experimental mouse models of lung disease.

Selection of optimal experimental *in vivo* model is crucial for preclinical drug discovery (119). In asthma, many different models are in use, each mimicking different aspects of the disease (39,53,89,90). Our laboratory developed model of asthma relapse to mimic intermittent reversible course of the disease and to investigate importance of allergen-specific Th2 memory cells for its maintenance (48,120,121). In publication 2, we successfully used the asthma relapse model to evaluate efficacy of novel treatment modality, tiotropium bromide, in asthma.

A prerequisite for successful development of new anti-asthmatic therapies is detailed understanding of asthma phenotypes and endotypes. Achievement of this goal is, however, impossible without discovery of biomarkers from body fluids and/or affected tissues (16,68). This thesis, therefore, provided a step-wise approach towards detection of novel biomarkers and anti-asthmatic medications: (i) our detailed gene expression profile of an acute allergic asthma provides numerous novel biomarker and treatment targets; (ii) our novel imaging technology enables elegant way for visualization of allergic lung inflammation *in vivo*; while (iii) our data do not only provide supportive evidence for the use of anticholinergic drug tiotropium bromide in asthma, but also describe an elegant experimental setting for testing novel drugs or validation of novel biomarkers.

## 5. DECLARATION OF CONTRIBUTION

### *Revealing the acute asthma ignorome: characterization and validation of uninvestigated gene networks*

Berislav Bosnjak participated in selection of studies for this microarray meta-analysis, contributed to its data interpretation, as well as designed validation experiments using quantitative real-time PCR on total lung RNA samples from mice in allergic asthma model. He participated in manuscript preparation and approved its final version.

### *Dendritic Polyglycerolsulfate Near Infrared Fluorescent (NIRF) Dye Conjugate for Non-Invasively Monitoring of Inflammation in an Allergic Asthma Mouse Model*

Berislav Bosnjak contributed to the study with the analysis of lung inflammation on H&E-stained lung sections and mucus hypersecretion on PAS-stained lung sections, as well as determining of serum OVA-specific IgG1 titers. He also read and approved the final version of the manuscript.

### *Tiotropium bromide inhibits relapsing allergic asthma in BALB/c mice*

Berislav Bosnjak was involved in the design of experiments included in this study, he performed immunization, treatment and aerosol challenges of animals, collected BAL, lung and sera and analyzed airway inflammation data, eosinophil counts in lungs, as well as allergen-specific IgG1 and IgE titers in sera. He also contributed to manuscript preparation and approved its final version.

## 6. REFERENCES

1. Marketos SG, Ballas CN. Bronchial asthma in the medical literature of Greek antiquity. *J Asthma*. 1982;19(4):263–9.
2. Akdis CA, Immunology EAOAAC. *Global Atlas of Asthma*. 2013. 1 p.
3. Martinez FD, Vercelli D. Asthma. *Lancet*. 2013 Oct 19;382(9901):1360–72.
4. *Global Strategy for Asthma Management and Prevention*. 2011. 1 p.
5. Eder W, Ege MJ, Mutius von E. The asthma epidemic. *N Engl J Med*. 2006 Nov 23;355(21):2226–35.
6. Masoli M, Fabian D, Holt S, Beasley R, Global Initiative for Asthma (GINA) Program. The global burden of asthma: executive summary of the GINA Dissemination Committee report. *Allergy*. Munksgaard International Publishers; 2004 May;59(5):469–78.
7. Schernhammer ES, Vutuc C, Waldhör T, Haidinger G. Time trends of the prevalence of asthma and allergic disease in Austrian children. *Pediatr Allergy Immunol*. 2008 Mar;19(2):125–31.
8. Harris JR, Magnus P, Samuelsen SO, Tambs K. No evidence for effects of family environment on asthma. A retrospective study of Norwegian twins. *Am J Respir Crit Care Med*. 1997 Jul;156(1):43–9.
9. Torgerson DG, Ampleford EJ, Chiu GY, Gauderman WJ, Gignoux CR, Graves PE, et al. Meta-analysis of genome-wide association studies of asthma in ethnically diverse North American populations. *Nat Genet*. 2011 Jul 31;43(9):887–92.
10. Moffatt MF, Gut IG, Demenais F, Strachan DP, Bouzigon E, Heath S, et al. A Large-Scale, Consortium-Based Genomewide Association Study of Asthma. *N Engl J Med*. 2010 Sep 23;363(13):1211–21.
11. March ME, Sleiman PM, Hakonarson H. Genetic polymorphisms and associated susceptibility to asthma. *Int J Gen Med*. 2013;6:253–65.
12. Wenzel SE. Asthma phenotypes: the evolution from clinical to molecular approaches. *Nature Medicine*. 2012 May;18(5):716–25.
13. Henderson AJ. Childhood asthma phenotypes in the twenty-first century. *Breathe*. European Respiratory Society; 2014 Jun 1;10(2):100–8.
14. Agache I, Akdis C, Jutel M, Virchow JC. Untangling asthma phenotypes and endotypes. *Allergy*. 2012 Jul;67(7):835–46.
15. Anderson GP. Endotyping asthma: new insights into key pathogenic

- mechanisms in a complex, heterogeneous disease. *Lancet*. 2008 Sep 20;372(9643):1107–19.
16. Lötvall J, Akdis CA, Bacharier LB, Bjermer L, Casale TB, Custovic A, et al. Asthma endotypes: a new approach to classification of disease entities within the asthma syndrome. *J Allergy Clin Immunol*. 2011 Feb;127(2):355–60.
  17. George BJ, Reif DM, Gallagher JE, Williams-DeVane CR, Heidenfelder BL, Hudgens EE, et al. Data-driven asthma endotypes defined from blood biomarker and gene expression data. *PLoS ONE*. 2015;10(2):e0117445.
  18. Baines KJ, Simpson JL, Wood LG, Scott RJ, Gibson PG. Transcriptional phenotypes of asthma defined by gene expression profiling of induced sputum samples. 2011 Jan;127(1):153–60.e1–9.
  19. Verrills NM, Irwin JA, He XY, Wood LG, Powell H, Simpson JL, et al. Identification of novel diagnostic biomarkers for asthma and chronic obstructive pulmonary disease. *Am J Respir Crit Care Med*. American Thoracic Society; 2011 Jun 15;183(12):1633–43.
  20. Holt PG, Macaubas C, Stumbles PA, Sly PD. The role of allergy in the development of asthma. *Nature*. 1999 Nov 25;402(6760 Suppl):B12–7.
  21. Johansson SGO, Hourihane JO, Bousquet J, Brujnzeel Koomen C, Dreborg S, Haahtela T, et al. A revised nomenclature for allergy: An EAACI position statement from the EAACI nomenclature task force. *Allergy*. Munksgaard International Publishers; 2001 Sep 1;56(9):813–24.
  22. Wenzel SE. Asthma: defining of the persistent adult phenotypes. *Lancet*. Elsevier; 2006 Aug 26;368(9537):804–13.
  23. Holgate ST. Innate and adaptive immune responses in asthma. *Nature Medicine*. 2012 May;18(5):673–83.
  24. Fahy JV, Locksley RM. The airway epithelium as a regulator of Th2 responses in asthma. *Am J Respir Crit Care Med*. 2011 Aug 15;184(4):390–2.
  25. Lambrecht BN, Hammad H. Asthma: The importance of dysregulated barrier immunity. *Eur J Immunol*. 2013 Dec 1;43(12):3125–37.
  26. Erle DJ, Sheppard D. The cell biology of asthma. *J Cell Biol*. 2014 Jun 9;205(5):621–31.
  27. Mjösberg J, Spits H. Type 2 innate lymphoid cells-new members of the “type 2 franchise” that mediate allergic airway inflammation. *Eur J Immunol*. 2012 May;42(5):1093–6.

28. Ito T, Wang Y-H, Duramad O, Hori T, Delespesse GJ, Watanabe N, et al. TSLP-activated dendritic cells induce an inflammatory T helper type 2 cell response through OX40 ligand. *J Exp Med. Rockefeller Univ Press*; 2005 Nov 7;202(9):1213–23.
29. Bacharier LB, Geha RS. Molecular mechanisms of IgE regulation. *2000 Feb*;105(2 Pt 2):S547–58.
30. Punnonen J, Aversa G, Cocks BG. Interleukin 13 induces interleukin 4-independent IgG4 and IgE synthesis and CD23 expression by human B cells. 1993.
31. Luger EO, Fokuhl V, Wegmann M, Abram M, Tillack K, Achatz G, et al. Induction of long-lived allergen-specific plasma cells by mucosal allergen challenge. *2009 Oct*;124(4):819–26.e4.
32. Li L, Xia Y, Nguyen A, Feng L, Lo D. Th2-induced eotaxin expression and eosinophilia coexist with Th1 responses at the effector stage of lung inflammation. *J Immunol*. 1998 Sep 15;161(6):3128–35.
33. Li XM, Schofield BH, Wang QF, Kim KH, Huang SK. Induction of pulmonary allergic responses by antigen-specific Th2 cells. *J Immunol*. 1998 Feb 1;160(3):1378–84.
34. Gavett SH, Chen X, Finkelman F, Wills-Karp M. Depletion of murine CD4+ T lymphocytes prevents antigen-induced airway hyperreactivity and pulmonary eosinophilia. *American Journal of Respiratory Cell and Molecular Biology*. 1994 Jun;10(6):587–93.
35. Robinson DS, Hamid Q, Ying S, Tsicopoulos A, Barkans J, Bentley AM, et al. Predominant TH2-like bronchoalveolar T-lymphocyte population in atopic asthma. *N Engl J Med*. 1992 Jan 30;326(5):298–304.
36. Eckl-Dorna J, Niederberger V. What is the source of serum allergen-specific IgE? *Curr Allergy Asthma Rep*. 2013 Jun;13(3):281–7.
37. Talay O, Yan D, Brightbill HD, Straney EEM, Zhou M, Ladi E, et al. IgE+ memory B cells and plasma cells generated through a germinal-center pathway. *Nat Immunol*. 2012 Apr;13(4):396–404.
38. Bousquet J, Jeffery PK, Busse WW, Johnson M, Vignola AM. Asthma. From bronchoconstriction to airways inflammation and remodeling. *Am J Respir Crit Care Med*. 2000 May;161(5):1720–45.
39. Hall S, Agrawal DK. Key mediators in the immunopathogenesis of allergic asthma. *Int Immunopharmacol. Elsevier B.V*; 2014 Jun 21;:1–14.
40. Shiraishi Y, Asano K, Nakajima T, Oguma T, Suzuki Y, Shiomi T, et al. Prostaglandin D2-induced eosinophilic airway inflammation is mediated by CRTH2 receptor. *J Pharmacol Exp Ther*. 2005 Mar;312(3):954–60.

41. Gyles SL, Xue L, Townsend ER, Wetley F, Pettipher R. A dominant role for chemoattractant receptor-homologous molecule expressed on T helper type 2 (Th2) cells (CRTH2) in mediating chemotaxis of CRTH2+ CD4+ Th2 lymphocytes in response to mast cell supernatants. *Immunology*. 2006 Nov;119(3):362–8.
42. Finkelman FD, Hogan SP, Hershey GKK, Rothenberg ME, Wills-Karp M. Importance of Cytokines in Murine Allergic Airway Disease and Human Asthma. *The Journal of Immunology*. 2010 Feb 3;184(4):1663–74.
43. Jose PJ, Griffiths-Johnson DA, Collins PD, Walsh DT, Moqbel R, Totty NF, et al. Eotaxin: a potent eosinophil chemoattractant cytokine detected in a guinea pig model of allergic airways inflammation. *J Exp Med*. Rockefeller Univ Press; 1994 Mar 1;179(3):881–7.
44. Deckers J, Branco Madeira F, Hammad H. Innate immune cells in asthma. *Trends in Immunology*. 2013 Nov;34(11):540–7.
45. Lloyd CM, Hessel EM. Functions of T cells in asthma: more than just TH2 cells. *Nature Publishing Group*. 2010 Nov 9;10(12):838–48.
46. Lommatzsch M, Julius P, Kuepper M, Garn H, Bratke K, Irmscher S, et al. The course of allergen-induced leukocyte infiltration in human and experimental asthma. *Journal of Allergy and Clinical Immunology*. Elsevier; 2006 Jul;118(1):91–7.
47. Epstein MM. Do mouse models of allergic asthma mimic clinical disease? *Int Arch Allergy Immunol*. 2004 Jan;133(1):84–100.
48. Mojtabavi N, Dekan G, Stingl G, Epstein MM. Long-lived Th2 memory in experimental allergic asthma. *J Immunol*. 2002 Nov 1;169(9):4788–96.
49. Elliot JG, Jensen CM, Mutavdzic S, Lamb JP, Carroll NG, James AL. Aggregations of lymphoid cells in the airways of nonsmokers, smokers, and subjects with asthma. *Am J Respir Crit Care Med*. 2004 Mar 15;169(6):712–8.
50. Farber DL, Yudanin NA, Restifo NP. Human memory T cells: generation, compartmentalization and homeostasis. *Nature Publishing Group*. 2014 Jan;14(1):24–35.
51. Turner DL, Bickham KL, Thome JJ, Kim CY, D'Ovidio F, Wherry EJ, et al. Lung niches for the generation and maintenance of tissue-resident memory T cells. *Mucosal Immunol*. 2014 May;7(3):501–10.
52. Mikhak Z, Strassner JP, Luster AD. Lung dendritic cells imprint T cell lung homing and promote lung immunity through the chemokine receptor CCR4. *Journal of Experimental Medicine*. 2013 Aug 26;210(9):1855–69.

53. Shin YS, Takeda K, Gelfand EW. Understanding Asthma Using Animal Models. *Allergy Asthma Immunol Res.* 2009;1(1):10.
54. Rosner F. Moses Maimonides' treatise on asthma. *Thorax.* 1981;36:245–51.
55. National Asthma Education and Prevention Program. Expert Panel Report 3 (EPR-3): Guidelines for the Diagnosis and Management of Asthma-Summary Report 2007. 2007. pp. S94–138.
56. Burks AW, Calderon MA, Casale T, Cox L, Demoly P, Jutel M, et al. Update on allergy immunotherapy: American Academy of Allergy, Asthma & Immunology/European Academy of Allergy and Clinical Immunology/PRACTALL consensus report. 2013. pp. 1288–96.e3.
57. Akdis M, Akdis CA. Mechanisms of allergen-specific immunotherapy: multiple suppressor factors at work in immune tolerance to allergens. 2014 Mar;133(3):621–31.
58. Warrington R. Immunotherapy in asthma. *Immunotherapy.* 2010 Sep;2(5):711–25.
59. Jeffery PK, Godfrey RW, Adelroth E, Nelson F, Rogers A, Johansson SA. Effects of treatment on airway inflammation and thickening of basement membrane reticular collagen in asthma. A quantitative light and electron microscopic study. *Am Rev Respir Dis.* 1992 Apr;145(4 Pt 1):890–9.
60. Juniper EF, Kline PA, Vanzielegem MA, Ramsdale EH, O'Byrne PM, Hargreave FE. Effect of long-term treatment with an inhaled corticosteroid (budesonide) on airway hyperresponsiveness and clinical asthma in nonsteroid-dependent asthmatics. *Am Rev Respir Dis.* 1990 Oct;142(4):832–6.
61. Ward C, Pais M, Bish R, Reid D, Feltis B, Johns D, et al. Airway inflammation, basement membrane thickening and bronchial hyperresponsiveness in asthma. *Thorax.* 2002 Apr;57(4):309–16.
62. Bateman ED, Bousquet J, Keech ML, Busse WW, Clark TJH, Pedersen SE. The correlation between asthma control and health status: the GOAL study. *Eur Respir J.* 2007 Jan;29(1):56–62.
63. Bateman ED, Boushey HA, Bousquet J, Busse WW, Clark TJH, Pauwels RA, et al. Can guideline-defined asthma control be achieved? The Gaining Optimal Asthma Control study. *Am J Respir Crit Care Med.* 2004 Oct 15;170(8):836–44.
64. Bousquet J, Mantzouranis E, Cruz AA, Aït-Khaled N, Baena-Cagnani CE, Bleecker ER, et al. Uniform definition of asthma severity, control, and exacerbations: document presented for the World Health Organization Consultation on Severe Asthma. 2010. pp. 926–38.

65. Cockcroft DW, Swystun VA. Asthma control versus asthma severity. 1996 Dec;98(6 Pt 1):1016–8.
66. Chen H, Gould MK, Blanc PD, Miller DP, Kamath TV, Lee JH, et al. Asthma control, severity, and quality of life: quantifying the effect of uncontrolled disease. 2007 Aug;120(2):396–402.
67. Masoli F, Fabian D, Holt S, Beasley R. Global Burden of Asthma, 2004. Available at <http://www.ginasthma.org> ( ...; 2004.
68. Baines KJ, Pavord ID, Gibson PG. The role of biomarkers in the management of airways disease. *Int J Tuberc Lung Dis*. 2014 Nov;18(11):1264–8.
69. Ortega HG, Liu MC, Pavord ID, Brusselle GG, FitzGerald JM, Chetta A, et al. Mepolizumab treatment in patients with severe eosinophilic asthma. *N Engl J Med*. 2014 Sep 25;371(13):1198–207.
70. Wenzel S, Ford L, Pearlman D, Spector S, Sher L, Skobieranda F, et al. Dupilumab in persistent asthma with elevated eosinophil levels. *N Engl J Med*. 2013 Jun 27;368(26):2455–66.
71. Gauvreau GM, O'Byrne PM, Boulet L-P, Wang Y, Cockcroft D, Bigler J, et al. Effects of an anti-TSLP antibody on allergen-induced asthmatic responses. *N Engl J Med*. 2014 May 29;370(22):2102–10.
72. Kyle Strimbu JAT. What are Biomarkers? Current opinion in HIV and AIDS. NIH Public Access; 2010 Nov 1;5(6):463–6.
73. Wu VS, Kanaya N, Lo C, Mortimer J, Chen S. From bench to bedside: What do we know about hormone receptor-positive and human epidermal growth factor receptor 2-positive breast cancer? *J Steroid Biochem Mol Biol*. 2015 May 18.
74. Crimi E, Spanevello A, Neri M, Ind PW, Rossi GA, Brusasco V. Dissociation between airway inflammation and airway hyperresponsiveness in allergic asthma. *Am J Respir Crit Care Med*. 1998 Jan;157(1):4–9.
75. Reddel HK, Taylor DR, Bateman ED, Boulet L-P, Boushey HA, Busse WW, et al. An official American Thoracic Society/European Respiratory Society statement: asthma control and exacerbations: standardizing endpoints for clinical asthma trials and clinical practice. *American Journal of Respiratory and Critical Care Medicine*. 2009. pp. 59–99.
76. Rosi E, Ronchi MC, Grazzini M, Duranti R, Scano G. Sputum analysis, bronchial hyperresponsiveness, and airway function in asthma: results of a factor analysis. *Journal of Allergy and Clinical Immunology*. 1999 Feb;103(2 Pt 1):232–7.
77. Leung TF, Ko FWS, Wong GWK. Recent advances in asthma biomarker research. *Therapeutic Advances in Respiratory Disease*. 2013 Oct;7(5):297–308.

78. Connett GJ. Bronchoalveolar lavage. *Paediatr Respir Rev*. 2000 Mar;1(1):52–6.
79. Vijverberg SJ, Hilvering B, Raaijmakers JA, Lammers J-WJ, Maitland-van der Zee A-H, Koenderman L. Clinical utility of asthma biomarkers: from bench to bedside. *Biologics*. 2013;7:199–210.
80. Szeffler SJ, Wenzel S, Brown R, Erzurum SC, Fahy JV, Hamilton RG, et al. Asthma outcomes: biomarkers. *J Allergy Clin Immunol*. 2012 Mar;129(3 Suppl):S9–23.
81. Cowan DC, Taylor DR, Peterson LE, Cowan JO, Palmay R, Williamson A, et al. Biomarker-based asthma phenotypes of corticosteroid response. *J Allergy Clin Immunol*. 2015 Apr;135(4):877–83.e1.
82. Garcia-Marcos L, Brand PL. The utility of sputum eosinophils and exhaled nitric oxide for monitoring asthma control with special attention to childhood asthma. *Allergol Immunopathol (Madr)*. 2010 Jan;38(1):41–6.
83. Persson MG, Zetterström O, Agrenius V, Ihre E, Gustafsson LE. Single-breath nitric oxide measurements in asthmatic patients and smokers. *The Lancet*. 1994 Jan 15;343(8890):146–7.
84. Woodruff PG, Modrek B, Choy DF, Jia G, Abbas AR, Ellwanger A, et al. T-helper type 2-driven inflammation defines major subphenotypes of asthma. *Am J Respir Crit Care Med*. 2009 Sep 1;180(5):388–95.
85. Woodruff PG, Boushey HA, Dolganov GM, Barker CS, Yang YH, Donnelly S, et al. Genome-wide profiling identifies epithelial cell genes associated with asthma and with treatment response to corticosteroids. *PNAS. National Acad Sciences*; 2007 Oct 2;104(40):15858–63.
86. Bjornsdottir US, Holgate ST, Reddy PS, Hill AA, McKee CM, Csimma CI, et al. Pathways activated during human asthma exacerbation as revealed by gene expression patterns in blood. *PLoS ONE*. 2011;6(7):e21902.
87. Choy DF, Modrek B, Abbas AR, Kummerfeld S, Clark HF, Wu LC, et al. Gene expression patterns of Th2 inflammation and intercellular communication in asthmatic airways. *The Journal of Immunology. American Association of Immunologists*; 2011 Feb 1;186(3):1861–9.
88. Sircar G, Saha B, Jana T, Dasgupta A, Gupta Bhattacharya S, Saha S. DAAB: A manually curated database of Allergy and Asthma Biomarkers. *Clin Exp Allergy*. 2015 May 14;:n/a–n/a.
89. Graham MT, Nadeau KC. Lessons learned from mice and man: Mimicking human allergy through mouse models. *Clinical Immunology*. 2014 Aug.
90. Nials AT, Uddin S. Mouse models of allergic asthma: acute and chron-

- ic allergen challenge. *Dis Model Mech*. The Company of Biologists Limited; 2008 Nov;1(4-5):213–20.
91. Kips JC, Anderson GP, Fredberg JJ, Herz U, Inman MD, Jordana M, et al. Murine models of asthma. *Eur Respir J*. 2003 Aug;22(2):374–82.
  92. Stevenson CS, Birrell MA. Moving towards a new generation of animal models for asthma and COPD with improved clinical relevance. *Pharmacol Ther*. 2011 May;130(2):93–105.
  93. Gregory LG, Causton B, Murdoch JR, Mathie SA, O'Donnell V, Thomas CP, et al. Inhaled house dust mite induces pulmonary T helper 2 cytokine production. *Clin Exp Allergy*. 2009 Oct;39(10):1597–610.
  94. Johnson JR, Wiley RE, Fattouh R, Swirski FK, Gajewska BU, Coyle AJ, et al. Continuous exposure to house dust mite elicits chronic airway inflammation and structural remodeling. *Am J Respir Crit Care Med*. 2004 Feb 1;169(3):378–85.
  95. Jannasch K, Missbach-Guentner J, Alves F. Using *in vivo* imaging for asthma. *Drug Discov Today Dis Models*. 2009;6(4):129–35.
  96. Castro M, Fain SB, Hoffman EA, Gierada DS, Erzurum SC, Wenzel S, et al. Lung imaging in asthmatic patients: the picture is clearer. 2011 Sep;128(3):467–78.
  97. Jobse BN, Johnson JR, Farncombe TH, Labiris R, Walker TD, Goncharova S, et al. Evaluation of allergic lung inflammation by computed tomography in a rat model *in vivo*. *European Respiratory Journal*. 2009 Jun;33(6):1437–47.
  98. Lederlin M, Ozier A, Montaudon M, Begueret H, Ousova O, Marthan R, et al. Airway remodeling in a mouse asthma model assessed by *in vivo* respiratory-gated micro-computed tomography. *Eur Radiol*. 2010 Jan;20(1):128–37.
  99. de Lange EE, Altes TA, Patrie JT, Parmar J, Brookeman JR, Mugler JP, et al. The variability of regional airflow obstruction within the lungs of patients with asthma: assessment with hyperpolarized helium-3 magnetic resonance imaging. 2007 May;119(5):1072–8.
  100. Samee S, Altes T, Powers P, de Lange EE, Knight-Scott J, Rakes G, et al. Imaging the lungs in asthmatic patients by using hyperpolarized helium-3 magnetic resonance: assessment of response to methacholine and exercise challenge. 2003 Jun;111(6):1205–11.
  101. Thien F. Measuring and imaging small airways dysfunction in asthma. *Asia Pac Allergy*. 2013 Oct;3(4):224–30.
  102. Vogel-Claussen J, Renne J, Hinrichs J, Schönfeld C, Gutberlet M, Schaumann F, et al. Quantification of pulmonary inflammation after segmental allergen challenge using turbo-inversion recovery-

- magnitude magnetic resonance imaging. *Am J Respir Crit Care Med*. 2014 Mar 15;189(6):650–7.
103. Richter T, Bellani G, Scott Harris R, Vidal Melo MF, Winkler T, Venegas JG, et al. Effect of prone position on regional shunt, aeration, and perfusion in experimental acute lung injury. *Am J Respir Crit Care Med*. 2005 Aug 15;172(4):480–7.
104. Richard J-C, Zhou Z, Ponde DE, Dence CS, Factor P, Reynolds PN, et al. Imaging pulmonary gene expression with positron emission tomography. *Am J Respir Crit Care Med*. 2003 May 1;167(9):1257–63.
105. Jones HA, Marino PS, Shakur BH, Morrell NW. In vivo assessment of lung inflammatory cell activity in patients with COPD and asthma. *Eur Respir J*. 2003 Apr;21(4):567–73.
106. Taylor IK, Hayes M, O'Connor BJ, Jones HA. Imaging allergen-induced airway inflammation in atopic asthma with [<sup>18</sup>F]-fluorodeoxyglucose and positron emission tomography. *The Lancet*. 1996.
107. Markus MA, Dullin C, Mitkovski M, Prieschl-Grassauer E, Epstein MM, Alves F. Non-invasive optical imaging of eosinophilia during the course of an experimental allergic airways disease model and in response to therapy. Stumbles PA, editor. *PLoS ONE*. 2014;9(2):e90017.
108. Montet X, Figueiredo JL, Alencar H, Ntziachristos V, Mahmood U, Weissleder R. Tomographic fluorescence imaging of tumor vascular volume in mice. *Radiology*. 2007 Mar;242(3):751–8.
109. Ushiki T, Kizaka-Kondoh S, Ashihara E, Tanaka S, Masuko M, Hirai H, et al. Noninvasive tracking of donor cell homing by near-infrared fluorescence imaging shortly after bone marrow transplantation. Rapoport JZ, editor. *PLoS ONE*. 2010;5(6):e11114.
110. Korideck H, Peterson JD. Noninvasive quantitative tomography of the therapeutic response to dexamethasone in ovalbumin-induced murine asthma. *J Pharmacol Exp Ther*. 2009 Jun;329(3):882–9.
111. Cortez-Retamozo V, Swirski FK, Waterman P, Yuan H, Figueiredo JL, Newton AP, et al. Real-time assessment of inflammation and treatment response in a mouse model of allergic airway inflammation. *J Clin Invest*. 2008 Dec;118(12):4058–66.
112. Ma G, Gallant P, McIntosh L. Sensitivity characterization of a time-domain fluorescence imager: eXplore Optix. *Appl Opt*. 2007 Apr 1;46(10):1650–7.
113. Bates S. The role of gene expression profiling in drug discovery. *Curr Opin Pharmacol*. 2011 Oct;11(5):549–56.

114. Stupka E. The emergence of genomics in mouse asthma models. *Drug Discovery Today - Disease Models*. 2009;6(4):119–27.
115. Chengalvala MV, Chennathukuzhi VM, Johnston DS, Stevis PE, Kopf GS. Gene expression profiling and its practice in drug development. *Curr Genomics*. 2007 Jun;8(4):262–70.
116. Weissleder R. Scaling down imaging: molecular mapping of cancer in mice. *Nat Rev Cancer*. Nature Publishing Group; 2002 Jan;2(1):11–8.
117. Conway JRW, Carragher NO, Timpson P. Developments in preclinical cancer imaging: innovating the discovery of therapeutics. *Nat Rev Cancer*. 2014 May;14(5):314–28.
118. Gammon ST, Foje N, Brewer EM, Owers E, Downs CA, Budde MD, et al. Preclinical anatomical, molecular, and functional imaging of the lung with multiple modalities. *AJP: Lung Cellular and Molecular Physiology*. 2014 May 15;306(10):L897–914.
119. Zhang D, Luo G, Ding X, Lu C. Preclinical experimental models of drug metabolism and disposition in drug discovery and development. *Acta Pharmaceutica Sinica B*. 2012 Dec;2(6):549–61.
120. Jungsuwadee P, Dekan G, Stingl G, Epstein MM. Recurrent aerosol antigen exposure induces distinct patterns of experimental allergic asthma in mice. *Clin Immunol*. 2002 Feb 1;102(2):145–53.
121. Jungsuwadee P, Dekan G, Stingl G, Epstein MM. Inhaled dexamethasone differentially attenuates disease relapse and established allergic asthma in mice. *Clin Immunol*. 2004;110(1):13–21.

## 7. ACKNOWLEDGMENTS

I express my sincere gratitude to Dr. Michelle M. Epstein for providing me a chance to work in her lab on this thesis. Her enthusiasm, scientific knowledge and inspiration contribute to the success of my thesis.

I also greatly thank ao. Prof. Dr. Oskar Hoffmann at Institute of Pharmacology and Toxicology on University of Vienna. Completion of this PhD thesis would me much more difficult without his constant encouragement and support.

I appreciate contributions from all collaborators to whom we cooperated on different parts of this thesis.

I wish also to thank all past and current members of Experimental Allergy lab for all help on different parts of experiments and friendly working environment.

I wish to thank a lot to my parents, sisters and friends for their undivided support and care.

Last but not least, I wish to thank my wife Gordana and children Vida and Vilim. This work would have been difficult to complete without their love and support.

## 8. CURRICULUM VITAE

### Personal information

Name Berislav Bošnjak  
Address Harmoniegasse 3/1, 1090 Wien, Austria  
Telephone +43 65 03480360  
E-mail berislav.bosnjak@meduniwien.ac.at  
Nationality Croatian  
Date of birth 28. 05. 1979  
Gender Male

### Work experience

#### *November 2009 - present*

PhD student employed on FP7 EU projects P3AGI (GA 230739) and Innovabone (GA 263363)

Medical University of Vienna, Department of Dermatology, Division of Immunology, Allergy and Infectious Diseases, Experimental Allergy, Währinger Gürtel, A-1090 Vienna, Austria

#### *January 2009 - October 2009*

ÖAD scholarship for student research project on immunobiology of asthma

Medical University of Vienna, Department of Dermatology, Division of Immunology, Allergy and Infectious Diseases, Experimental Allergy, Lazarettgasse 19, A-1090 Vienna, Austria

#### *May 2006 - December 2008*

Senior researcher – immuno-pharmacologist (from April 2007 to December 2008), Senior researcher – pharmacologist (from January 2007 to March 2007), Researcher – pharmacologist (from May 2006 to December 2006)

GlaxoSmithKline Research Centre Zagreb Limited, Prilaz baruna Filipovića 29, HR- 10000 Zagreb, Croatia

*December 2004 - May 2006*

Researcher – pharmacologist (from April 2005 to April 2006), Researcher – immunologist (from December 2004 to March 2005)

PLIVA Research Institute Ltd., Prilaz baruna Filipovica 29, HR-10000 Zagreb, Croatia

*February 2002 - December 2004*

Researcher – immunologist

PLIVA Inc., pharmaceutical company, Prilaz baruna Filipovica 25, HR-10000 Zagreb, Croatia

**Education**

*April 2009 - present*

PhD studies in Biology, field of Molecular biology  
University of Vienna, Vienna, Austria

*October 2002 - December 2006*

Master of science degree in Biology, field of Physiology and Immunobiology

Master of science thesis title: "Characteristics of airway inflammation after ovalbumin challenge in sensitized mice", investigation of the mechanisms by which airway inflammation induces airway hyperresponsiveness in asthma

Faculty of medicine, University of Rijeka, Croatia (from December 2002 to February 2004) and Faculty of Science, University of Zagreb, Croatia (from February 2004 to December 2006)

*June 1996 - October 2001*

Bachelor of science (BS) in Molecular biology

Graduation thesis title: "Activation of transcription factor NF- $\kappa$ B in the spleens of Wistar rats after treatment with Jectofer", investigation of the effect of iron in form of non-toxic compound Jectofer (ferric-sorbitol-citrate) on activation of transcription factor NF- $\kappa$ B in the spleen cells

Faculty of Science, University of Zagreb, Croatia

**Memberships**

- Austrian Society of Allergology and Immunology (ÖGAI; since 2012)
- Croatian Immunological Society (HDI; since 2005)
- Croatian Society for Biochemistry and Molecular Biology (HDBMB; since 2004)
- European Academy of Allergy and Clinical Immunology (EAACI; since 2011)
- European Respiratory Society (ERS; since 2011)

**Scholarships/Awards**

- Travel grant from ÖGAI for attendance of 15<sup>th</sup> International Congress of Immunology in Milan, Italy, August 22-27, 2013
- Travel grant from EAACI for attendance of EAACI Allergy School “Clinical impact and mechanisms of infections in allergy”, in Edinburgh, UK, September 15-18, 2011
- Exceptional Science Award given by Research and Development of GlaxoSmithKline Inc. for a front-line contribution to advancing understanding and application of the science that will create better medicines (2008)
- Annual award given by PLIVA Inc. for excellent team work (2005)
- The best student at the Department of Biology, Faculty of Science, University of Zagreb (2000)
- University of Zagreb Rector's prize for the thesis “The role of iron in progression of lung tumors” (1999)

**Published articles:**

1. Schliehe C, Flynn EK, Vilagos B, Richson U, Swaminathan S, Bosnjak B, Bauer L, Kandasamy RK, Griesshammer IM, Kosack L, Schmitz F, Litvak V, Sissons J, Lercher A, Bhattacharya A, Khamina K, Trivett AL, Tessarollo L, Mesteri I, Hladik A, Merkler D, Kubicek S, Knapp S, Epstein MM, Symer DE, Aderem A, Bergthaler A. (2015) The methyltransferase Setdb2 mediates virus-induced susceptibility to bacterial superinfection. *Nat Immunol.* 16(1):67-74.

2. Hrvacic B, Situm K, Duric K, Bosnjak B, Ferencic Z, Brajsa K, Markovic S, Glojnaric I. (2014) Relative potencies of three glucocorticoids to induce hypoplasia of the physis and concomitant biochemical alterations in the rat. *Drug Chem Toxicol.* 2014 Aug 11:1-6. [Epub ahead of print]
3. Bosnjak B, Tilp C, Tomsic C, Dekan G, Pieper MP, Erb KJ, Epstein MM. (2014) Tiotropium bromide inhibits relapsing allergic asthma in BALB/c mice. *Pulm Pharmacol Ther.* 27(1): 44-51.
4. Elenkov IJ, Hrvacic B, Markovic S, Mesic M, Cempuh Klunkay A, Lerman L, Filipovic Sucic A, Vujasinovic I, Bosnjak B, Brajsa K, Zihir D, Kosutic Hulita N, Malnar I. (2013) Synthesis and Anti-inflammatory Activity of Novel Furochromenes. *Croat Chem Acta* 86(3): 253-64.
5. Biffi S, Dal Monego S, Dullin C, Garrovo C, Bosnjak B, Licha K, Welker P, Epstein MM, Alves F. (2013) Dendritic Polyglycerolsulfate Near Infrared Fluorescent (NIRF) Dye Conjugate for Non-Invasively Monitoring of Inflammation in an Allergic Asthma Mouse Model. *PLoS ONE* 8(2): e57150.
6. Bosnar M, Kragol G, Kostrun S, Vujasinovic I, Bosnjak B, Bencetic Mihaljevic V, Marusic Istuk Z, Kapic S, Hrvacic B, Brajsa K, Tavcar B, Jellic D, Glojnaric I, Verbanac D, Culic O, Padovan J, Alihodzic S, Erakovic Haber V, Spaventi R. (2012) N'-substituted-2'-O,3'-N-carbonimidoyl bridged macrolides: novel anti-inflammatory macrolides without antimicrobial activity. *J Med Chem* 55(13): 6111-23.
7. Ivetic Tkalcevic V, Hrvacic B, Bosnar M, Cuzic S, Bosnjak B, Erakovic Haber V, Glojnaric I. (2012) Cantharidin-induced inflammation in mouse ear model for translational research of novel anti-inflammatories. *Transl Res* 160(2): 137-45.
8. Bosnjak B, Stelzmueller B, Erb KJ, Epstein MM. (2011) Treatment of allergic asthma: Modulation of Th2 cells and their responses. *Respir Res.* 12: 114 (review)
9. Bosnar M, Cuzic S, Bosnjak B, Nujic K, Ergovic G, Marjanovic N, Pasalic I, Hrvacic B, Polancec D, Glojnaric I, Haber VE. (2011) Azithromycin inhibits macrophage interleukin-1 $\beta$  production through inhibition of activator protein-1 in lipopolysaccharide-induced murine pulmonary neutrophilia. *Int Immunopharmacol* 11: 424-34.

10. Pasalic I, Bosnjak B, Ivetic Tkalcevic V, Jaran DS, Javorscak Z, Markovic D, Hrvacic B (2011) Cage enrichment with paper tissue, but not plastic tunnels, increases variability in mouse model of asthma. *Lab Anim* 45(2): 121-3. (short report)
11. Bosnar M\*, Bosnjak B\*, Cuzic S, Hrvacic B, Marjanovic N, Glojnaric I, Culic O, Parnham MJ, Erakovic Haber V (2009) Azithromycin and clarithromycin inhibit lipopolysaccharide-induced murine pulmonary neutrophilia mainly through effects on macrophage-derived GM-CSF and IL-1 $\beta$ . *J Pharmacol Exp Ther* 331: 104-113 (\* authors equally contributed to the paper)
12. Hrvacic B\*, Bosnjak B\*, Bosnar M, Ferencic Z, Glojnaric I, Erakovic Haber V (2009) Clarithromycin suppresses airway hyperresponsiveness and inflammation in mouse models of asthma. *Eur J Pharmacol* 616: 236-243. (\* authors equally contributed to the paper)
13. Bosnjak B, Ivetic Tkalcevic V, Duric K, Belamaric D, Cuzic S, Ferencic Z, Brajsa K, Glojnaric I, Antolovic R, Hrvacic B (2009) Intranasal challenge with increasing ovalbumin doses differently affects airway hyperresponsiveness and inflammatory cell accumulation in mouse model of asthma. *Inflamm Res* 58: 773-81
14. Brajsa K, Ferencic Z, Katicic M, Bosnjak B, Presecki V, Spaventi R, Dominis M (2008) Influence of *Helicobacter pylori* infection persistence on bcl-2 expression in gastric mucosa inflammatory cells. *Acta Clin Croat* 47: 123-127
15. Ivetic Tkalcevic V, Bosnjak B, Pasalic I, Hrvacic B, Situm K, Dominis Kramaric M, Glojnaric I, Erakovic Haber V (2008) The anti-inflammatory activity of clarithromycin inhibits TNF $\alpha$  production and prolongs survival following lipopolysaccharide administration in mice. *Int J Antimicrob Agents* 32: 195-196 (letter to the editor)
16. Hrvacic B, Bosnjak B, Tudja M, Mesic M, Mercep M (2006) Applicability of an ultrasonic nebulization system for the airways delivery of beclomethasone dipropionate in a murine model of asthma. *Pharm Res* 23: 1765-1775
17. Ivetic Tkalcevic V, Bosnjak B, Hrvacic B, Bosnar M, Marjanovic N, Ferencic Z, Situm K, Culic O, Parnham MJ, Erakovic V (2006) Anti-

- inflammatory activity of azithromycin attenuates the effects of lipopolysaccharide administration in mice. *Eur J Pharmacol* 539: 131-138
18. Katic M, Bosnjak B, Gall-Troselj K, Dikic I, Pavelic K (2006) A clinoptilolite effect on cell media and the consequent effects on tumor cells in vitro. *Front Biosci* 11: 1722-1732
  19. Tomas D, Kruslin B, Cupic H, Stanimirovic A, Bosnjak B, Lovricevic I, Belicza M (2006) Correlation between Bcl-2 and Bax in atrophic and hypertrophic type of actinic keratosis. *JEADV* 20: 51-57
  20. Stanimirovic A, Cupic H, Bosnjak B, Tomas D, Kruslin B, Belicza M (2005) TP53, Bcl-2 and growth hormone receptor expression in cutaneous squamous cell carcinoma. *Acta Dermatovenerol Croat* 13: 201-205
  21. Stanimirovic A, Cupic H, Tomas D, Bosnjak B, Balicevic D, Kruslin B, Belicza M (2004) Immunohistochemical determination of the growth hormone receptor in squamous cell carcinoma of the skin. *Acta Dermatoven APA* 13: 3-6
  22. Bosnjak B, Katic M, Hrvacic B, Zupanovic Z, Poljak-Blazi M (2004) Effect of ferric sorbitol citrate on transcription factor NF- $\kappa$ B in rat spleen cells. *Immunopharmacol Immunotoxicol* 26: 43-52
  23. Stanimirovic A, Cupic H, Bosnjak B, Tomas D, Balicevic D, Kruslin B, Belicza M (2004) Expression of p53, bcl-2 and growth hormone receptor in atrophic type of actinic keratosis. *J Dermatol Sci* 34: 49-53 (letter to the editor)
  24. Stanimirovic A, Cupic H, Bosnjak B, Kruslin B, Belicza M (2003) Expression of p53, bcl-2 and growth hormone receptor in actinic keratosis, hypertrophic type. *Arch Dermatol Res* 295: 102-108
  25. Pavelic K, Katic M, Sverko V, Marotti T, Bosnjak B, Balog T, Stojkovic R, Radacic M, Poljak-Blazi M (2002) Immunostimulatory effect of natural clinoptilolite as a possible mechanism of its antimetastatic ability. *Cancer Res Clin Oncol* 128: 37-44
  26. Zarkovic N, Hartleb M, Zarkovic K, Borovic S, Golubic J, Kalisnik T, Frech S, Kingmuller M, Loncaric I, Bosnjak B, Jurin M, Kuhlmeij J (1998) Spleen peptides (Polyerga<sup>TM</sup>) inhibit development of artificial

lung metastases of murine mammary carcinoma and increase efficiency of chemotherapy in mice. *Cancer Biother Radiopharm* 13: 25-32

**Patent applications:**

1. Mercep M, Malnar I, Hrvacic B, Markovic S, Filipovic Sucic A, Bosnjak B, Cempuh Klunkay A, Rupcic R, Hutinec A, Elenkov IJ, Mesic M (2006) Bis-coumarin compounds with anti-inflammatory activity. International patent application Pub. No.: WO/2006/111858
2. Culic O, Bosnar M, Marjanovic N, Jelic D, Alihodzic S, Vela V, Marusic-Istuk Z, Erakovic V, Bosnjak B, Hrvacic B, Tomaskovic M, Munic V, Ivetic V, Hutinec A, Kragol G, Leljic M (2006) Macrolides with anti-inflammatory activity. International patent application Pub. No.: WO/2006/087644

**Book chapter**

1. Poljak-Blazi M, Katic M, Kralj M, Zarkovic N, Marotti T, Bosnjak B, Sverko V, Balog T, Pavelic K (2001) In vitro and in vivo effect of natural clinoptilolite on malignant tumors. In: Galarneau A, Di Renzo F, Fajula F, Vedrine J (eds.) *Studies in Surface Science and Catalysis; Zeolites and Mesoporous Materials at the Dawn of 21st Century*. Amsterdam, London, Oxford, Paris, Shannon, Tokyo, Elsevier.